PNL-8862
UC-702

Subcontractor Report

Summary of 1990 Eolian Characterization Studies, Hanford Site, Washington

January 1991 - Prepared
December 1993 - Published

Prepared by Washington State University
and University of Wyoming
for Pacific Northwest Laboratory
under Contract DE-AC06-76RLO 1830
with the U.S. Department of Energy

Pacific Northwest Laboratory
Operated for the U.S. Department of Energy
by Battelle Memorial Institute

Battelle

PNL-8862

PACIFIC NORTHWEST LABORATORY
operated by
BATTELLE MEMORIAL INSTITUTE
for the
UNITED STATES DEPARTMENT OF ENERGY
under Contract DE-AC06-76RLO 1830

Printed in the United States of America

Available to DOE and DOE contractors from the Office of Scientific and Technical Information, P.O. Box 62, Oak Ridge, TN 37831; prices available from (615) 576-8401. FTS 626-8401.

Available to the public from the National Technical Information Service, U.S. Department of Commerce, 5285 Port Royal Rd., Springfield, VA 22161.

The contents of this report were printed on recycled paper

PNL-8862
UC-702

Summary of 1990 Eolian Characterization Studies, Hanford Site, Washington

D. R. Gaylord, L. D. Stetler, and G. D. Smith
Washington State University
Pullman, Washington

R. W. Mars, University of Wyoming
Laramie, Wyoming

January 1991

Prepared by Washington State University
and University of Wyoming
for Pacific Northwest Laboratory
under Contract DE-AC06-76RLO 1830
with the U.S. Department of Energy
under Agreement No. 097718-A-L2

Pacific Northwest Laboratory
Richland, Washington 99352

Summary

A study of eolian activity was initiated to improve understanding of past climate change and the likely effect of wind on engineered protective barriers at the Hanford Site. Eolian features from a Holocene sand dune field located in the southeastern portion of the Hanford Site were investigated using a variety of field and laboratory techniques including stratigraphic examinations of hand-dug pits, textural and compositional analyses of dune sand and potential source detritus, and air photo interpretations. These investigations were undertaken to evaluate the provenance and eolian dynamics of the sand dunes.

Air photo interpretations and ground truth checks revealed that eolian-influenced areas on the Hanford Site are divisible into: 1) wind-scoured alluvium and bedrock, 2) stabilized dune sand and subordinate alluvium, 3) mixed stabilized dune sand and alluvium, and 4) active dune sand. A total of 29 hand-dug test pits excavated on an approximately 2-mile grid across the southern part of the Hanford Site provided basic stratigraphic control for interpreting Holocene-Recent sand dune activity and revealed that sand dune sediments become finer grained and better sorted downwind (to the east and northeast). Textures and compositions of potential source sediments exposed along the Cold Creek Valley and Yakima River most closely match those of sediments incorporated into the dunes. Methods by which basic equations of eolian entrainment and sand flow together with grain size and meteorological data can be used to predict sand dune migration rates are demonstrated. Actual measured rates of sand dune migration at the Hanford Site during the past approximate 40 years are from 2.5 to 4.5 m/yr.

Interpretations of sand dune migration using archival air photo stereopairs document a 20% reduction in the volume of active sand dunes (measured from an approximate 15-km^2 test area) between 1948 and 1987. Changes in annual precipitation appear to have influenced active dune migration strongly.

Contents

Figures

Tables

Introduction

Understanding the character of eolian activity likely to affect the Hanford Site during the next 10,000 years is a crucial element in implementing the Hanford Protective Barriers Program. Both eolian-caused accumulation and deflation of sediment from the protective barriers could adversely affect the soil-water balance, a critical factor of barrier design that would influence dissolution and transport of hazardous wastes (Peterson 1989; Wing and Gee 1990).

An agreement was reached between Washington State University (WSU) and Pacific Northwest Laboratory (PNL)[a] in April, 1990 to address the relationship between climate, eolian deflation, and eolian accumulation at the Hanford Site using an integrated, three-phase, multiyear study. The first phase of the study has focused on the preliminary characterization of eolian systems and eolian chronology at the Site; as outlined below, Phase 1 was accomplished via two, interrelated tasks. The second phase of the study will build on the findings of phase 1 and will address the regional aspects of eolian-terrain interactions needed to clarify causal relationships between the climate and eolian landforms, sedimentology, and stratigraphy. The third phase will build upon the findings of phases 1 and 2 to develop a conceptual model of eolian-climatic interactions.

The following report summarizes in-progress findings from Phase 1 activities. The emphasis of the first year of the program has been to characterize the modern eolian system at Hanford via a field- and laboratory- based investigation conducted by the principal investigator, two geology graduate students, and cooperating PNL personnel. Existing Hanford area meteorological data has been examined and, in a preliminary fashion, integrated with findings from field and laboratory investigations of the sedimentology, stratigraphy, and geomorphology of eolian features at the Hanford Site. The primary goal of the first year of research has been the identification of the most appropriate and efficient techniques and/or strategies necessary to reconstruct the eolian history of the Site.

Task 1 of Phase 1 commenced with a review of existing meteorological (especially anemometer) data from the Site. The summary of Hanford meteorological data by Stone et al. (1983) provided the necessary climatic background and was utilized extensively. Glantz et al. 1990 preliminary estimates of potential sand transport at Hanford via analyses of wind direction and speed data provided a thorough introduction to modern airflow tendencies at the Site. Task 1 also included the detailed examination of aerial photos from which an eolian features map was compiled and a sampling program was devised. Completion of the eolian features map and sampling program provided the basis for summer, 1990 field investigations. Finally, as an adjunct to Task 1 activities, modern airflow patterns and strengths at Hanford were used in concert with sedimentary and morphologic data to predict and reconstruct rates of sand dune migration at the Site. Detailed measurements of sand dune migration from an approximately 40-year interval (using aerial photographs) were compared with the projected rates of migration.

Task 2 of Phase 1 investigated the chronology of eolian deposition at the Site. Test sites identified in Task 1 were trenched, described, sampled, and analyzed. Sediments sampled from selected dunes around and on the Site during December 1989 are still being processed for Optical Stimulated Luminescence (OSL) age dating as described by Smith et al. (1991) and Stokes (1991). OSL age dating of such inert dune sediment could potentially revolutionize our ability to constrain the timing of eolian/climatic events at the Site.

Following a brief introduction to the physiography, geology, and climate of the Hanford Site, this report is subdivided into five other major areas of discussion. The first considers the geomorphology, sedimentology, and distribution of major eolian features across the Site, the second

(a) Pacific Northwest Laboratory is a multiprogram national laboratory operated by the U.S. Department of Energy by Battelle Memorial Institute under contract DE-AC06-76RLO 1830.

describes eolian pit stratigraphies and inferred chronologies, the third reviews preliminary findings from provenance studies, the fourth considers eolian processes and airflow-sediment relations, and the fifth summarizes 1990 activities and proposes strategies necessary to accomplish Phase 2 and Phase 3 objectives.

Hanford Site Overview

Hanford Site Physiography and Geology

The Hanford Site is located in the Pasco Basin, a generally low-relief structural and topographic basin within the Yakima Fold Belt subprovince of the Columbia River Plateau Physiographic Province (Thornbury 1965) (Figure 1). A series of WNW ESE-trending anticlinal basalt ridges and hills at the Site rise as much as 515 m (1700 ft) above steep colluvial slopes, elongate synclinal troughs and valleys, and low-sloping alluvial surfaces. Except for the anticlinal basalt bedrock ridges and hills, the primary surface materials are alluvial, eolian, or a mixture of both.

The geology of the Hanford Site is characterized by deformed to undeformed Miocene to Recent volcanic and sedimentary strata. Four principal stratigraphic units are recognized at the Site (Figure 2). In ascending order these are the Miocene Columbia River Basalt Group, Miocene - Pliocene Ringold Formation, Pleistocene Hanford formation (informal name), and Holocene alluvial, colluvial, and eolian deposits.

The Columbia River Basalt Group is composed of a thick sequence of tholeiitic basalt flows intercalated with subordinate sedimentary, volcaniclastic, and pedogenic interbeds. Between approximately 17 and 8.5 Ma, over two kilometers of basalt accumulated in the Pasco Basin (Watkins and Baksi 1974; DOE 1986a). A series of folds in the basalt (the Yakima folds) developed under the influence of basin-wide compressional stresses (Figure 3). These folds trend approximately WNW-ESE (Myers et al. 1979; Reidel et al. 1990) and are reflected by the most prominent topographic features in the area (Figure 4) including the anticlinal Saddle Mountains (immediately north of the Hanford Site), Rattlesnake Hills (along the southern periphery of the Site), Yakima and Umtanum Ridges (along the western margin of the Site), Gable Butte and Gable Mountain (north-centrally located on the Site), and the synclinal Cold Creek Valley (in the southern part of the Site).

The Ringold Formation is composed primarily of quartzo-feldspathic and lithic conglomerate, sandstone, siltstone, mudstone, and claystone (Newcomb 1958; Newcomb et al. 1972; Grollier and Bingham 1978; Myers et al. 1979; Lindsey and Gaylord 1989; 1990). Ringold strata accumulated to thicknesses greater than 200 m on and near the Site, but exposures of this unit are largely restricted to the White Bluffs along the eastern margin of the Columbia River.

The Hanford formation is composed of a variably thick sequence (40 to 70 m) of fine- to coarse-grained clastic, glacial-fluvial sediments that overlie much of the Site west and south of the Columbia River. Two subunits of the Hanford formation are recognized: the underlying (older), 35 to 60 m thick Pasco gravels (Brown 1975; Myers et al. 1979) and the overlying (younger), 7^{+} m thick, locally intercalated sand- to silt-rich Touchet beds (Flint 1938; Myers et al. 1979). Sedimentary detritus includes basalt-rich gravels and basaltic-lithic and quartzo-feldspathic sandy gravel, sand, silt, and mud. Strata of the Hanford formation were deposited by catastrophic floods triggered by ice-dam collapse in western Montana and northeastern Idaho near the end of the last glacial epoch (ca. 13000 yr B.P.) (Mullineaux et al. 1977; Myers et al. 1979).

Broadly dissected alluvial surfaces in the Hanford formation long have been subjected to eolian reworking and locally are obscured beneath up to 30 m of eolian (primarily dune sand) sedimentary detritus. The thickest sand dune accumulations on the Site occur south of Gable Mountain and Gable Butte and north of the 'horn' of the Yakima River.

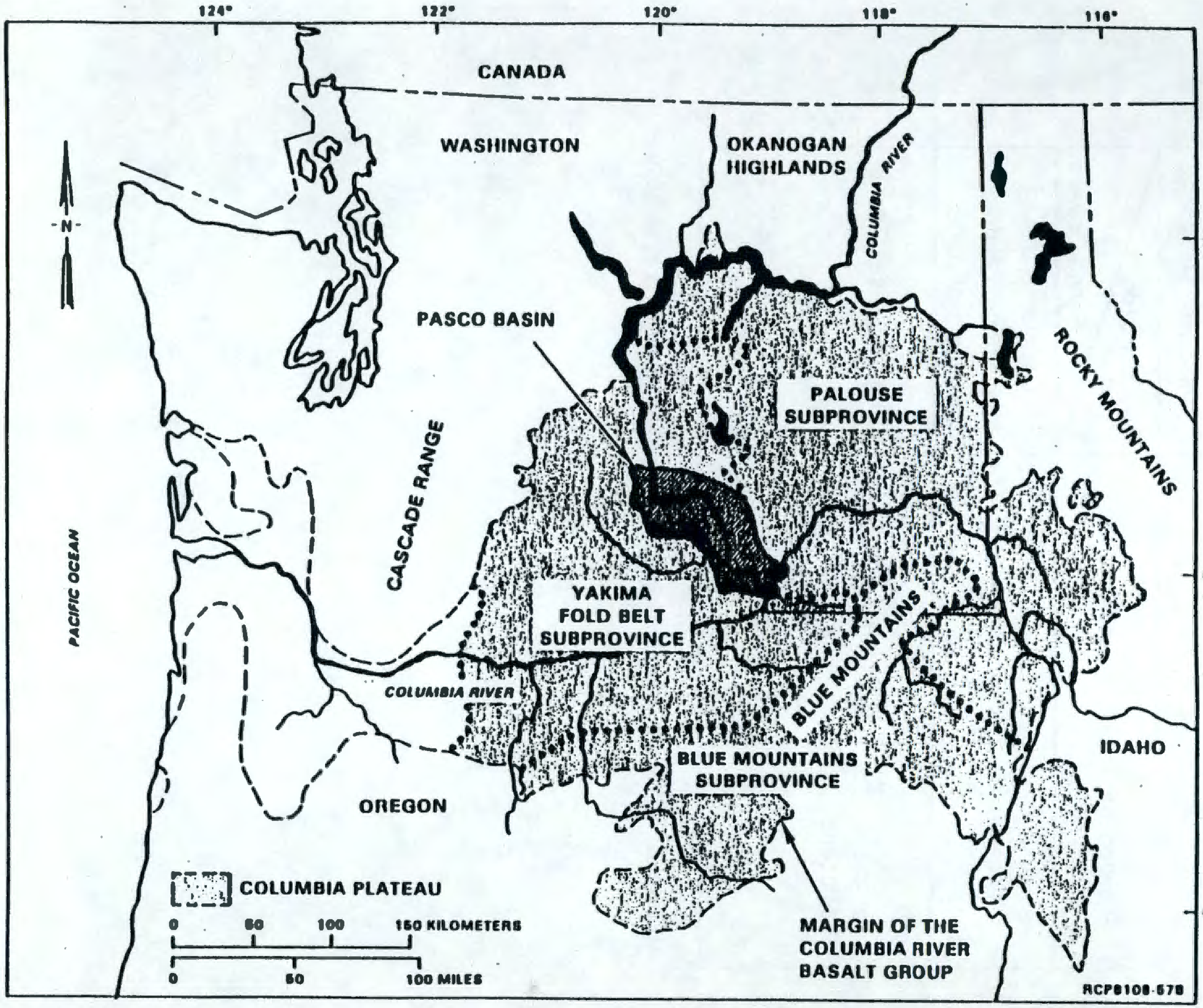

Figure 1. Physiographic Provinces and Subprovinces of the Columbia Plateau Region, Washington, Oregon, and Idaho (DOE 1986; Glantz et al. 1990)

Epoch	Formation	Stratigraphy
Holocene	Surficial Deposits	Alluvial, Colluvial, and Eolian Deposits
Pleistocene	Hanford	Touchet Beds / Pasco Gravels
Pliocene	Ringold	Conglomerates, Sandstone, Siltstone w/mud, claystones
Miocene	Columbia River Basalt Group	Tholeitic Basalt Flows Sedimentary & Volcaniclastic Interbeds

Figure 2. Generalized Stratigraphy of the Hanford Site (Myers et al. 1979)

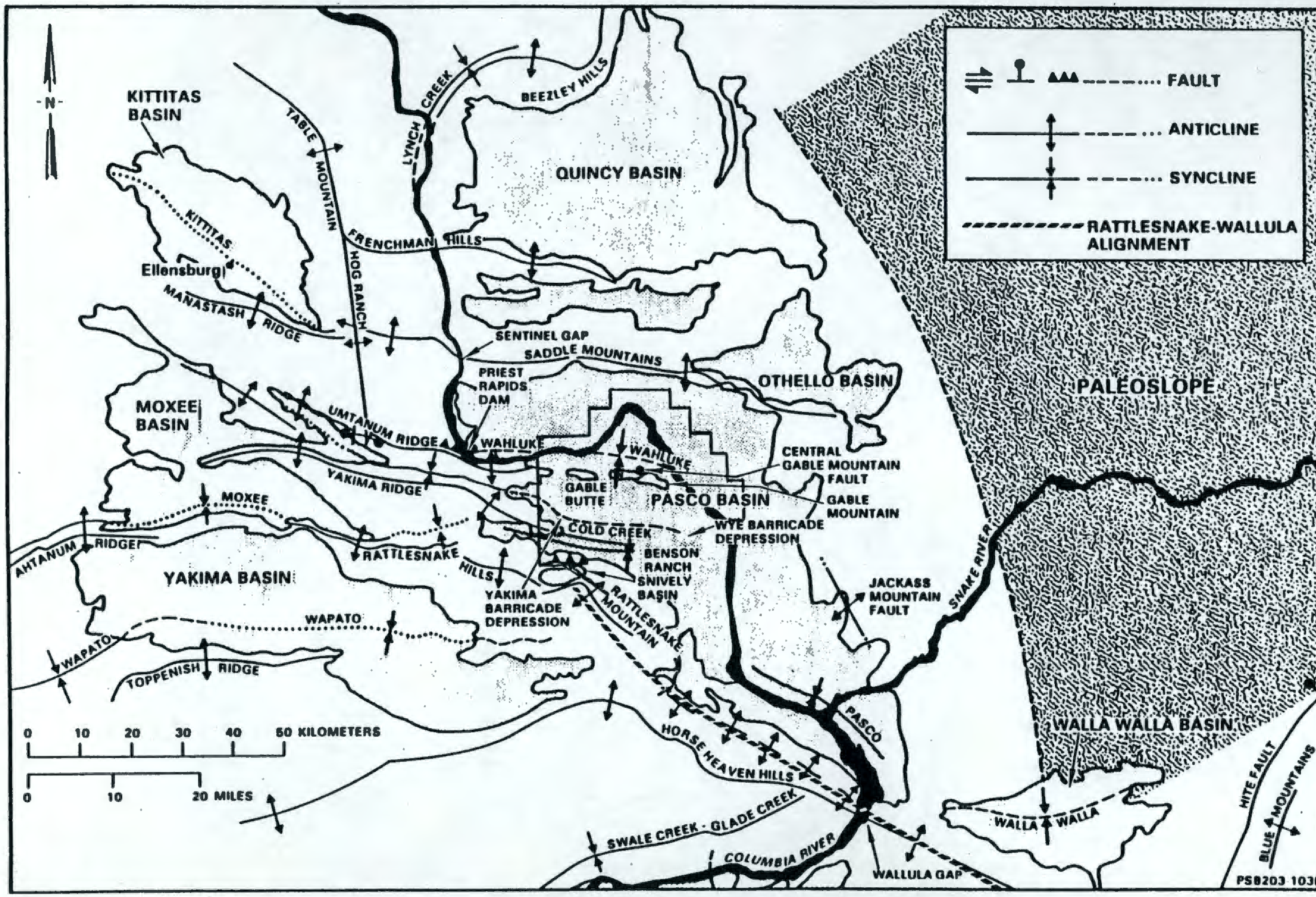

Figure 3. Generalized Geologic Structure Map of the Columbia Plateau Region, Washington (DOE 1986b; Glantz et al. 1990)

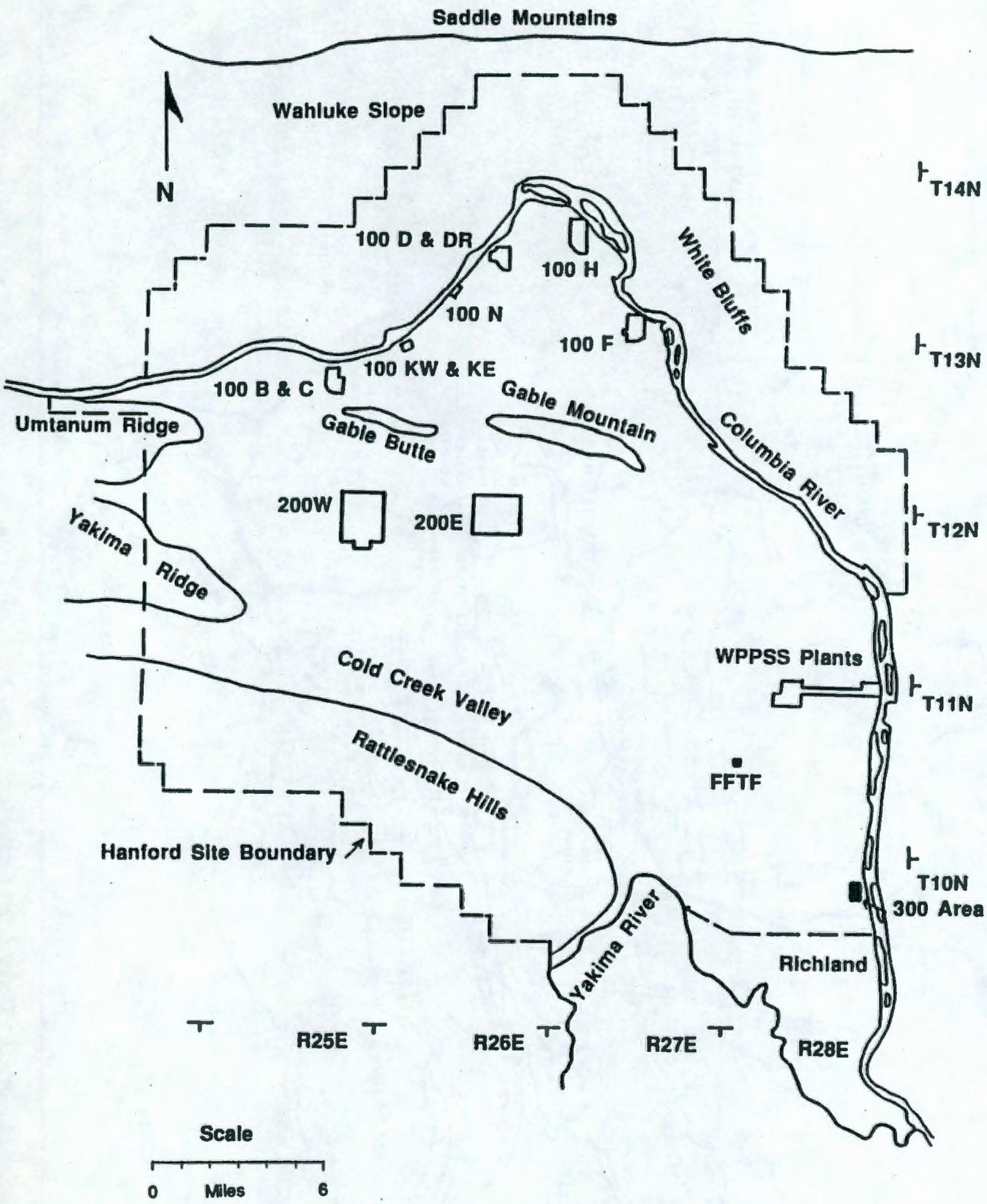

Figure 4. Major Topographic Features in and Adjacent to the Hanford Site

Hanford Site Climate

Overview

The Hanford Site climate is characterized by warm, dry summers, and cool, damp winters. The nearby Cascade and Rocky Mountains play a major role in modifying the modern Hanford Site weather. The Cascades tend to lessen the maritime influence of the nearby Pacific Ocean creating a more semi-arid continental climate than otherwise would be expected (Stone et al. 1983). The Rocky Mountains, on the other hand, tend to protect the region from the extreme cold and severe winter storms so prevalent east of the Continental Divide.

Stone et al. (1983) have summarized meteorological data collected on and near the Site for the period 1912 to 1980. The most complete onsite climate record comes from the Hanford Meteorological Station (HMS) where meteorological data has been collected more or less continuously since December, 1944 (Stone et al. 1983). Data recorded at the HMS include: ambient air temperature, temperature of the dew point, relative humidity, solar radiation, atmospheric pressure, precipitation, and wind speed and direction (Stone et al. 1983).

Precipitation

Average annual precipitation at the Site is 16 cm (6.3 in.) (Stone et al. 1983). The low annual precipitation in this area reflects the drying out of predominantly west-east flowing air masses that descend through the rain shadow leeward of the Cascade Mountains. Over half (~ 52%) of total annual precipitation falls during November, December, January, and February, while less than 12% of total annual precipitation falls during July, August, and September (Figure 5).

Temperature

Mean annual temperature at the Site is 53°F with only the January mean temperature falling below 32°F (Stone et al. 1983). On average the temperature reaches at least 32°F on all but 24 days of the year; those days all occur during November, December, January, and February. The first frost (minimum temperature of 32°F) typically occurs by October 15 and the last frost usually occurs by April 23. Temperatures in excess of 90° F typically occur by May 23 each year while the last 90°F temperature day usually is recorded by September 13. Typically, the average temperature of the soil measured at a depth of 0.20 cm (~0.5 in.) is less than 32°F only during January; however, in severe winters, these near-surface soils may remain below freezing during all or parts of December, January, and February (Stone et al. 1983).

Wind

The most complete analysis available of wind data from the Hanford Site and vicinity is summarized in Glantz et al. (1990). These investigators examined wind speed and directional data from all stations in the Hanford Monitoring Network (HWMN) (also known as the Hanford Wind Telemetry Network) and used data from 21 of these stations to compile a preliminary summary of effective sand-moving winds at the Hanford Site (Figures 6a and 6b). Effective sand-moving winds as defined in the Glantz et al. (1990) study were those necessary to entrain and transport fine-grained quartz sand (0.30 mm in diameter) as measured 9.14 m (30 ft) above the surface. In general, effective sand-moving winds at the Site vary during the year and reach their peak during the spring and early summer. Note: The calculations and equations necessary to make an assessment of eolian entrainment and transport are derived in a later section of this report.

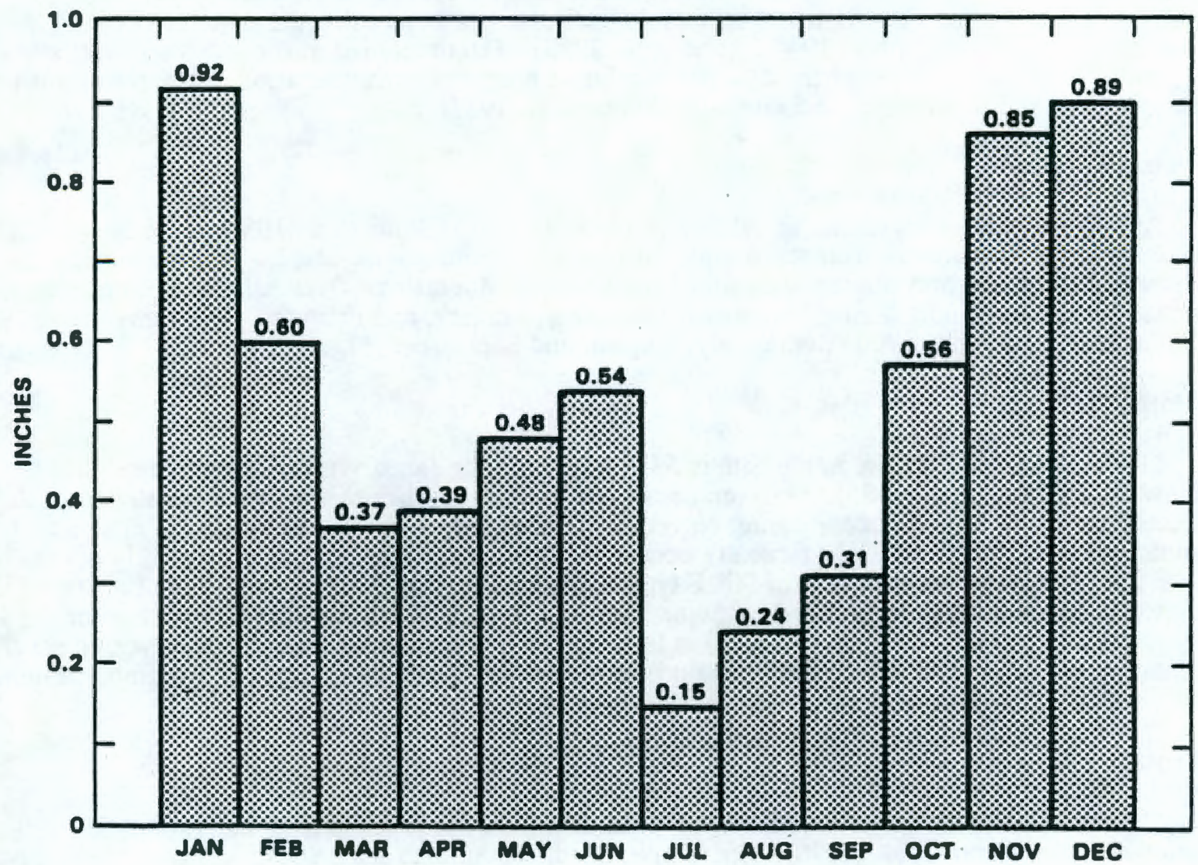

Figure 5. Average Monthly Precipitation, 1919 to 1980 (Stone et al. 1983)

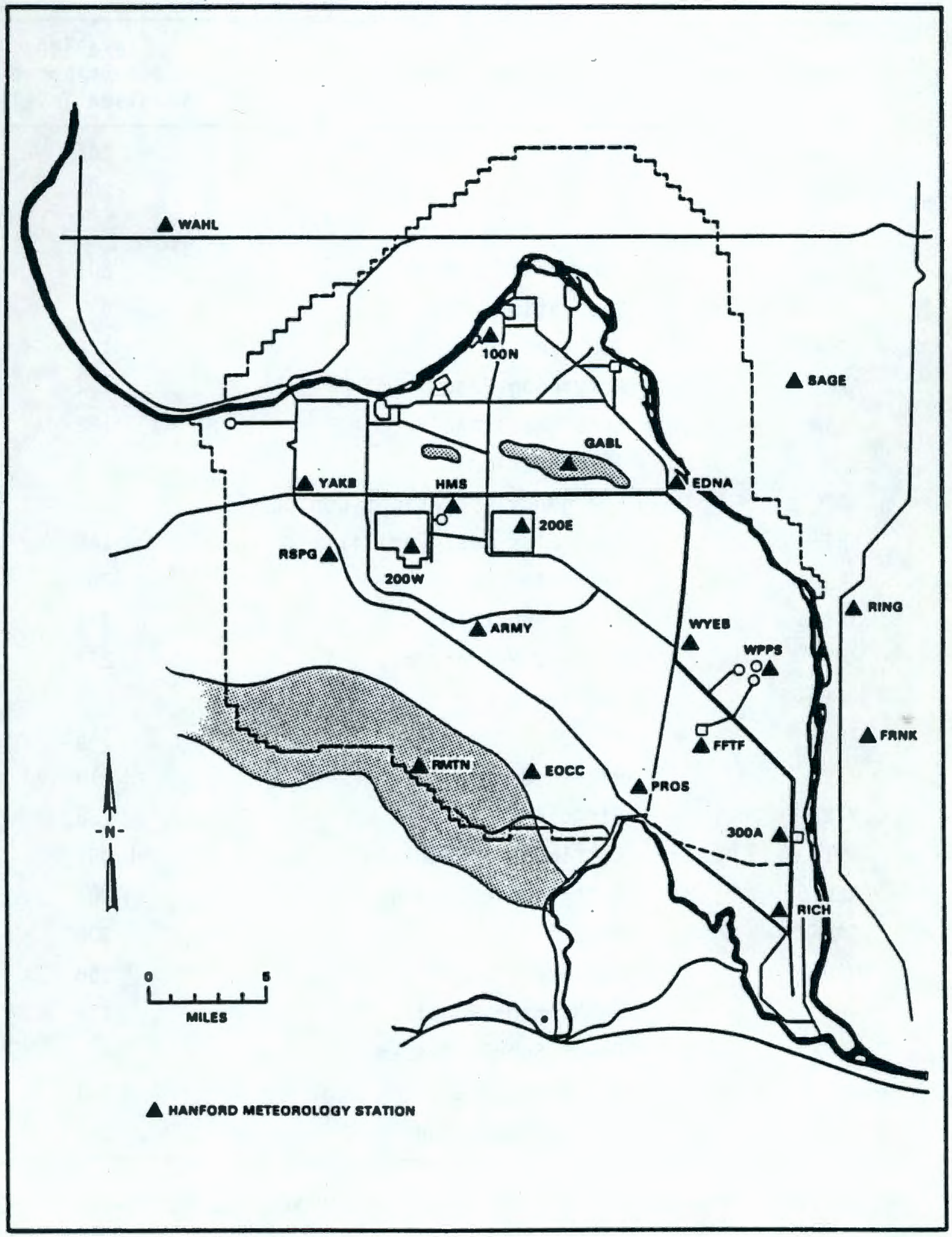

Figure 6a. Index Map of Stations in the Hanford Wind Monitoring Network (HWMN) (Glantz et al. 1990)

Abbreviation	Station name	Elevation (meters above mean sea level)
100N	100N Reactor Area	146
200E	200 East Chemical Separations Area	204
200W	200 West Chemical Separations Area	201
300A	300 Area	122
ARMY	Army Loop Road	172
EDNA	Edna (Railroad Intersection)	122
EOCC	Emergency Operations Center	378
FFTF	Fast Flux Test Facility	168
FRNK	Franklin County	268
GABL	Gable Mountain	331
HMS	Hanford Meteorology Station	222
PROS	Prosser	146
RICH	Richland	119
RING	Ringold	189
RMTN	Rattlesnake Mountain	1,087
RSPG	Rattlesnake Springs	207
SAGE	Sagehill	300
WAHL	Wahluke Slope	258
WPPS	Washington Public Power Supply System	137
WYEB	Wye Barricade	168
YAKB	Yakima Barricade	242

Figure 6b. Abbreviations for Stations in the Hanford Wind Monitoring Network (HWMN) (Glantz et al. 1990)

Both Stone et al. (1983) and Glantz et al. (1990) observed that the airflow at each of HWMN stations differs because of local and regional terrain effects (e.g., Gable Mountain, Rattlesnake Mountain, Columbia River valley, White Bluffs). These terrain effects made and make assessment of an 'average' wind at the Site very difficult. As an added complication, only the HMS has acquired anemometer data continuously (with one minor exception) since Hanford was established. Other stations in the HWMN have much less continuous anemometer records Glantz et al. 1990. Nevertheless, their work demonstrates that the strongest winds at the Site occur during the spring and early summer.

The preliminary estimates of effective sand transport made by Glantz et al. 1990 identified distinctive airflow patterns for a: 1) cool-season, 2) warm-season, 3) cool to warm season transition, and 4) warm to cool season transition. Cool-season winds occur during November, December, January, and February) and are dominantly from the SW; warm season winds occur during May, June, July, and part of August, and are dominantly from the NW (Figures 7 and 8). Transitional winds shift from dominantly SW to NW during March and April and from dominantly NW to SW during September and October.

HWMN stations located in the northwest portion of the Site (e.g., 200-West Area, 200-East Area, Yakima Barricade, HMS) had different relative strengths and tended to be more NW-dominated than stations in the southeastern portion of the Site (FFTF, Wye Barricade, Prosser). For this reason, Glantz et al. (1990) do not believe the HMS long-term wind record is as representative of Sitewide airflow tendencies as the combined wind record from other stations in the HWMN. However, because their assessment of onsite airflow is based primarily on twenty short-term (less than 6 years) anemometer records from other HWMN stations, it is not clear how truly representative their database is of long-term airflow at the Site. With this in mind, and because a complete evaluation of all data from the rest of the HWMN stations is beyond the scope of this year's work, the calculations of effective sandflow and sand dune migration (described in later sections) are based on 25 years of anemometer data from the 15.25 m (50 ft) level of the HMS (Table 1). Note: Subsequent work on this project will incorporate additional NWMN anemometer data into calculations of predicted sandflow and sand dune migration.

Holocene Paleoclimate of the Columbia Basin

The relationship between eolian sand dune activity, airflow character, and paleoclimates in the Columbia Basin, Washington including the Hanford Site is not well known. Fortunately, the paleoclimate for this region is known in some detail from investigations of other proxy climate indicators. Chatters[a] has synthesized the paleoclimate of the Columbia Basin for the last approximately 10,000 yr by incorporating details from reports on the timing of glacial and alluvial geomorphology, rockfall frequencies in caves and rock shelters, timberline fluctuations, eolian sedimentation rates in caves and lakes, palynology, vertebrate and invertebrates paleontology, and archaeology.

Chatters[a] surmised that paleoclimates in the Columbia Basin during the last approximately 10,000 years have been characterized by fluctuating seasonal temperatures and levels of effective moisture. He reasoned that hot summers, cold, long winters, and wet springs affected the region from ca. 10000 to 8000 yr B.P. Between ca. 8000 and 5500 yr B.P the region experienced the driest and possibly warmest episode of the Holocene; eolian activity in the Columbia Basin may have reached a maximum during this climatic interval.[a] Chatters[a] further surmised that effective moisture in the Basin increased from ca. 5500 to 2400 yr B.P. Following ca. 2400 yr B.P. the climate became temporarily warmer and drier; but this gave way to our modern climate by approximately ca. 2000 yr B.P. This modern climate has been maintained excepted for a cooler and relatively more moist interval from ca. 750 to <100 yr B.P.[a]

(a) Chatters, J. C. 1990. "Paleoecology and Paleoclimates of the Columbia Basin Region: Article for Review by the Defense Waste Barrier Program." Pacific Northwest Laboratory, Richland, WA.

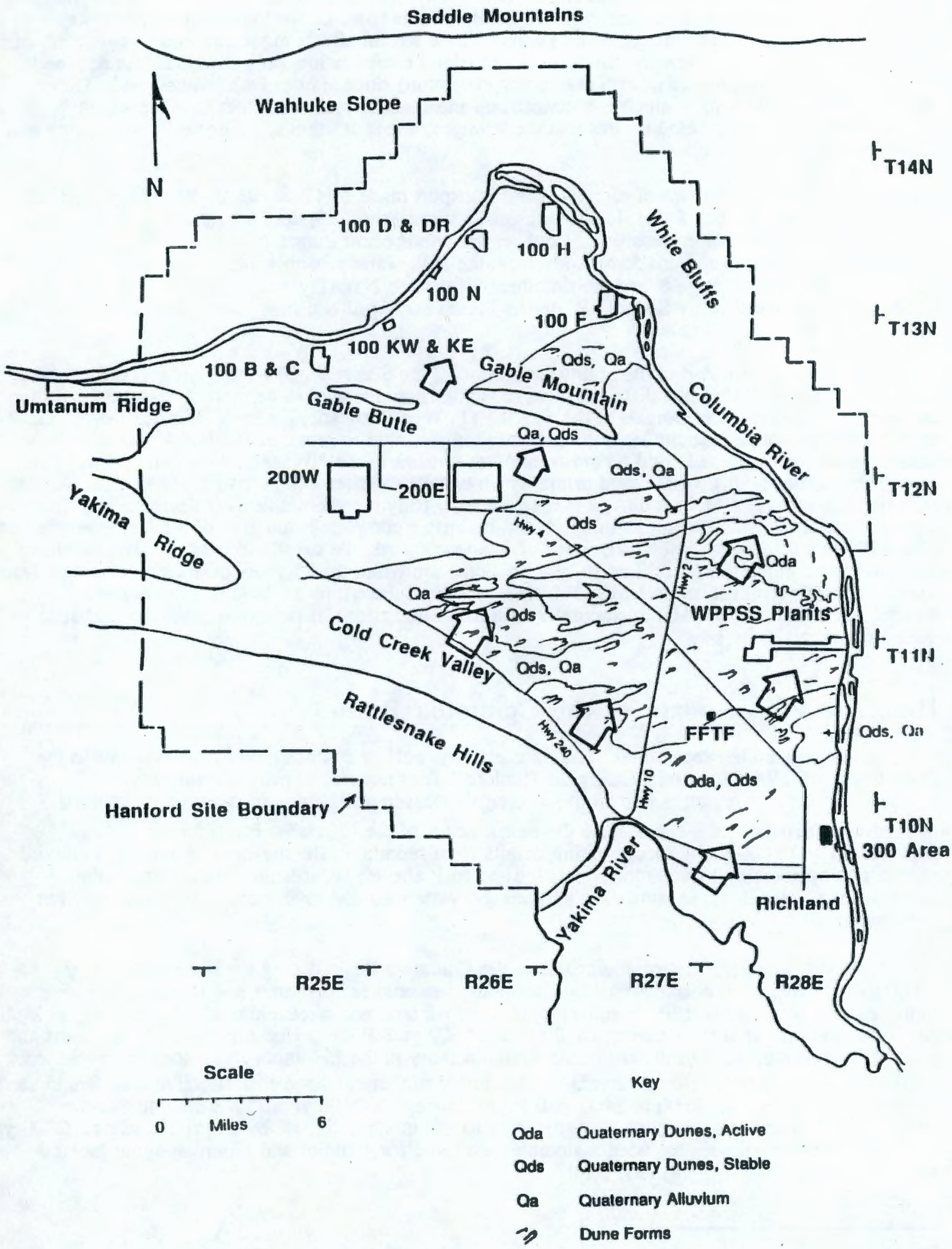

Figure 7. General Cool Season Airflow Over the Hanford Site (relative size of arrows proportional to available wind energy) (Glantz et al. 1990) Overlain on General Geomorphic Map of Eolian Features

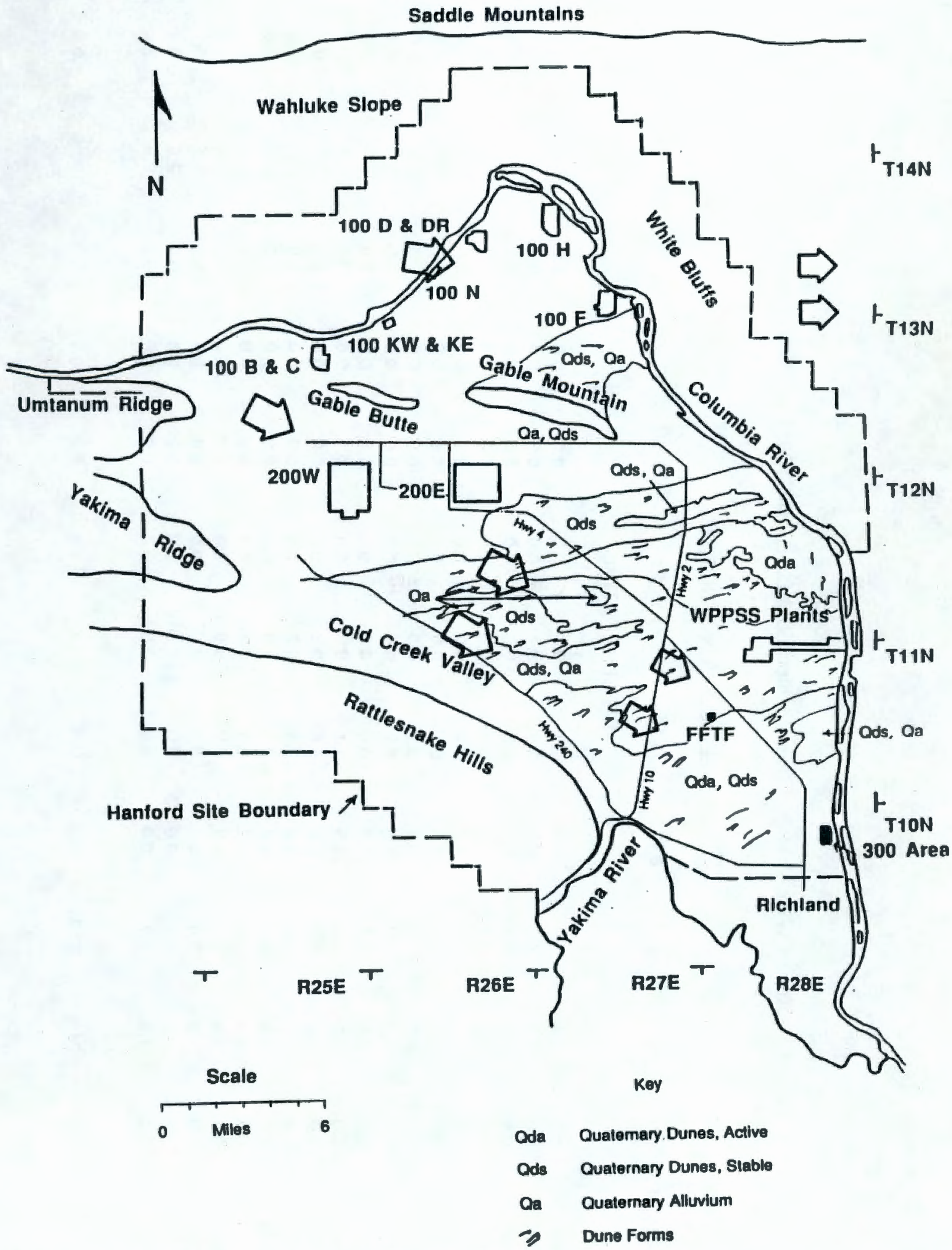

Figure 8. General Warm Season Airflow Over the Hanford Site (relative size of arrows proportional to available wind energy) (Glantz et al. 1990) Overlain on General Geomorphic Map of Eolian Features

Table 1. Annual Wind Velocity Classes in mph, 50-ft Level, HMS, 1955 to 1980 (Stone et al. 1983)

	SPEED CLASS OF WINDS (MPH)										
DIRECTION	0	1 - 3	4 - 7	8 - 12	13 - 18	19 - 24	25 - 31	32 - 38	39 - 46	> 46	TOTAL	AV. SPEED
	PERCENT OF TIME											
NNE	0.0	1.4	1.4	0.6	0.3	0.1	0.0	0.0	0.0	0.0	3.7	5.7
NE	0.0	1.4	1.2	0.3	0.2	0.1	0.0	0.0	0.0	0.0	3.2	5.1
ENE	0.0	1.0	0.9	0.2	0.0	0.0	0.0	0.0	0.0	0.0	2.1	4.3
E	0.0	1.2	1.1	0.2	0.0	0.0	0.0	0.0	0.0	0.0	2.6	4.1
ESE	0.0	1.1	1.2	0.2	0.0	0.0	0.0	0.0	0.0	0.0	2.6	4.2
SE	0.0	1.5	1.6	0.4	0.1	0.0	0.0	0.0	0.0	0.0	3.6	4.5
SSE	0.0	0.9	1.2	0.5	0.1	0.0	0.0	0.0	0.0	0.0	2.8	5.6
S	0.0	1.0	1.3	0.5	0.2	0.1	0.0	0.0	0.0	0.0	3.3	6.4
SSW	0.0	0.8	1.3	0.7	0.6	0.3	0.1	0.0	0.0	0.0	4.0	9.4
SW	0.0	0.9	1.9	1.5	1.4	0.8	0.3	0.1	0.0	0.0	6.8	11.1
WSW	0.0	0.9	2.5	2.8	1.6	0.6	0.2	0.0	0.0	0.0	8.5	9.9
W	0.0	1.3	4.1	3.6	1.1	0.2	0.0	0.0	0.0	0.0	10.3	7.9
WNW	0.0	1.3	4.3	6.2	2.9	1.0	0.1	0.0	0.0	0.0	15.8	9.8
NW	0.0	1.7	4.7	5.2	2.8	1.2	0.2	0.0	0.0	0.0	15.8	9.8
NNW	0.0	1.5	2.5	0.9	0.2	0.0	0.0	0.0	0.0	0.0	5.2	5.5
N	0.0	1.8	2.0	0.7	0.2	0.0	0.0	0.0	0.0	0.0	4.7	5.1
CALM	2.5	0.0	0.0	0.0	0.0	0.0	0.0	0.0	0.0	0.0	2.5	0.0
VAR	0.0	1.9	0.7	0.0	0.0	0.0	0.0	0.0	0.0	0.0	2.5	2.6
TOTAL	2.5	21.8	33.8	24.6	11.6	4.4	1.2	0.2	0.0	0.0	100.0	8.0

Geomorphology and Sedimentology

Geomorphology

Overview

The Hanford Site is blanketed by eolian deposits and deflationary surfaces reflecting Holocene and possibly late Pleistocene eolian activity (Figures 9 and 10). Sand dunes are the most obvious and abundant eolian accumulations and are confined primarily to the lower elevations of the Site. Four primary eolian and eolian-alluvial map units are identified as part of the preliminary assessment of onsite eolian morphology (Figure 9). These are: 1) wind scoured alluvium and bedrock with subordinate eolian deposits (Qa), 2) stabilized dune sand and subordinate alluvium (Qds), 3) mixed stabilized dune sand and alluvium (Qds & Qa), and 4) active dune sand (Qda).

Wind-Scoured Alluvium and Bedrock (Qa)

Approximately 10% of the mapped area falls within eolian subtype Qa (Figures 9 and 10). Qa is characterized by wind-scoured basalt bedrock and polished alluvial gravels (primarily of the Hanford formation) and is concentrated north of the 200-West and 200-East areas and along the lower (northern) flanks of the Rattlesnake Hills. Alluvial gravels are commonly pebble- to cobble-sized, but range from granules to boulders and comprise flat to broadly undulating, hard-packed surfaces. Eolian deposits in Qa are usually less than a few centimeters thick, are composed of silt and sand and cover less than 20% of the surface. In rare cases, Qa eolian sediments have accumulated to thicknesses of a few tens of centimeters in the lee of obstacles such as boulders and vegetation.

Stabilized Dune Sand (Qds)

Approximately 50% of the surface sediments are mapped as Qds, 3 to 10 m thick accumulations of stabilized dune sand intermixed with minor amounts of alluvium (Figures 9 and 10). Sand dunes within the Qds are composed predominantly parabolic dunes of deflation (terminology of Melton 1940); parabolic dunes of accumulation (Melton 1940) and blowout dunes comprise the remainder of the dunes of this map unit. Stabilized parabolic sand dunes have characteristic hairpin shapes whose parallel limbs (ridges) open upwind and close downwind (Figure 11). The stabilized limbs of these dunes commonly are elongated and roughly parallel to the prevailing sand-moving winds (generally from the NW, WSW, SW at the Hanford Site). Stabilized sand dune limbs may extend from 100s to 1000s of meters upwind from stabilized noses or, where the noses have been deflated, may stand alone as isolated ridges. Local relief between dune and interdune areas commonly is 3 to 10 m. Dunes have been stabilized by a variety of xerophytic vegetation including sages and grasses. In general, the surface cover ('soils') of these stabilized dune sands are characterized by < 20 cm thick organic and rootlet disturbed zones; these surface covers often are capped by firm, centimeters-thick silty, crusts.

Significant accumulations of Qds occur along two dominant tracts (Figure 9). The northern concentration of Qds extends along an irregular 4 to 10 km wide, 22 km long, northeast-trending tract extending from near the Dry Creek-Cold Creek junction to a large area of active dunes immediately northeast of the Wye Barricade. The southern concentration of stabilized dunes occurs along an irregular northeast-trending, 4 to 12 km wide tract centered on the Yakima River 'horn' and extending to the Columbia River from south of WPPSS to approximately the 300 Area. Sand dune accumulations in the northern tract are thickest north and east of Highway 4. Sand dunes in the southern tract have attained their maximum thicknesses along an approximately 4 to 6 km wide swath between the Yakima River 'horn' and the FFTF.

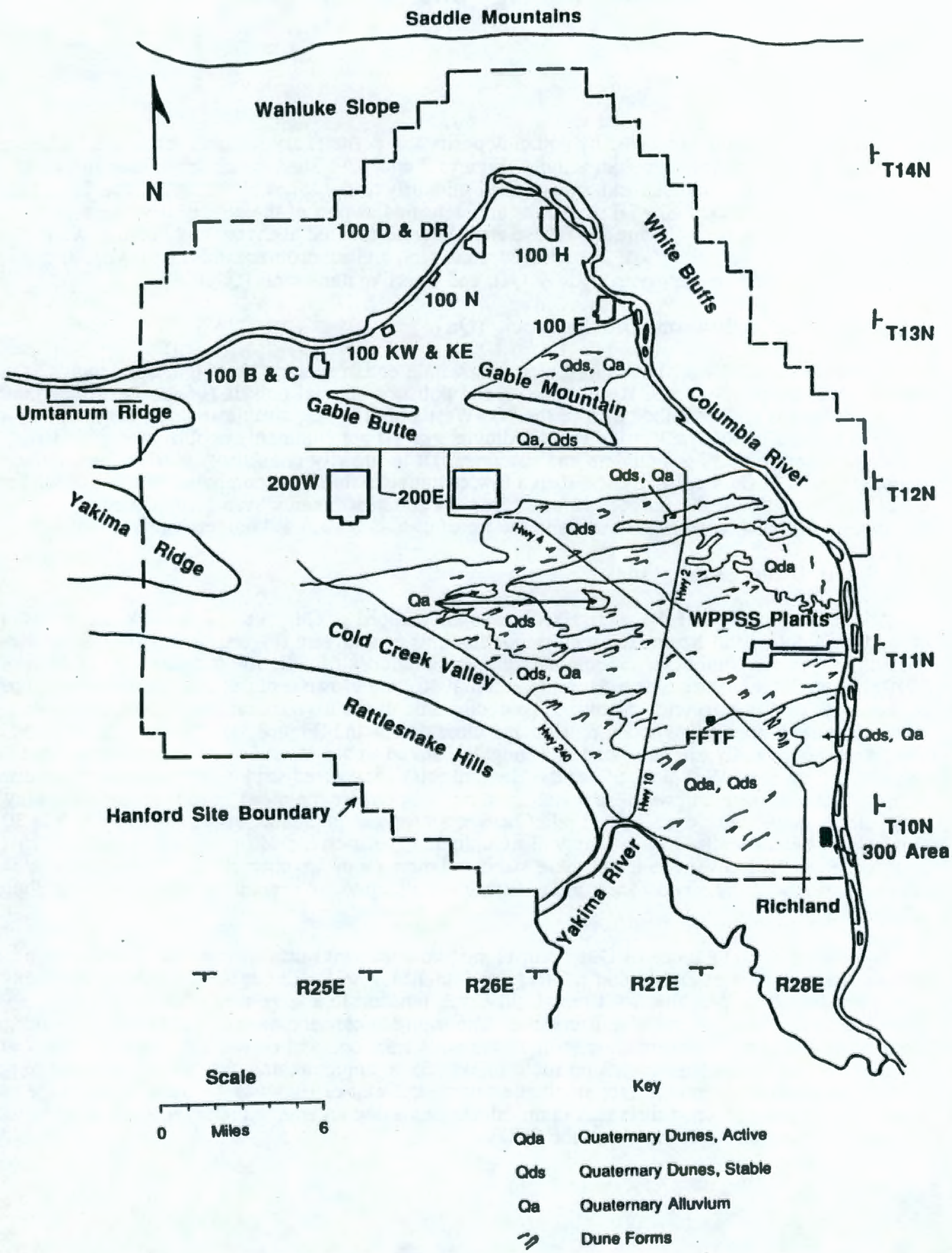

Figure 9. Map of Eolian and Alluvial Map Units Used in 1990 Field Studies at the Hanford Site

Figure 10. High Altitude Air Photo of Northeastern Portion of Hanford Site. Note Qda (active sand dune), Qds (stabilized sand dune), Qa (alluvium), and mixed Qa, Qds mapped areas, scale 1:110,000.

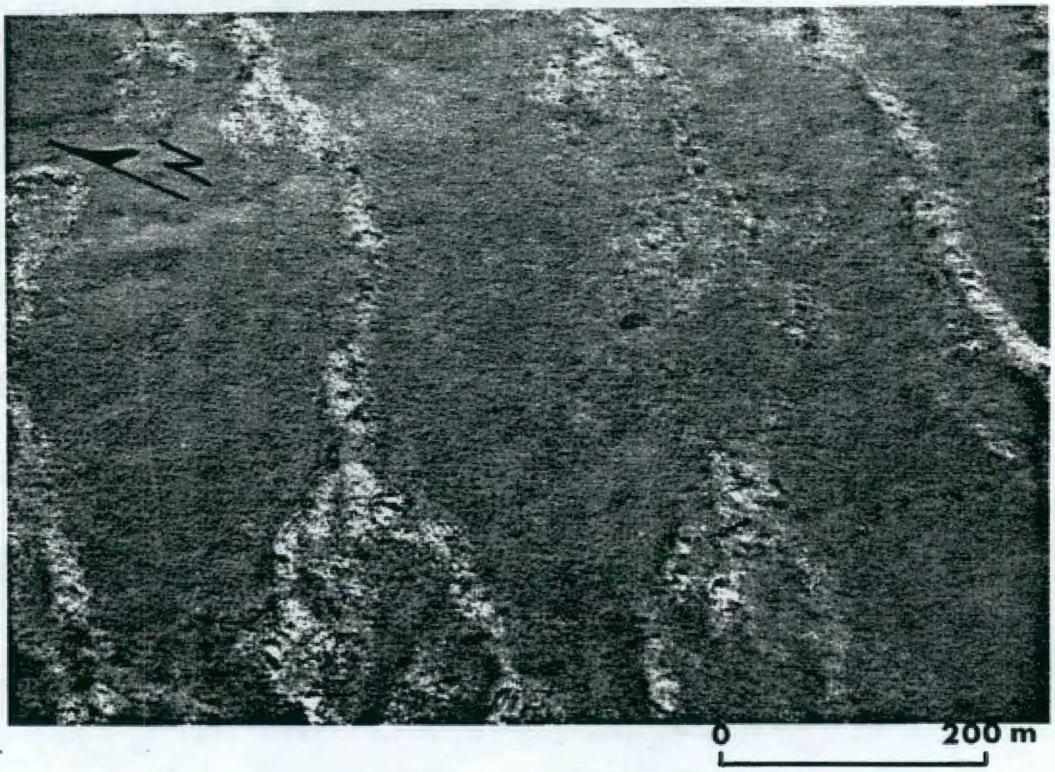

Figure 11. Parabolic Dune of Accumulation South of Main Concentration of Active Dunes. Migration was from SW-NE (bottom to top of August 1987 oblique air photo).

Mixed Stabilized Dune Sand and Alluvium (Qds, Qa)

Approximately 30% of the surface sediments are mapped as mixed Qds & Qa; 1 to 3 m thick accumulations of stabilized dune sand are intermixed with wind-blown and scoured alluvium (Figures 9 and 10). Qds and Qa are concentrated in irregularly elongated areas that roughly trend SW-NE. Sand dunes within the Qds and Qa are primarily parabolic dunes of accumulation (Melton 1940); parabolic dunes of deflation and blowout dunes are subordinate. Stabilized parabolic sand dunes in this map unit have characteristic hairpin shaped limbs (ridges) as discussed in the previous section (Figure 11). The stabilized limbs of these dunes commonly are elongated and roughly parallel to the prevailing sand-moving winds (generally from the NW, WSW, SW at the Hanford Site). Stabilized sand dune limbs commonly extend from 100s to 1000s of meters upwind from stabilized noses or, where the noses have been deflated, stand alone as isolated ridges. Local relief between dune and interdune areas commonly is 1 to 3 m.

Alluvium comprises 50 to 70% of the mapped Qds and Qa. Qa is characterized by wind-blown and sand-polished alluvial gravels (primarily of the Hanford formation). Alluvium is composed of hard-packed clayey, silty, sandy gravels; gravels are commonly granule- to pebble-sized. Sand dunes and alluvium have been colonized by a variety of xerophytic vegetation including sages and grasses. In general, the surface cover ('soils') on these sediments are characterized by < 20 cm thick organic and rootlet disturbed zones; typically these surface covers often are capped by firm, centimeters-thick silty, crusts.

Active Dune Sand (Qda)

Active dune sands (Qda) comprise approximately 10% of the map area and are concentrated in an approximately 25 square km area immediately north of WPPSS and across the Columbia River from Ringold Flats (Figures 9 and 10), and locally within stabilized dune areas where the surface vegetation cover has been disturbed. Active sand dune morphologies have changed systematically since the late 1940s, apparently (at least in part) due to changes in the amounts and timing of precipitation. At various times from 1948 to 1988 (as discerned primarily from vertical and oblique air photos), active dune types have included barchan, barchanoid ridge, transverse, parabolic, blowout, and various compound dunes (Figure 12). For a review of dune classification and their relation to airflow, the reader is referred to McKee (1979). Morphologies in the main concentration of active dunes generally reflect southwest to northeast transport. Most actively migrating dunes possess angle-of-repose slipfaces (Figure 13). However, dunes near the center and along the northern periphery of the active dunes reflect more bidirectional winds with a significant component of northwest-southeast eolian transport indicated.

Air Photo Interpretation of Active Dunes

Thirty six arbitrarily chosen active sand dunes from the southern margin of the large concentration of active dunes were located precisely for comparison and calculation of migration rates using a PGII Stereoplotter (housed at the University of Wyoming). These dunes migrated from approximately 2.5 to 4.5 m/yr during the 29-year period 1948 to 1987 (Figure 14). Dune heights were also measured using the PGII to an accuracy of ± 2 ft for 1948, 1977, and 1987. Areas of the dunes were measured using an automatic planimeter function on the Map and Image Processing System (MIPS) at the University of Wyoming. These area computations together with height measurements permitted dune volumes to be calculated; these revealed an approximately 26% decrease in total volume of active sand dunes (from 708,000 to 520,000 cubic feet) over this same 29-year period (Figures 15, 16, and 17; Table 2). Average dune heights for these thirty-six dunes ranged from 8.2 m in 1948 to 9.4 m in 1977 and 7.9 m in 1987 (Table 2).

Figure 12. Oblique Air Photo of 10 to 20 m High Active Sand Dunes That are Migrating NE (toward the Columbia River), August 1987. Dunes are dominantly parabolic but include complex barchanoid and transverse forms at the extreme left of photo. View looking NNE.

Figure 13. **Angle-of-Repose Slipface of Active Parabolic Dune, July 1990**

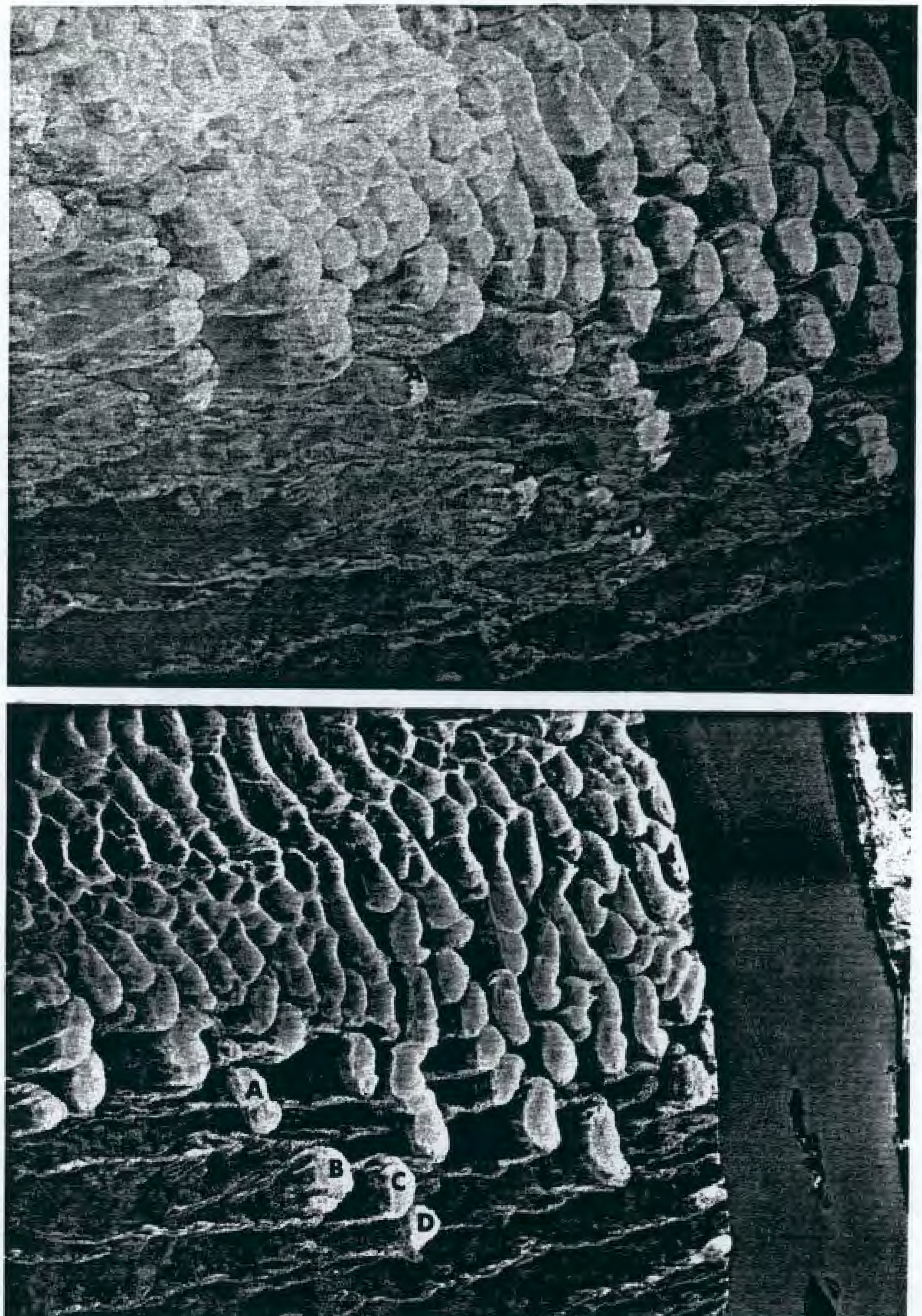

Figure 14. Comparison of Active Dunes From 1948 (bottom) and 1987 (top) Air Photos. Note changes in reference dunes A, B, C, and D. Dune types from both years include parabolic, barchan, barchanoid, and transverse dunes.

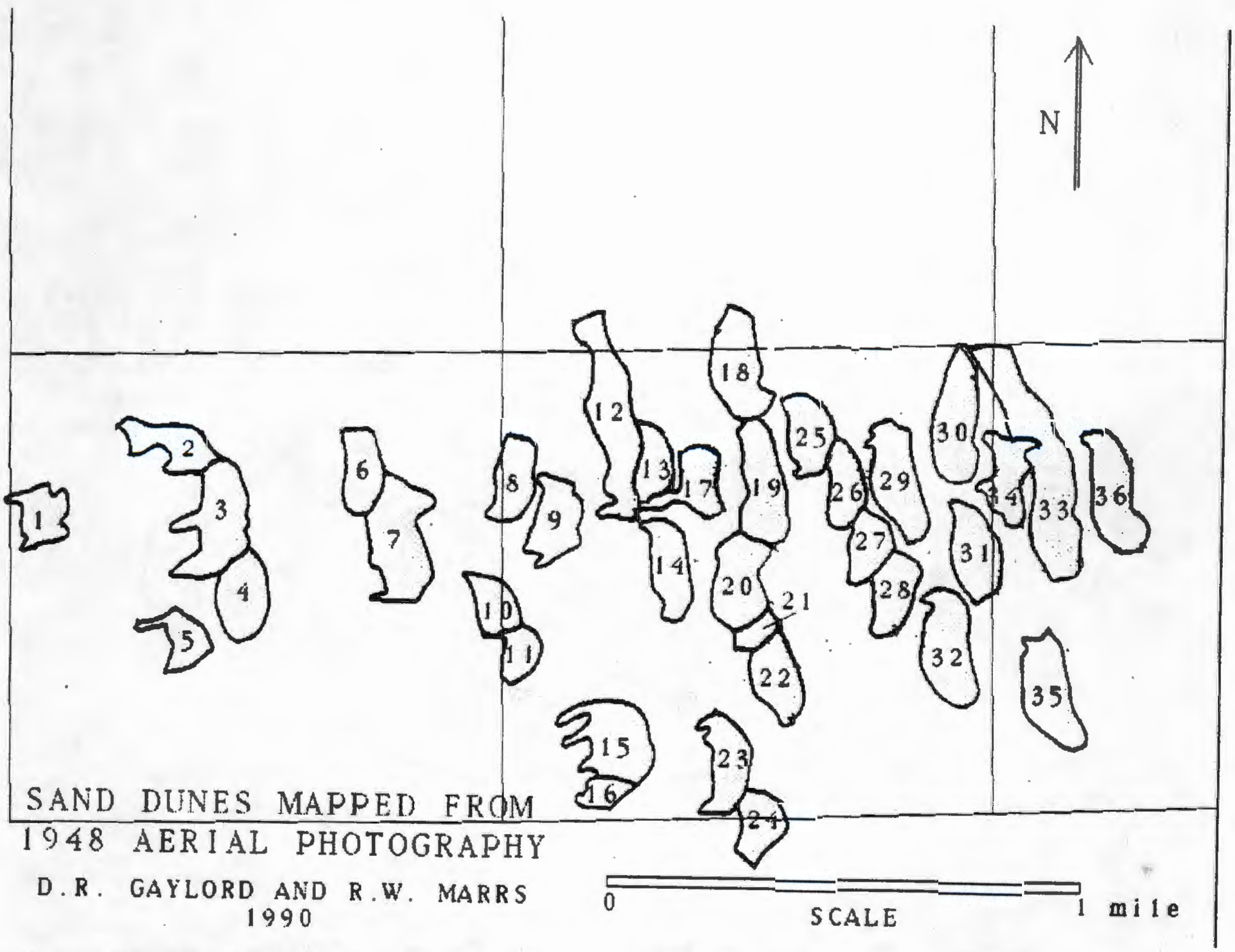

Figure 15. Outline Map of Active Sand Dunes in June 1948 Compiled From PGII Stereoplotter and Highlighted by Map and Image Processing System (MIPS). Dune numbers correspond to those listed in Table 2.

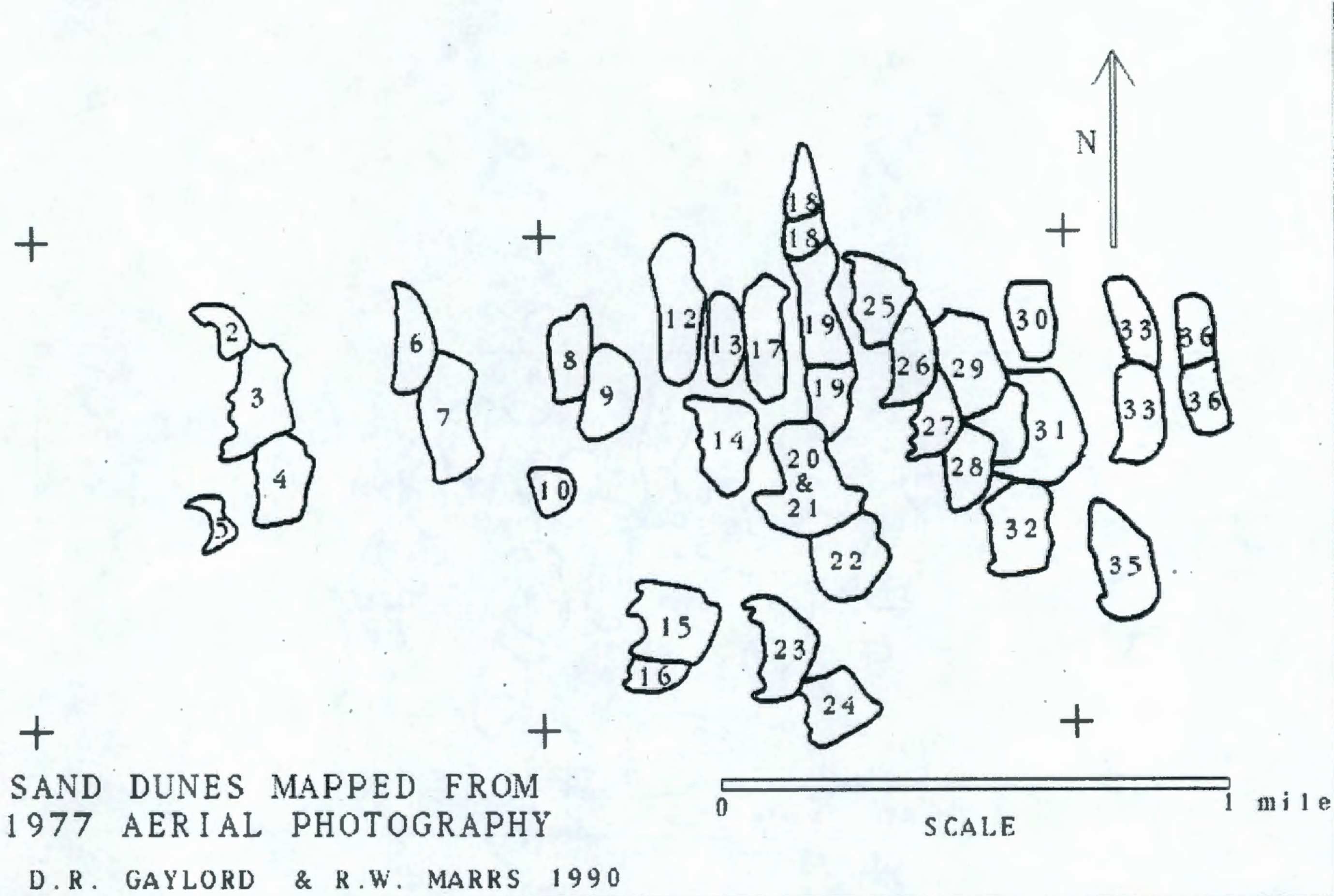

Figure 16. Outline Map of Active Sand Dunes in July 1977 Compiled From PGII Stereoplotter and Highlighted by Map and Image Processing System (MIPS). Dune numbers correspond to those listed in Table 2.

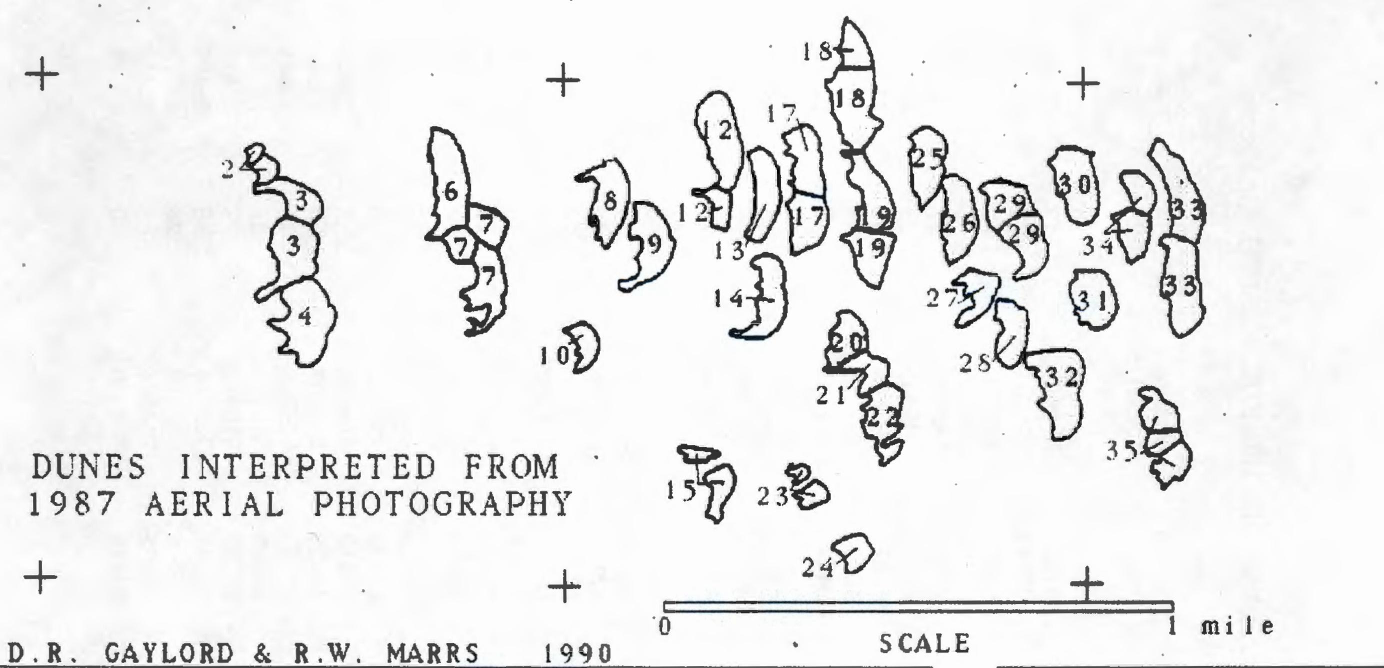

Figure 17. **Outline Map of Active Sand Dunes in May 1987 Compiled From PGII Stereoplotter and Highlighted by Map and Image Processing System (MIPS). Dune numbers correspond to those listed in Table 2.**

Table 2. Sand Dune Measurements From Analysis of 1948, 1977, and 1987 Air Photos

Dune #	1948 Height (ft)	1948 Area (sq.ft.)	1948 Volume (cu.ft.)	1977 Height (ft)	1977 Area (sq.ft.)	1977 Volume (cu.ft.)	1987 Height (ft)	1987 Area (sq.ft.)	1987 Volume (cu.ft.)
1	23.5	41541	488107	0.0	0	0	0	0	0
2	19.0	54964	522158	24.5	31019	379983	12	22414	134484
3	35.0	68388	1196790	34.0	60043	1020731	26.5	72846	965210
4	30.5	40815	622429	31.0	42629	660750	29.5	46754	689622
5	18.0	42992	386928	23.0	31382	360893	0	0	0
6	19.5	39001	380260	26.0	42992	558896	27	44302	598077
7	53.5	64397	1722620	53.0	56053	1485405	28	84578	1184092
8	29.5	39727	585973	42.0	37913	796165	21.5	41151	442373
9	34.5	48071	829225	37.0	40922	757063	27.5	43602	599528
10	22.0	31745	349195	22.0	24482	269301	15	22589	169418
11	24.5	27754	339987	0.0	0	0	0	0	0
12	14.0	94509	661563	25.0	55576	694696	27.5	58837	809009
13	8.0	39727	158908	23.0	33774	388404	23.5	34847	409452
14	26.0	44080	573040	29.0	48428	702202	25	42902	536275
15	28.0	70202	982828	21.5	53789	578229	20	36773	367730
16	20.0	25215	252150	20.0	26269	262689	0	0	0
17	37.0	51699	956432	37.0	48428	895912	25	63740	796750
18	41.5	52787	1095330	40.0	52180	1043608	24	58837	706044
19	25.5	53150	677663	22.0	88886	977746	22	67592	743512
20	18.5	71834	664465	45.0	66655	1499740	28.5	51482	733619
21	12.5	47345	295906	0.0	0	0	19	42202	400919
22	23.5	51699	607463	27.5	53789	739595	25	24515	306438
23	26.0	37187	483431	18.0	44139	397250	26.5	20488	271466
24	20.5	41903	429506	36.0	53431	961763	32.5	33096	537810
25	26.5	40452	535989	20.0	43782	437815	28	35547	497658
26	17.5	34285	299994	26.0	40922	531990	40	33096	661920
27	31.0	40815	632633	34.0	35919	610618	33.5	29243	489820
28	25.5	54239	691547	36.0	48428	871699	26.5	60588	802791
29	34.0	58955	1002235	35.5	33059	586806	40.5	33446	677282
30	21.0	44080	462840	31.0	62366	966678	38	28543	542317
31	22.0	56053	616583	42.0	46998	986960	28	43602	610428
32	43.0	123896	2663764	31.5	82917	1305940	28.5	85103	1212718
33	14.5	71290	516853	0.0	0	0	26	43778	569114
34	23.0	54601	627912	29.0	52002	754025	22.5	60413	679646
35	51.5	56415	1452686	0.0	63975	0	0	0	0

Sedimentology

Grain Size Analyses of Eolian Sediment

Eolian sediments were sampled from ninety-seven locations across the Hanford Site including the hand-dug pit stratigraphy sites. Samples were collected from depths of 60 to 70 cm below the surface at all sites (Figure 18). Sieve analyses using the method outlined by Ingram (1971) from forty-eight sample sites were used to generate the mean grain size distribution contour map presented in Figure 19. Mean grain sizes of eolian (primarily dune) sediments are dominantly in the fine to medium sand range. As can be seen in the mean grain size distribution map, eolian sediments generally fine downwind (towards the east and northeast). Sorting also improves downwind. A more complete description of textural trends is included in the 'Provenance' section.

Soil Development on the Hanford Site

Soil development on eolian deposits (Qds & Qda) at the Hanford Site generally is weak to nonexistent. Many stabilized sand dunes (Qds) have weak concentrations of carbonate cement (often on the undersides of grains) which are consistent with aridisols; but this apparent pedogenic feature lacks any physical soil structure. Deposits of Qa (with subordinate, thin eolian detritus), especially those with > 20 % silt and clay, often display more convincing characteristics of soil development. Typically, these sediments display distinct concentrations of organic matter in the upper 5 cm (A-horizon). In turn, the A-horizon is underlain by an orange-stained, 20 to 35 cm thick cambic (Bw) horizon. The cambic horizon grades down into a 35 to 40 cm thick carbonate-rich horizon, which overlies unweathered parent material. It must be noted that no single facet of these near surface sediments necessarily identifies them as soils. However, the sequence of organic-rich A horizon, Cambic Bw horizon, carbonate-rich Bk horizon and unweathered parent material is consistent with aridisol development (Soil Survey Staff 1988).

Eolian Stratigraphy and Sand Dune Chronology

Test Pits

Twenty-nine 1.0 to 1.2 m deep hand-dug test pits were excavated to observe, describe, and interpret the stratigraphy and sedimentology of eolian deposits [Figures 18, 20, and 21a-t (Appendix B)]. Most test pits are located on 2-mile grid centers, though in a few areas (such as surrounding the bison kill site north of the Wye Barricade) pits were located on half- and/or quarter-mile centers. Detailed descriptions from twenty representative pit stratigraphies are included in Appendix B. Note: Interpretations of the bison kill site stratigraphies and sediment samples are still ongoing and are not presented here. Pit walls from these hand-dug trenches were sketched, orientations of primary sedimentary structures measured, and strata sampled. Data from each pit were used to reconstruct site-specific depositional and erosional histories.

In general, pits excavations exposed massive to weakly cross-stratified eolian and mixed eolian-alluvial deposits with weak to non-existent surface soils and paleosols. For sands with mean grain sizes < 0.5 mm, the detrital components are: quartz (60 to 65%), followed by basalt (20 to 25%), feldspar (5 to 10%), mica and chert (< 2%), and other accessory minerals and lithic fragments (< 1%). For sands with mean grain sizes > 0.5 mm, the detrital components are: basalt (60 to 65%), followed by quartz (20 to 25%), feldspar (5 to 10%), mica and chert (< 2%), and other accessory minerals and lithic fragments (< 1%).

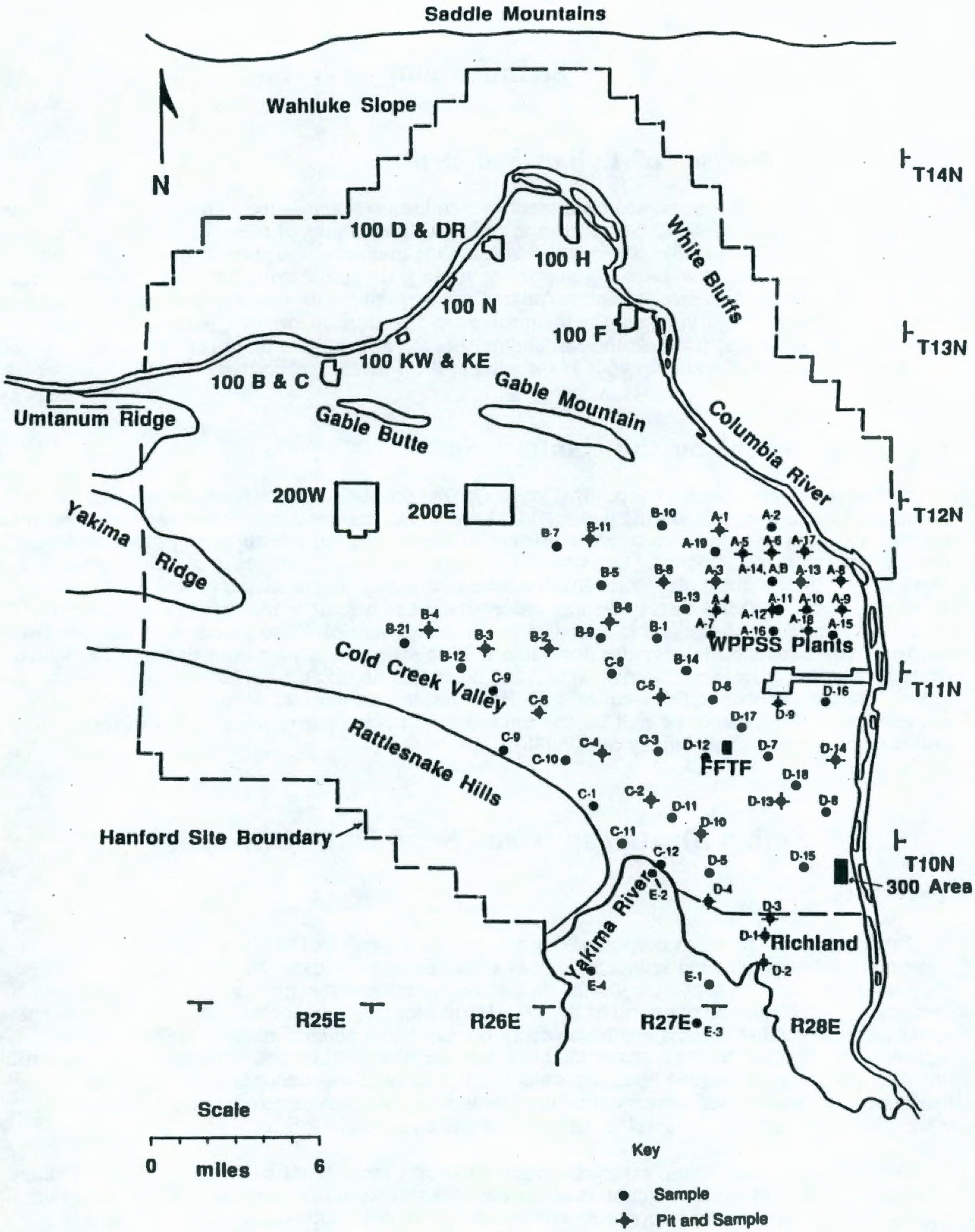

Figure 18. Sample Site and Test Pit Locations for 1990 Field Season

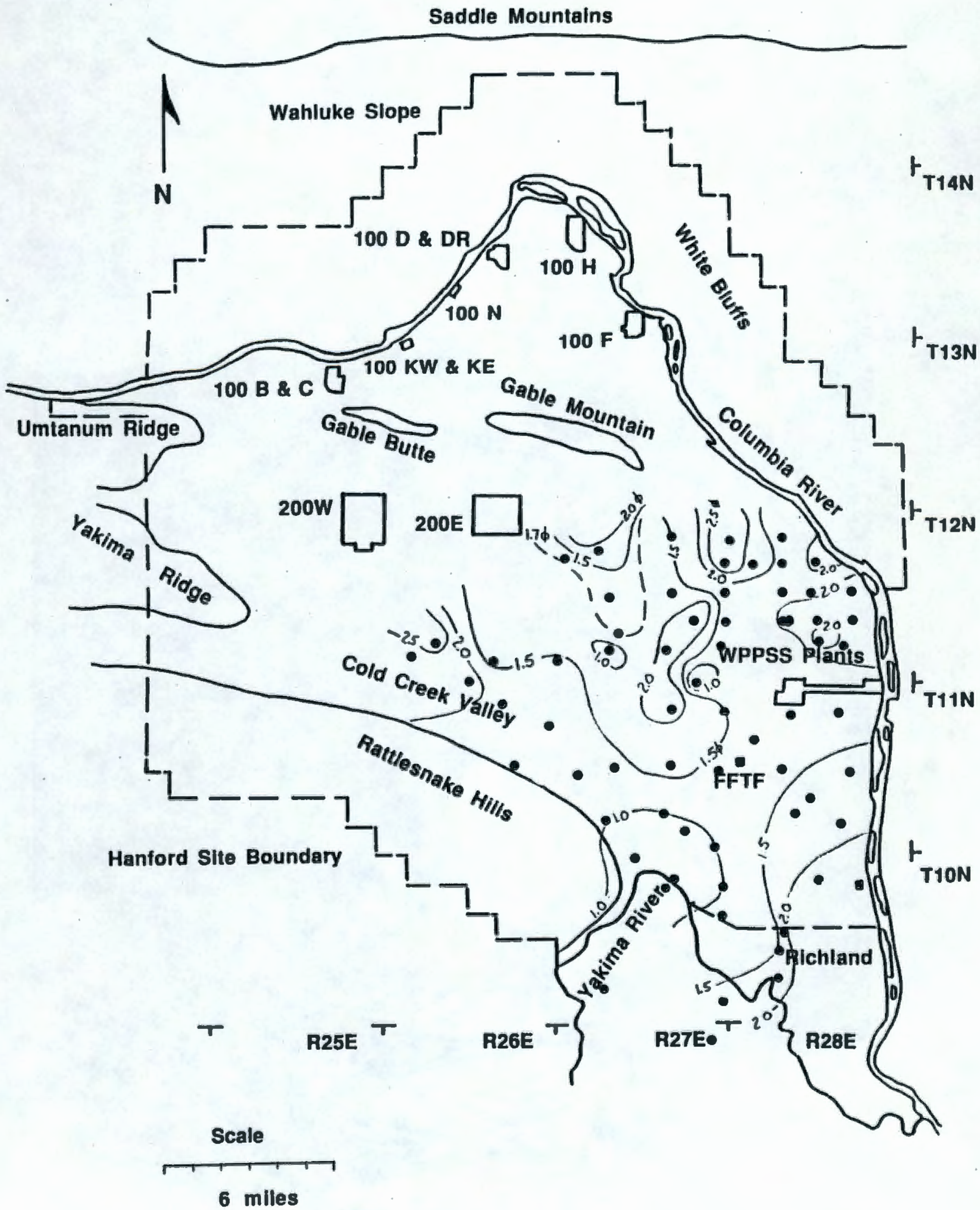

Figure 19. Contour Map of Mean Grain Size [computed using Folk's (1980) graphic mean grains size statistic] for Sand Dune Sediments Collected During 1990 Field Season. Contour interval is 0.5 phi.

Figure 20. Pit Stratigraphy From Site HA-90-13, July 1990. Note high-angle foresets overlain by nearly horizontal subcritically climbing cross-strata in upper one-quarter of pit.

Most pits in eolian sediments were dominated by fine- to medium-grained, poorly to moderately well sorted massive to weakly stratified sand. Paleocurrent roses of foreset attitudes reflect the prevailing modern eastwardly-directed wind (Figure 22). Minor gravels appeared in the eolian sequences primarily as lag concentrates and were identified in strata throughout the area studied. Gravels were particularly common in dune sands located near and/or adjacent to Cold Creek Valley.

Pits in fluvial-dominated sequences are characterized by relatively poorly sorted, fine- to coarse-grained sand and gravelly sand. Sediments from these deposits tended to have better paleosols and/or recent soil development than observed in sand dune strata.

Summary of Depositional Histories from Pit Stratigraphies

The pit stratigraphies within stabilized and active sands record comparable depositional histories (Figure 21a-t). In general, the preponderance of wavy, low-angle cross-strata and inversely-graded, subcritically climbing translatent cross-strata that characterize both recently active and stabilized sand dunes suggest that eolian aggradation occurred under the influence of vegetation and often following the climbing and aggradation of eolian ripples, respectively. The common massive strata suggest rapid deposition from suspension and/or the disruption of stratification by phytoturbation. Calculations of the entrainment velocities necessary to entrain and transport granule and small-pebbles (in excess of 43 mph at 15.2 m height) within eolian dominated deposits suggest that these gravels are relict alluvial, and not primary eolian-derived detritus.

The incipient soils developed at the top of most pits are the only evidence of extensive stabilization and soil formation within approximately a meter of the surface. The apparent youth of the modern surfaces (as evidence by the 'sharpness' of the topographic relief) and the absence of buried soils in the strata examined, suggests that the sediments we studied post-date the Mazama ash (ca. 6700 to 6800 yr B.P.).

Deeper trenches must be excavated to reveal more complete stratigraphic histories of eolian, eolian-fluvial, and fluvial sequences dating back to the Pleistocene. It will be particularly informative to excavate such trenches to depths where marker beds such as the Mazama ash and archaeologically-significant horizons can better constrain the timing of eolian, eolian-fluvial, and fluvial deposits. Thick sand dune deposits between the FFTF and Yakima River 'horn', and west of the main active dunes should be prime targets for backhoe trenching.

Ash and Archaeological Reconnaissance Field Studies

A portion of the summer, 1990 field effort was dedicated to location of chronologically distinct markers including ash beds, archaeological site, and radiocarbon-datable materials within eolian and fluvial deposits. Identification of such chronologically distinctive markers is essential to: 1) the confirmation of OSL age dates (of quartz sand grains), and 2) determination of the timing of eolian/ climatic variations at the Site.

Eolian deposits containing surface exposures of Mazama ash were relatively scarce. A total of five eolian localities and one fluvial locality (along Dry Creek) contain volcanic ash; these were trenched, described, and sampled. Only one archaeological site, the bison kill site (north of the Wye Barricade), was trenched, described, and sampled. Trench stratigraphies from Dry Creek will augment the Site-wide trench studies described in the previous section of this report.

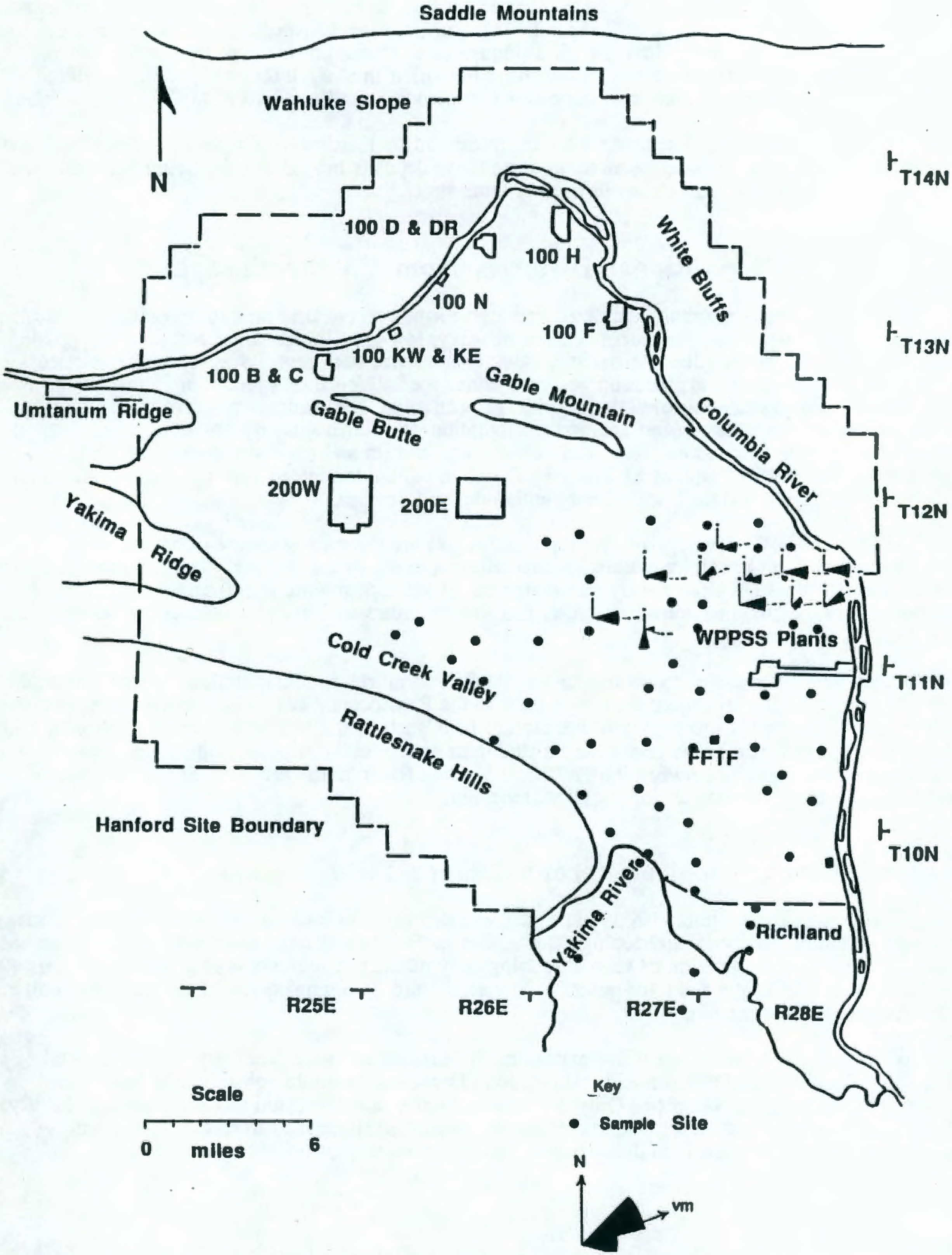

Figure 22. Paleocurrent Roses Indicating Vector Mean Azimuths for 11 Sites (n = 6 to 10). Winds were directed predominantly to E and ENE.

Provenance Investigations

Overview

The provenance of the eolian sediments reflects overall dispersal patterns away from inferred source areas. Three potential source locales were sampled and described including: 1) fluvial sediments exposed along Dry Creek, 2) alluvial sediments weathering out along the northeastern flanks of the Rattlesnake Hills, and 3) alluvial-eolian sediments exposed near the 'horn' of the Yakima River. The Dry Creek area was examined most extensively (Figures 23 and 24). Six, 8 to 11 m thick stratigraphic sections were measured in a sequence containing interstratified alluvium, volcanic ash beds, and paleosols. Eight charcoal samples were collected from these strata and will be used to constrain the sedimentary sequence chronologically.

Sand Dune Textures and Provenance

A limited number of grain size analyses and visual field and laboratory observations have shown that dune sands sampled across the Site suggest distinct downwind variations in both texture and composition. Mean grain size (from sieve analyses) decreases to the northeast from both the Cold Creek Valley and the Yakima River floodplain to the Columbia River (Figure 19). Mean grain sizes of upwind dune sands range from 0.5 to 0.35 mm in diameter (1 to 1.5 Φ) and often contained admixed pebbles; mean grain sizes of downwind dune sands range from 0.28 to 0.25 mm in diameter (1.8 to 2.0 Φ). Sorting also improves downwind. As yet unquantified laboratory observation suggests that sand grains appear to be better rounded downwind. Overall, estimates of dune sand composition vary little across the Site. Quartz predominates and makes up from 60 to 70%, basalt 25 to 30%, feldspars 2 to 4%, and micas and chert approximately 2% of a well-mixed sand containing a full range of grain size. However, the coarsest sands seem to possess the highest percentages of basalt.

Texturally, and compositionally, the sediments exposed along the Cold Creek Valley and the Yakima River most closely match those incorporated in downwind sand dunes. Sediments, paleosols, and ashes exposed along Dry Creek appear to be too fine grained to have been a significant source of dune sediment. Grain counts of heavy (accessory) minerals, light framework minerals, and lithic fragments from both potential source areas and dune sands will shed more light on the ultimate provenance and distribution of the dune sands away from a likely source area(s). Once a source area is established, the question of the type and timing of climatic events that triggered and/or promoted the generation of dune sands in the volumes now found on the Site will have to be addressed.

Eolian Processes and Airflow-Sediment Relations

Introduction

Recent experimental and theoretical treatment of particle entrainment and migration have included stochastic arguments to better portray the complexity of natural eolian activity (e.g., Anderson 1986; Anderson and Hallet 1986). Use of such a stochastic treatment is beyond the scope of this work presently; so, for the purposes of this report, Bagnold's (1941) equations of eolian entrainment, transport, and sand dune migration will be used to approximate, project, and evaluate the modern airflow-surface interactions.

Figure 23. View Looking SW Along Dry Creek Valley. Valley walls are 6 to 10 m high.

Figure 24. Predominantly Alluvial Sediments Exposed Along Valley Walls of Dry Creek. Person in foreground holding meter stick.

Documentation of the mechanics of eolian transport and deposition largely has arisen from studies of sand-sized detritus and sand dunes (Bagnold 1941; Zingg 1953; Horikawa and Shen 1960; Belly 1964; Fryberger 1979). Rates of eolian sediment transport depend primarily upon the duration and strength of the wind above some threshold windspeed necessary to initiate particle movement. The grain size range and amount of sediment transported likewise depend on interactions between a number of variables including the velocity and turbulence of the wind, density and viscosity of the air (temperature dependent), cohesiveness (including moisture content), size, shape, sorting, and density of the sediments, and size, shape, and density of surface roughness features including vegetation, and/or other surface obstructions and topographic features (Bagnold 1941; Chepil 1945; Horikawa and Shen 1960; Goldsmith 1985).

It is very difficult to quantify the effects of all of the above variables on eolian transport in a natural system. As a result, sets of simplified equations often are used to provide insight into the natural system. The most important variables controlling eolian entrainment and transport of sediment (assuming a loose, cohesionless surface) are the velocity gradient, the size of surface roughness features, relative density, grain size, and sorting of the sediments (Bagnold 1941; Zingg 1953; Fryberger 1979). The following discussion introduces the basic equations of entrainment, sandflow, and predicted dune migration. These equations are used to generate the predicted rates of dune migration at and near the Hanford Site using available wind speed data from the HMS.

Eolian Entrainment

Eolian entrainment first begins when the wind reaches a threshold velocity. Bagnold (1941, p. 52) used basic physics and mathematics to demonstrate that the wind velocity (V) at height (z) above a loose sediment surface is closely approximated by:

$$v_z = 5.75\, V_t^* \log \frac{z}{k} \tag{1}$$

where V_z = velocity as measured at some height above the surface.

5.75 = empirically derived constant expressing the proportionality between the change in wind velocity and the log-height.

V_t^* = threshold shear velocity, a velocity acting on the ground surface; (= $\sqrt{\frac{\tau}{\rho}}$); where τ = shear stress, and ρ = fluid density.

z = height at which wind velocity V_z is measured.

k = roughness factor (~ 1/30 mean grain diameter).

Once sediment grains (assume quartz) are ejected from the surface, the great density difference between the grain and the air (~ 2000 times) promotes saltation as the dominant sediment transport mode (~ 75%) (Bagnold 1941). Saltating grains bounce to heights from hundreds to thousands of grain diameters above the surface. The entanglement of these grains in the airstream extracts forward momentum from the wind and thus changes the wind profile above the surface. Bagnold (1941, p. 61, 104), characterized the wind velocity profile during active sediment transport by the following equation:

$$v_z = 5.75\, V_t^* \log \frac{z}{k'} + V_T \tag{2}$$

where V_z = velocity as measured at some height (z) above the surface.

5.75 = empirically derived constant expressing the proportionality between the change in wind velocity and the log-height.

V_t^* = threshold shear velocity (= $\sqrt{\frac{\tau}{\rho}}$); where τ = shear stress, and ρ = fluid density.

z = height at which wind velocity is measured.

k' = roughness factor (~ 1/30 bounce height of saltating grains).

V_T'= impact threshold velocity measured at a height of k' **

** Note: Values for k' and V_t' have been measured in wind tunnel experiments (e.g., Zingg 1953).

Example 1:

The following example calculates the wind velocity (v) that must be registered at a height of 15.2 m (50 ft) above the surface during saltation transport of a 0.027 cm diameter sand grain. The height of 15.2 m is chosen because it is the height from which the anemometer data used in Table 1 was taken. The grain size is the mean size determined from sieve analyses of actively migrating dune sand.

To proceed, we use equation 2:

$$V_{(15.2\text{ m})} = 5.75\, V_t^* \log \frac{z}{k'} + V_T' \qquad (2)$$

where $V_{(15.2\text{ m})}$ = velocity at 15.2 m (1520 cm).

5.75 = empirically derived constant expressing the proportionality between the change in wind velocity and the log-height.

V_t^* = impact threshold velocity (~ 19.2 cm/sec), (after Bagnold 1941, p. 88).

z = height at which wind velocity is measured = 1520 cm.

k' = roughness factor (~ 1/30 bounce height of saltating grains), = 0.274 cm, (after Zingg 1953).

V_T' = impact threshold velocity measured at a height of k', = 258 cm/sec, (after Zingg 1953).

$$V_{(15.2\text{m})} = (5.75)\ (19.2\text{ cm/sec}) \log \frac{1520\text{ cm}}{0.274\text{ cm}} + 248\text{ cm/sec}$$

$$V_{(15.2\text{m})} = 661\text{ cm/sec}$$

The value 661 cm/sec approximates the minimum velocity that must be recorded at the 15.2 m anemometer level to initiate sand movement on the surface. In subsequent calculations of sand flow rate for the same size sand, this value also will be referred to as V_T'.

Bagnold (1941, p. 204) determined that the rate of advance of a sand dune varies directly to the rate of sand movement over the brink of the dune and inversely to the height of the slipface. More precisely, Bagnold (1941, p. 216-217) derived and tested the following formula to predict the rate of sand dune migration (c):

$$c = \frac{q}{(\gamma)(H)} \tag{3}$$

where c = rate of dune migration

q = rate of sand flow in gms/unit width

γ = bulk density of dune sand (typically between 1.7 and 1.9 gm/cm^3

Bagnold (1941, p. 67) calculated sandflow (q) using the following equation:

$$q = \alpha C \sqrt{\frac{d}{D}}\frac{\rho}{g}(v_z - V_T')^3 \tag{4}$$

where q = rate of sandflow in gm/cm width/sec

α = constant = $\left(\frac{0.174}{\log \frac{z}{k'}}\right)^3$

C = constant = 1.5, for nearly uniform dune sand; 1.8 for naturally graded dune sand; 2.8 for poorly sorted dune sand

d = grain diameter in question (0.027 cm).

D = standard grain diameter of 0.025 cm.

ρ = density of air (1.22×10^{-3} gm/cm^3).

g = gravitational acceleration (981 cm/sec^2).

V_T' = impact threshold velocity at height z for 0.027 cm diameter sand; calculated using equation (2) (see Example 1).

v_z = velocity as measured 1520 cm above the surface (see Example 1).

k' = roughness factor (~ 1/30 bounce height of saltating grains), = 0.274 cm, (after Zingg 1953).

Example 2:

The prediction of sand dune migration depends on incorporation wind data from a meteorological stations into equations (3) and (4). The following example has three parts. In the first part, wind data is interpreted and reduced. Part two incorporates data from pertinent wind speed classes and inputs this data into equation (4). Part three incorporates a total yearly sandflow value (computed from part two) into equation (3). Various solutions of equation (3) [projected sand dune migration rates] are computed using a range of likely dune heights and bulk densities.

Note: The following calculations depend upon the following assumptions: 1) The HMS anemometer data is representative of wind strength and direction since the late Pleistocene, 2) The sand dunes in question were not affected by seasonal moisture or the effects of temperature, 3) The mean grain diameter of 0.27 mm is representative of the dune material transported, and 4) The sand-sized sediments were composed of quartz or quartz-density particles. These assumptions obviously will limit the accuracy of the predicted sand dune migration rates especially given the need for location-specific wind speeds, integration of the retardation of dune migration when sands are wet and/or frozen, of a different size than 0.27 mm, and/or composed of materials other than quartz. Thus, it is important to keep these assumptions in mind when interpreting the data.

Part 1:

Anemometer data from the HMS (Table 1) as compiled by Stone et al. (1983) is used as a first approximation of airflow likely to cause eolian transport at the Hanford Site. As already seen in Example 1, the effective sand-moving winds necessary to maintain transport (as measured at a height of 15.2 m) must reach at least 661 cm/sec (15.0 mph). Thus, any time the wind exceeds 15 mph, dune sands theoretically will migrate. Wind speed data from the HMS are subdivided into ten classes: (0), (1 to 3), (4 to 7), (8 to 12), (13 to 18), (19 to 24), (25 to 31), (32 to 38), (39 to 46), and (>46) mph for 16 different wind direction sectors (i.e., NNE, NE, ENE, etc.) (see Table 1). The total percent of time during a year that the wind blows within a given wind speed class is indicated at the bottom of each column.

Winds in the 13 to 18 mph wind speed class blow approximately 10.6% of the year. However, to compute net sand movement, it is important that countervailing winds be subtracted from the prevailing eastwardly-directed winds; this gives a value of 9.6% of the year. Still, because a 15 mph wind is necessary to transport sand, 13 to 15 mph winds may be ignored. Assuming a linear distribution of these winds, we find that effective sand-moving winds between 15 and 18 mph blow only 5.3% of the year. To facilitate computation, the mean wind speed between 15 and 18 mph (i.e., 16.5 mph) was used. This same method was used to determine the percentage of effective sand-moving winds for the other wind classes and was incorporated into the sandflow (q) calculations shown in Table 3.

Part 2:

In order to calculate the yearly rate of sand flow, it is necessary to solve equation (4) for each wind class and add the values together.

So, substituting appropriate values into:

$$q = \alpha C \sqrt{\frac{d}{D}} \frac{\rho}{g} (v_z - V_T')^3 \qquad (4)$$

we find:

$$= (1.0 \times 10^{-4})(1.8)\sqrt{\frac{0.27}{0.25}}(1.24 \times 10^{-6}(V_z - V_t')^3$$

$$= (2.3 \times 10^{-10})(738 - 661 \text{cm/sec})^3$$

$$= (1.0 \times 10^{-4}) \text{ gm/cm/sec}$$

Because such 15 to 18 mph winds transport sand to the east 5.3% of the year (= 19.3 days), total sandflow = (1.7×10^6 sec/year) x (1.0×10^{-4} gm/cm width/sec) ≅ 167.1 gm/cm width/year. Similar calculations to the above were made using 21.5, 28.0, and 35.0, winds (average values for 19 to 24, 25 to 31, 32 to 38, 39 to 46 mph winds) (Table 3).

Table 3. Total Sandflow Per Year for Representative Wind Speed Classes

MPH	Total Sandflow: gm/cm width/yr
16.5	1.77×10^2
21.5	8.33×10^3
28	1.82×10^4
35	1.08×10^4
Total q	3.75×10^4

Part 3:

Substituting the value for 'Total q' into equation (3),

$$c = \frac{q}{(\gamma)(H)} \tag{3}$$

choosing a range of dune heights (i.e., 300, 500, 1000, 1500, 2000, and 3000 cm), and incorporating an appropriate bulk density (1.7 to 1.9 gm/cm^{-3} are reasonable for the Hanford dunes) will yield a range of potential sand dune migration rates.

Implications of Predicted Rates of Sand Dune Migration

It is still premature to project with confidence how or what form dune sands have taken as they have been transported away from their source area(s). Many vexing problems remain regarding the: 1) availability of source detritus at various times during the Holocene and Pleistocene, 2) local wind variability, 3) moisture, and roughness factors, 4) influence of alluvial lags on sand transport rates, and 5) applicability of existing eolian entrainment and transport equations to actual rates of sand dune migration. These, and likely other subsequent problems will be addressed during the remaining years of the study. Still, the method demonstrated in the examples is itself is based on empirically tested equations which have proven to approximate natural eolian processes. The value of these equations, then, is the potential they have for assisting effort to realistically estimate the amount and effects of eolian activity at the Site, values of crucial importance to the barriers program.

Climatic and Eolian Interactions at the Hanford Site

We have just begun to examine the relationship between climate variables and eolian activity at the Hanford Site. This is a large and complex area of study and will ultimately require assessment of many variables. As a first step in this process, annual precipitation (solid line) was plotted against volume of active dune sand (dashed line) in 1948, 1977, and 1987 (volumes calculated using digitized air photo measurements made on the PGII Plotter) (Figure 25; Table 2).

Preliminary assessment of this composite graph apparently shows that 2 years of heightened precipitation during 1980 to 1984 (an increase of ~ 30% over the previous 5 years) resulted in an ~ 20% decrease in active sand dune volume. This apparent relationship and other potential relationships between eolian migration rates, volumes, heights, and various aspects of climate and vegetative cover have yet to be explored fully, but have great significance to the ongoing eolian-climate work.

Rapid restabilization of the previously stabilized dune surface following a 1984 wildfire at Hanford suggests that the climatic threshold needed to promote wholesale Site-wide sand dune reactivation was not breached for long. The continued documentation of the character of eolian/climatic activity at the Site will provide further insight into the nature of that climatic threshold.

Summary and Recommendations

All proposed phases of geomorphic, sedimentary, stratigraphic, and theoretical work to characterize the Pleistocene/Holocene eolian systems and eolian chronologies at the Hanford Site have been initiated. Data compilation and analyses are still ongoing, but results clearly demonstrate that the techniques and strategy being employed are leading us towards the ultimate goal of the program: development of a conceptual model of eolian-climatic interactions at the Hanford Site. This model may then be applied to the design and long-term stability of engineered protective barriers to be used at the Hanford Site.

The emphasis of the first year of the project has been to characterize the modern eolian system at Hanford via a field-and laboratory-based investigation conducted by the principal investigator, two geology graduate students, and cooperating PNL personnel. Existing Hanford area meteorological data has been examined and, preliminarily, integrated with field and laboratory data from the sedimentary, stratigraphic, and geomorphic aspects of the project.

Aerial photos were used to compile an eolian features map and sampling program and provided the data for historical rates of sand dune migration (using the PGII Plotter and computer enhancement equipment. Stabilized dune sands are dominantly parabolic, while actively migrating dunes include parabolic, barchan, barchanoid, and transverse types. The relationship between dune type, climate, and vegetation is still being investigated. Active sand dunes over the last approximate 40 years have migrated at a rate of 2.5 to 4.5 m/yr. During this same time, there was an approximately 26% decline in amount of actively migrating dune sand; though still under study, the cause may be related to a peak in effective precipitation during the early 1980s.

Eolian sediments were sampled from ninety-seven locations across the Hanford Site including twenty-nine hand-dug, 1.0 to 1.2 m deep pits. Sieve analyses from forty-eight samples sites indicate that mean grain size of sand dune sediments are dominantly fine-grained, fine downwind (to the east and northeast), and are better sorted downwind.

The provenance of the eolian sediments reflects overall dispersal patterns away from inferred source areas including: 1) fluvial sediments exposed along Dry Creek, 2) alluvial sediments weathering out along the northeastern flanks of the Rattlesnake Hills, and 3) alluvial-eolian sediments exposed near the 'horn' of the Yakima River. The Dry Creek area was examined most extensively where six, 8 to 11 m thick stratigraphic sections were measured in a sequence containing interstratified alluvium, volcanic ash beds, and paleosols. Eight charcoal samples were collected from these strata and will be used to constrain the sedimentary sequence chronologically.

A limited number of grain size analyses and visual field and laboratory observations indicate that dune sands sampled across the Site have distinct downwind variations in both texture and composition. Mean grain size (from sieve analyses) decreases to the northeast from both the Cold Creek Valley and the Yakima River floodplain to the Columbia River. Mean grain sizes of upwind dune sands range from 0.5 to 0.35 mm in diameter (1 to 1.5 Φ) and often contained admixed pebbles; mean grain sizes of downwind dune sands range from 0.28 to 0.25 mm in diameter

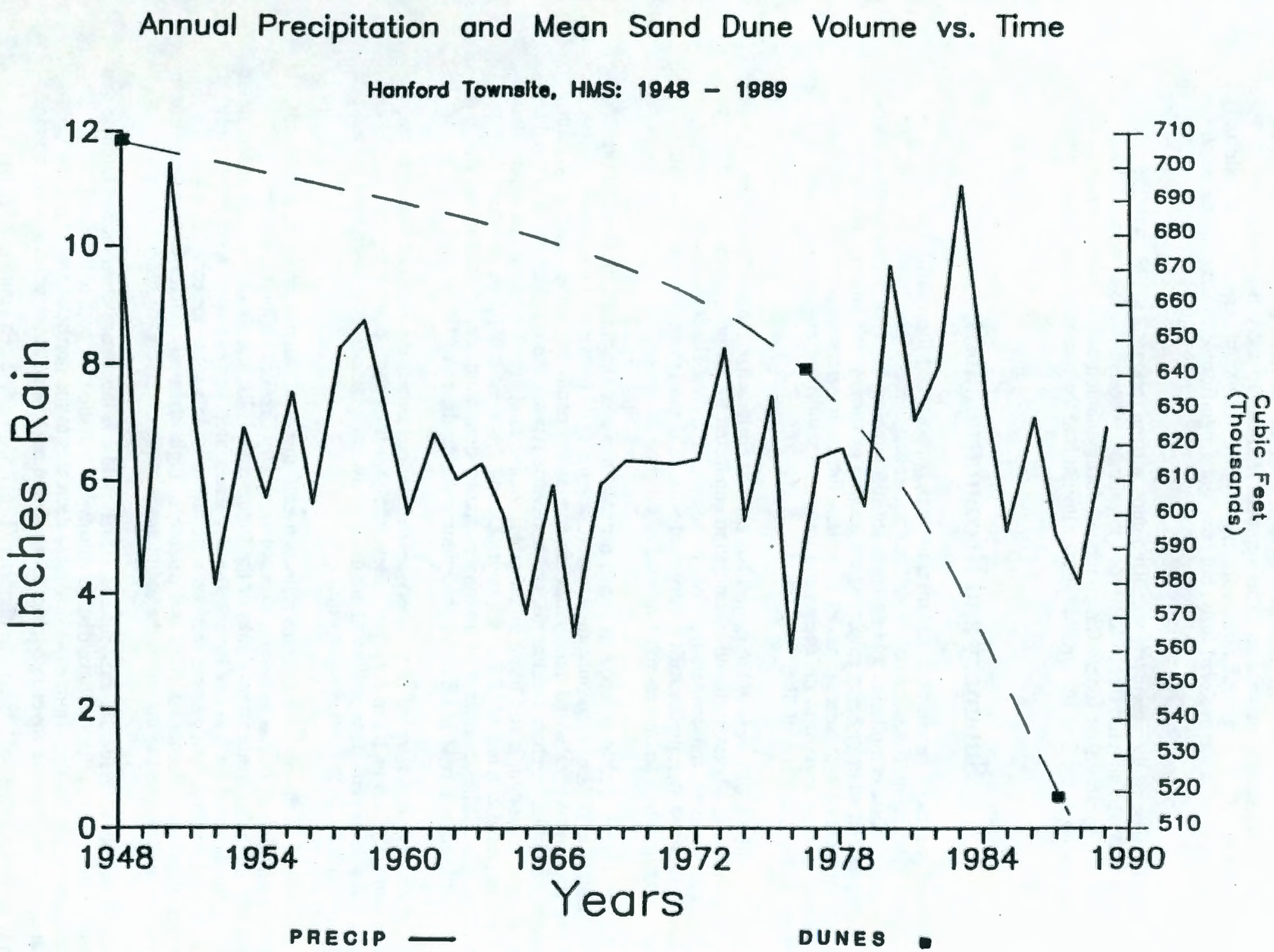

Figure 25. Graph of Mean Annual Precipitation Since 1948 Plotted With Estimated Volume of Active Dune Sand for 1948, 1977, and 1987

(1.8 to 2.0 Φ). As yet unquantified laboratory observation suggests that sand grains appear to be better rounded downwind. Overall, estimates of dune sand composition vary little across the Site. Quartz predominates and makes up from 60 to 70%, basalt 25 to 30%, feldspars 2 to 4%, and micas and chert approximately 2% of a well-mixed sand containing a full range of grain size. However, the coarsest sands seem to possess the highest percentages of basalt.

Texturally, and compositionally, the sediments exposed along the Cold Creek Valley and the Yakima River most closely match those incorporated in downwind sand dunes. Sediments, paleosols, and ashes exposed along Dry Creek appear to be too fine grained to have been a significant source of dune sediment. Grain counts of heavy (accessory) minerals, light framework minerals, and lithic fragments from both potential source areas and dune sands will shed more light on the ultimate provenance and distribution of the dune sands away from a likely source area(s). Once a source area is established, the question of the type and timing of climatic events that triggered and/or promoted the generation of dune sands in the volumes now found on the Site will have to be addressed.

The pit stratigraphies within stabilized and active sands record comparable depositional histories. In general, the preponderance of wavy, low-angle cross-strata and inversely-graded, subcritically climbing translatent cross-strata that characterize both recently active and stabilized sand dunes suggest that eolian aggradation occurred under the influence of vegetation and often following the climbing and aggradation of eolian ripples, respectively. The common massive strata suggest rapid deposition from suspension and/or the disruption of stratification by phytoturbation. Calculations of the entrainment velocities necessary to entrain and transport granule and small-pebbles (in excess of 43 mph at 15.2 m height) within eolian dominated deposits suggest that these gravels are relict alluvial, and not primary eolian-derived detritus.

The incipient soils developed at the top of most pits are the only evidence of extensive stabilization and soil formation within approximately a meter of the surface. The apparent youth of the modern surfaces (as evidence by the 'sharpness' of the topographic relief) and the absence of buried soils in the strata examined, suggest that the sediments we studied were post-date the Mazama ash (ca. 6700 to 6800 yr B.P).

The stratigraphic data collected thus far does not record the long term (thousands of years) record sought. It does, however, provide a record of the short-term character of dune activity and distribution which can be used to guide thinking and interpretation of older deposits as they are encountered. If OSL proves to be a viable method of dating inert dune sands then we will have the chronologic control we are seeking. Deeper trenches must be excavated to reveal more complete stratigraphic histories of eolian, eolian-fluvial, and fluvial sequences dating back to the Pleistocene. It will be particularly informative to excavate to a level where marker beds such as the Mazama ash and archaeologically-significant horizons can be used to better constrain the eolian, eolian-fluvial, and fluvial deposits. Thick sand dune deposits between the FFTF and Yakima River 'horn', and west of the main active dunes should be prime targets for backhoe trenching.

Determination of the relationship between climate and eolian activity at the Site, is a large and complex task and ultimately will require the incorporation of many more variables than used in this year's study. Particularly important variables to consider will be the effect of evapotranspiration, plant activity, and human/animal disruptions on the mobility of loose sediment.

Proposed 1991 Eolian Work

As can be seen from the above summary and recommendations, many problems still remain and need to be addressed. The research program outlined below has both field and laboratory components:

Field Studies

(1) Trenching (for documentation of stratigraphic and sedimentary development of eolian and related deposits). This task can be completed using both backhoe and hand trenching as outlined below.

Most of the near-surface, hand-dug trenches completed during the 1990 summer field season were not sufficiently deep to assess character and/or existence of the Mazama ash, the only reliable eolian marker bed identified thus far on or near the Site. As a result, a series of backhoe trenches in sand dune deposits should be considered both on and adjacent to the Site. We particularly favor a series of two to three meter deep backhoe trenches in the sand dunes located between the Yakima horn and the FFTF. Other backhoe trenches should be contemplated in stabilized dune concentrations west and north of the main concentration of active sand dunes (i.e., north of the WPPSS plants). Hand-dug trenches in eolian strata should be continued across the Site to complete the one mile grid system of sampling begun last summer. In addition, trenching of offsite eolian deposits should be considered for sand dunes in the Juniper Hills east of the Hanford Site and in dune sands north of the Site that may be intercalated with fluvial and possibly lacustrine deposits (e.g., sand dunes along the Ringold Flats). Clearly, those eolian strata associated with water-laid sediments have a much improved chance of being dated using conventional ^{14}C techniques.

The bison kill site needs further excavation to establish stratigraphic context and continuity. Hand and possibly backhoe trenching will be necessary to complete evaluation of the depositional/archaeological/climatic history of this locale.

Assuming the OSL age dating of Smith et al. (1991) and Stokes (1991) proves feasible, pit samples should be collected for this purpose during 1991. This one technique could revolutionize attempts to date geologic-climatic events at the Site.

(2) Provenance (for determination of eolian dispersal patterns as they relate to climatically-induced eolian sedimentation). This task will require detailed description and sampling of both eolian deposits on and off the Site and Holocene fluvial and fluvial/eolian source sediments. The additional trench sites identified in task 1 of this section will be used to acquire the extra samples.

(3) Eolian mechanics (to field test entrainment and transport processes simulated and documented in wind tunnel experiments already begun at the Department of Mechanical Engineering, WSU). This task will use WSU instruments to measure (in the field) the relationship between turbulence intensity, boundary layer wind profiles, and sediment entrainment. Identification of the relationship between these variables is fundamental to evaluation of eolian/climatic interactions preserved in eolian-derived sediments.

Laboratory Studies

(1) Sedimentary Petrology (to establish the textural and compositional character of eolian and source sediments as part of provenance studies). Many hundreds of hours will be spent: a) sieving and settling samples from surface and deep trenches in eolian and fluvial/eolian deposits for determination of textural parameters, and b) separating heavy from light minerals and point counting (via thin sections) mineral and lithic separates to document quartz and feldspar varieties, accessory mineral, and lithic compositions. These data will be plotted on contour maps to establish sediment dispersal paths. If stratigraphic control can be established for the sand dune samples, it may be possible to recognize changes in eolian sediment dispersal through time.

(2) Ash analyses (to geochemically substantiate the origin of volcanic ashes encountered in trenching). Analyses would be conducted using the microprobe at WSU (where such analytical work with Pleistocene ashes is already an established procedure).

(3) Air photo interpretation (to continue the evaluation of modern levels of sand dune migration). This research would build on 1990 results and incorporate additional 1930s, 50s, 60s, and early 70s air photos mounted in the PGII plotter to plot changes in active dune heights and migration rates. Calibrated computer imagery would be used to compute changes in active dune areas and volumes (when combined with dune height data). The results of this task are crucial to our efforts to establish the relationship and equilibrium between sand dune activity at the Site and the modern climate (including wind, precipitation, and temperature data. In this manner, more realistic projections can be made of former levels of eolian activity under differing (projected) climates.

References

Anderson, R. S. 1986. "Erosion Profiles Due to Particles Entrained by Wind: Application of an Eolian Sediment-Transport Model." *Geol. Soc. Am. Bull.* 97:1270-1278.

Anderson, R. S., and B. Hallet. 1986. "Sediment Transport by Wind: Toward a General Model." *Geol. Soc. Am. Bull.* 97:523-535.

Bagnold, R. A. 1941. *The Physics of Blown Sand and Desert Dunes*. Methuen and Co., Ltd., London.

Belly, P. 1964. *Sand Movement by Wind, with Addendum 2 by A. Kadib*. Tech. Memo 1, U.S. Army Corps of Engineers, Coastal Eng. Res. Center.

Brown, R. E. 1975. "Ground Water and Basalts in the Pasco Basin". In *Proceedings of the 13th Engineering Geology and Soils Engineering Symposium*, Moscow, Idaho.

Chepil, W. S. 1945. "The Transport Capacity of the Wind, Pt. 3 of Dynamics of Wind Erosion." *Soil Sci.* 60(6):475-480.

DOE. 1986a. *Environmental Assessment: Reference Repository Location, Hanford Site, Washington*. DOE/RW-0070, U.S. Department of Energy, Washington, D.C.

DOE. 1986b. *Draft Environmental Impact Statement: Disposal of Hanford Defense High Level, Transuranic and Tank Wastes*. DOE/EIS-0113, U.S. Department of Energy, Richland, Washington.

Flint, R. F. 1938. "Origin of the Cheney-Palouse Scabland Tract." *Geol. Soc. of Am. Bull.* 49:461-564.

Folk, R. L. 1980. *Petrology of Sedimentary Rocks*. Hemphill Publishing Co., Austin, Texas.

Fryberger, S. G. 1979. "Dune Forms and Wind Regime." In *A Study of Global Sands Seas*, ed. E. D. McKee, pp. 137-170. U.S. Geol. Survey Prof. Paper 1052.

Glantz, C. S., M. N. Swartz, K. W. Burk, R. B. Kasper, M. W. Ligotke, and P. J. Perrault. 1990. *Climatological Summary of Wind and Temperature Data for the Hanford Meteorology Monitoring Network*. PNL-7471, Pacific Northwest Laboratory, Richland, Washington.

Goldsmith, V. 1985. "Coastal Dunes," In *Coastal Sedimentary Environments*, ed. R. A. Davis, Jr., pp. 303-378. Springer-Verlag, New York.

Grollier, M. J., and J. W. Bingham. 1978. *Geology of Parts of Grants, Adams, and Franklin Counties, East-Central Washington*. Wash. Div. of Geology and Earth Resources Bulletin 71.

Horikawa, K., and H. W. Shen. 1960. *Sand Movement by Wind Action on the Characteristics of Sand Traps*. Tech. Mem. No. 119, U.S. Army Corps of Engineers, Coastal Eng. Res. Center.

Ingram, R. L. 1971. *Procedures in Sedimentary Petrology*. John Wiley and Sons, New York.

Lindsey, K. A., and D. R. Gaylord. 1989. *Sedimentology and Stratigraphy of the Miocene-Pliocene Ringold Formation, Hanford Site, South-Central Washington*. WHC-SA-0740-FP, Westinghouse Hanford Company, Richland, Washington.

Lindsey, K. A., and D. R. Gaylord. 1990. "Lithofacies and Sedimentology of the Miocene-Pliocene Ringold Formation, Hanford Site, South-Central Washington." *Northwest Science* 64:165-180.

McKee, E. D., ed. 1979. *A Study of Global Sand Seas.* U.S. Geol. Survey, Prof. Paper 1052.

Melton, F. A. 1940. "A Tentative Classification of Sand Dunes: Its Application to Dune History in the Southern High Plains." *Jour. of Geology* 48:113-174.

Mullineaux, D. R., R. E. Wilcox, W. F. Ebaugh, R. Fryxell, and M. Rubin. 1977. "Age of the Last Major Scabland Flood of Eastern Washington, as Inferred from Associated Ash Beds of Mount St. Helens Set S." *Geol. Soc. of Am. Abstracts with Programs* 9(7):1105.

Myers, D.W., S. M. Price, J. A. Caggiano, M. P. Cochran, W. H. Czimer, N. J. Davidson, R. C. Edwards, K. R. Fecht, G. E. Holmes, M. G. Jones, J. R. Kunk, R. D. Landon, R. K. Ledgerwood, J. T. Lillie, P. E. Long, T. H. Mitchell, E. H. Price, S. P. Reidel, and A. M. Tallman. 1979. *Geologic Studies of the Columbia Plateau: A Status Report.* RHO-BWI-ST-4, Rockwell Hanford Operations, Richland, Washington.

Newcomb, R. C. 1958. "Ringold Formation of Pleistocene Age in the Type Locality, The White Bluffs, Washington." *Am. Jour. Sci.* 256:328-340.

Newcomb, R. C., J. R. Strand, and F. J. Frank. 1972. *Geology and Groundwater Characteristics of the Hanford Reservation of the Atomic Energy Commission, Washington.* U.S. Geol. Survey Prof. Paper 717.

Petersen, K. L. 1989. *The Long-Term Climate Change Assessment Task of the Hanford Site, Washington, Protective Barrier Development Program.* WHC-SA-0537, Westinghouse Hanford Company, Richland, Washington.

Reidel, S. P., K. R. Fecht, M. C. Hagood, and T. L. Tolan. 1990. "The Geologic Evolution of the Central Columbia Plateau," eds. S. P. Reidel and P. R. Hooper, pp. 247-264. In *Volcanism and Tectonism in the Columbia River Flood Basalt Province*, Geol. Soc. Am., Spec. Paper 239.

Smith, B. W., E. J. Rhodes, S. Stokes, and N. A. Spooner. 1991. "Optical Dating of Quartz," *Radiation Protection Dosimetry* 34:75-78.

Soil Survey Staff. 1988. *Soil Taxonomy.* U.S. Dept. of Agriculture SMSS Tech. Monograph # 6.

Stokes, S. 1991. "Quartz-Based Optical Dating of Weichselian Cover Sands from the Eastern Netherlands," *Geologie en Mijnbouw* 70:327-337.

Stone, W. A., J. M. Thorp, O. P. Gifford, and D. J. Hoitink. 1983. *Climatological Summary for the Hanford Area in Subsurface Geology of the Cold Creek Syncline.* RHO-BWI-ST-14, Rockwell Hanford Operations, Richland, Washington.

Thornbury, W. D. 1965. *Regional Geomorphology of the United States.* John Wiley and Sons, New York.

Watkins, N. D., and A. K. Baksi. 1974. "Magnetostratigraphy and Oroclinal Folding of the Columbia River, Steens and Owyhee Basalts in Oregon, Washington, and Idaho." *Am. Jour. of Science* 274:148-189.

Wing, R. N., and G. W. Gee. 1990. H*anford Site Protective Barrier Development Program: Fiscal Year 1989 Highlights.* WHC-EP-0318, Westinghouse Hanford Company, Richland, Washington.

Zingg, A. W. 1953. "Wind-Tunnel Studies of the Movement of Sedimentary Material." *Iowa University Studies Engineering Bulletin* 34:111-135.

Appendix A

Parameters of Dune Migration Calculations

Appendix A

Parameters of Dune Migration Calculations

The sandflow equation using Bagnold's (1941) formula in CGS units is as follows:

$$q = aC(c/D)^{0.5}(p/g)(V-Vt)^3$$

Definition of parameters:

q = sandflow gm/cm/yr	<u>Values</u>
where	
a = constant equal to $[0.174/\log(z/k')]^3$	
z = 50 ft--height of velocity measurement:	50 ft
k' = roughness coefficient:	0.274 cm
C = empirical coefficent having the following values:	
1.5 for a nearly uniform sand	
1.8 for a naturally graded sand (dunes)	1.8
2.8 for sand with a wide range of grain sizes	
d = mean grain size of sand, cm	0.287 cm
D = standard grain size, cm:	0.25 cm
p = density of air, 60°F:	0.00122 gm/cc
g = acceleration due to gravity:	981 cm/sec^2
V = wind speed to evaluate sandflow, cm/sec	
V_t = impact threshold velocity, cm/sec:	672.1 cm/sec

Sandflow calculation for wind speeds of:

V = mph	16.5	21.5	28.0	35.0	42.5
V = cm/sec	737.6	961.1	1251.7	1564.6	1899.9
q = gm/cm/sec	.8E-5	5.8E-3	4.7E-2	1.7E-1	4.5E-1
q = gm/cm/day	5.8	5.0E+2	4.1E+3	1.6E+4	3.9E+4

% yr wind blows at or above V:

	9.00%	8.90%	5.30%	2.10%	0.50%
Days:	32.9	32.5	19.4	7.7	1.8
q = gm/cm/yr	192	16301	78279	113256	701996

Migration rates are calculated as a function of q, dune height, and sand bulk density and has the form:

$$C = q/[\text{dune height (cm)} * \text{bulk density}] \text{ cm/yr}$$

Appendix B

Pit Stratigraphies

Figure 21a.

Pit Stratigraphy

Location and Morphologic Setting:

HA-90-1 NW1/4NW1/4 Sec 7 T12N R28E

Sample from a small deflation bowl (30 m wide by 50 m long) located on flat, vegetated terrace about 1 mi. north of active dune field, 1.25 mi. east of May Junction, and 1.25 mi. southwest of Columbia River. Center of deflation area is 2 m below the surrounding flats.

% of Vegetative Cover:

Less than 5% of surface contains vegetation.

Pedogenic Development:

No soil development.

Pit Dimensions and Geometry:

80 cm at a trend of N80E; 1.3 m at a trend of N170E; 90 cm deep

Textural Characteristics:

Average Grain Size: 2.5 Phi (0.177 mm).
Sorting: Moderate
Silt & Clay: <2%
Roundness: Largest quartz grains are angular, many exhibit fractured edges. Remaining grains are subangular to subrounded.

Sand Composition:

Quartz--72%; Basalt--20%; Mica--4%; Feldspar--2%; Magnetite--2%.

Sedimentary Structures:

At 90 cm is a well-rounded, clast supported cobble (5 to 10 cm) lag deposit. Overlying the cobble lag is a massive, fine-grained, pebble rich (3 to 7 mm) sand. Pebble composition is chert, basalt, quartzite, and granite. No stratification is observed in this pit.

Interpretation:

The material exposed in this pit were deposited primarily by fluvial processes. The cobble lag represents a traction deposit formed as a result of flow which was competent to roll the cobbles along the channel bottom. Long axis of the cobbles parallel present flow of the Columbia River (approximately north-south in this reach) suggesting deposition by currents perpendicular to modern day flow directions. The overlying massive, fine-grained, pebbly sand indicates rapid deposition during the waning stages of a flood. It is unknown if the same flow event was responsible for deposition of the cobble lag and the massive, fine-grained, pebbly sand.

Eolian processes are presently active on the surface of the deflation bowl. Superimposed ripples are present in the deflation bowl on the northern rim (up wind direction), in areas directly downwind of vegetation, and in wind-induced scour-channels which are located on the southern rim (down wind direction) of the exposed area. The largest ripples are asymmetrical, sinuous crested, 4 to 6 cm high, 40 cm in wavelength, that bifurcate. Superimposed on these long wavelength ripples are smaller, asymmetrical, sinuous-crested wind ripples about 2 cm high with a wavelength from 8 to 10 cm. The large ripples contain a dense concentration of very coarse and coarse basalt grains on their stoss side. As fine sand was transported out of the area by eolian activity, pebbles were exposed and concentrated at the surface as lags. All elongate pebbles are oriented with long axes perpendicular to present day wind direction.

Fluvial sedimentation at the pit site appears to have been rapid. The dominance of massive, fine-grained, pebbly sand indicates that accumulation of the sediment was rapid, probably the result of a single fluvial event. The Mazama ash, although present regionally, was not encountered in this pit. The absence of this distinctive marker unit and the lack of any well-developed soil suggests that the deposits are quite young, and likely younger than the 6700 yr B.P. date assigned to the Mazama volcanic event.

Figure 21a.

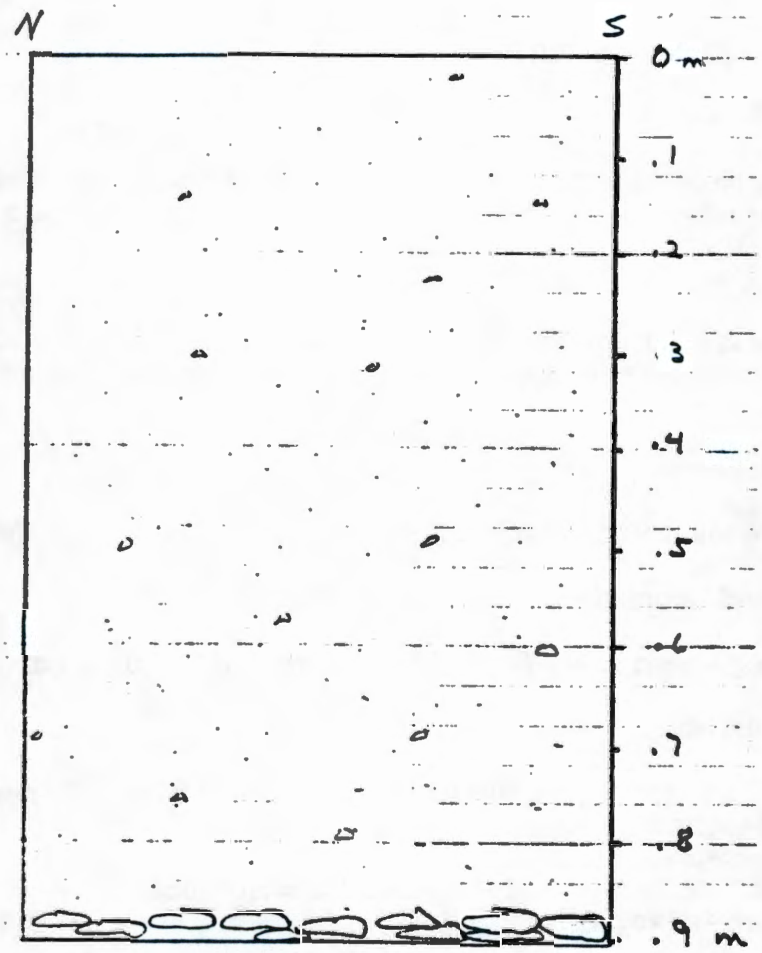

Key

Roots

Massive sand

Fine-grained sand

Coarse-grained sand

Cobbles

Pebbly sand

Pebbles

Pebble stringers

Cambic horizon

Figure 21b.

Pit Stratigraphy

Location and Morphologic Setting:

HA-90-3 SE1/4SE1/4 Sec13 T12N R27E

Pit located on top of a sparsely vegetated trailing arm of a partially stabilized parabolic dune in the northwest corner of the active dune field. Relief is about 2 to 3 m.

% of Vegetative Cover:

Vegetation is scant, covering about 25% of the surface. Grass is predominant with rare sage. Root mass continuous to about 20 cm with some extending the entire pit depth of 110 cm.

Pedogenic Development:

There is no soil development in this pit.

Pit Dimensions and Geometry:

70 cm along a trend of N60E; 1.3 m along a trend of N135E; 1.1 m deep

Textural Characteristics:

Average Grain Size: Bimodal: 1.25 Phi (0.42 mm); 2.0 Phi (0.25 mm)
Sorting: Moderate
Silt & Clay: <2%
Roundness: Medium-grained--subangular to subrounded;
Fine-grained--subrounded.

Sand Composition:

<u>Medium Fraction:</u> Quartz--55%, Basalt--35-38%, Chert--3%, Feldspar--2-3%, Mica--2%
<u>Fine Fraction:</u> Quartz--80%, Basalt--10-12%, Mica--2-3%, Feldspar--2%, Magnetite--1%

Sedimentary Structures:

No structures are present below 75 cm where the material is a fine-grained, massive sand. Stratification above 75 cm consists of alternating low-angle layers of dark, medium-grained, sand laminae and beds ranging from 0.5 to 2 cm thick interbedded with a light, fine-grained thinly laminated sand averaging one to two grains thick. Approximately 16 to 20 medium-grained sand laminae and beds occur between 10 and 75 cm. Contacts between medium- and fine-grained strata are sharp and dip about 12° to the northeast.

Interpretation:

The accumulation of sediment in this pit were deposited as a result of eolian processes. Massive sand in the pit represents rapid deposition of suspended fine-grained eolian sediment during eolian transport. The overlying alternating medium- and fine-grained sand laminae and beds are interpreted as subcritically climbing translatent cross-strata. Subcritically climbing translatent cross-strata result from translation and accumulation of eolian ripples. Eolian sedimentation at the pit site appears to have been continuous with no significant erosional or pedologic breaks. The dominance of low-angle stratification suggests that accumulation of sediment was slow throughout its history. The Mazama ash, though present regionally, was not encountered in this pit. The absence of this distinctive marker unit and the lack of any well-developed soil suggests that the deposit is quite young, and likely younger than the 6700 yr B.P. date assigned to the Mazama volcanic event.

Figure 21b.

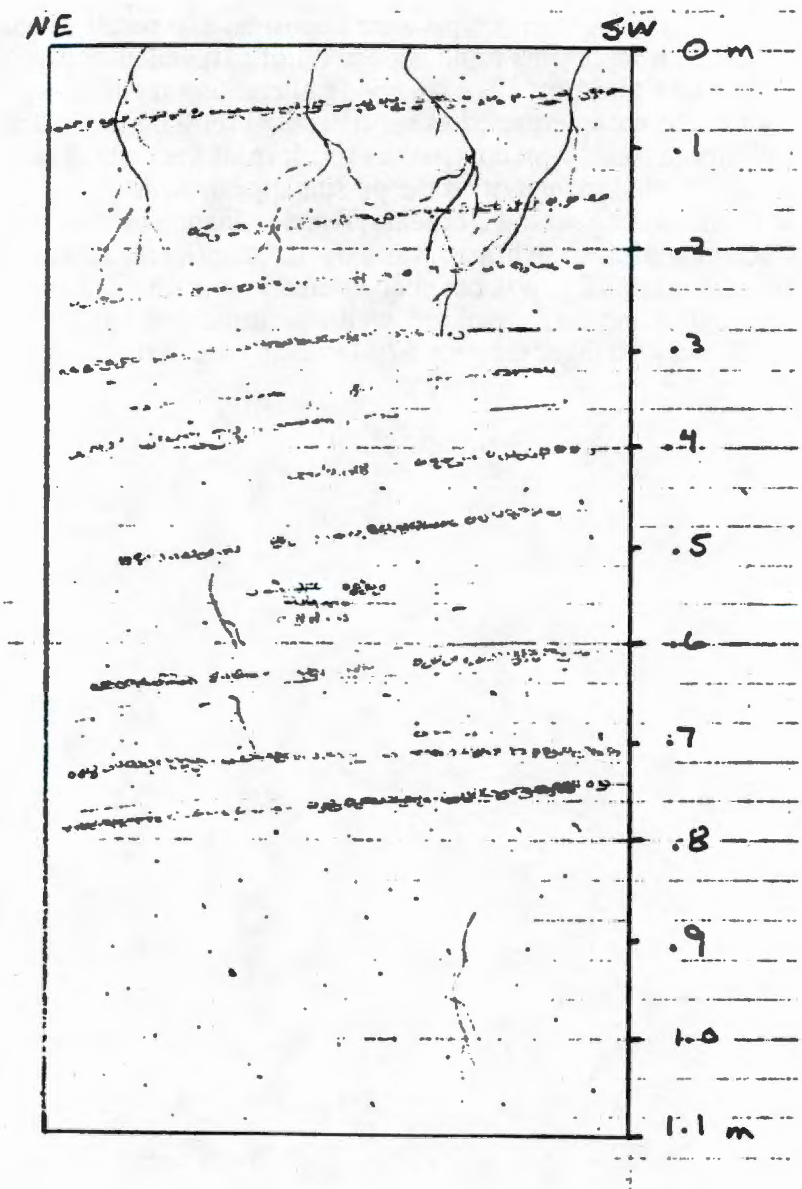
NE
SW
0 m
.1
.2
.3
.4
.5
.6
.7
.8
.9
1.0
1.1 m

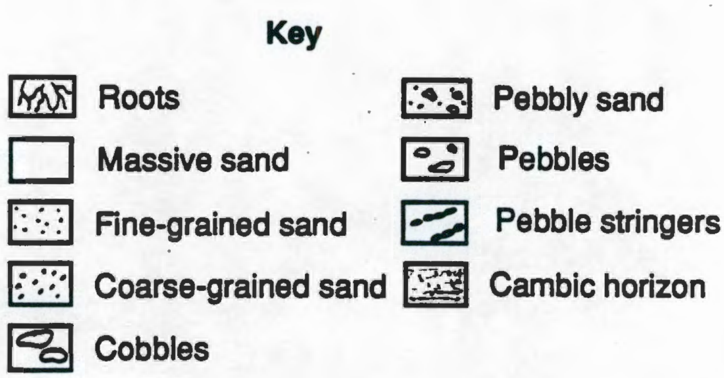
Key
Roots
Massive sand
Fine-grained sand
Coarse-grained sand
Cobbles
Pebbly sand
Pebbles
Pebble stringers
Cambic horizon

Figure 21c.

Pit Stratigraphy

Location and Morphologic Setting:

HA-90-5 SE1/4SE1/4 Sec 7 T12N R28E

Sample is from a partially stabilized trailing arm of a parabolic dune located in the northern periphery of the active dune field. The trend is N75E and it is between 10 to 12 m high. The rise in elevation observed here exists for several kilometers along the trend N75E and marks a terrace level rising above the flat ground to the north.

% of Vegetative Cover:

Moderately vegetated by grasses, cactus, and sage. ~30% cover. Roots are dense to 15 cm.

Pedogenic Development:

There is no soil present at the pit site.

Pit Dimensions and Geometry:

1.2 m along a trend of N30E; 1 m along a trend of N90E; 90 cm deep

Textural Characteristics:

Average Grain Size: Bimodal--Coarse: 1.0 to 1.5 Phi (0.5 to 0.35 mm); Fine: 2.0 to 2.5 Phi (0.25 to 0.177 mm).
Sorting: Moderate, clean
Silt & Clay: 2%
Roundness: Mainly subrounded. Few grains show fractured edges.

Sand Composition:

Quartz--70%; Basalt--24%; Phlogopite--3%; Muscovite--1%; Biotite--1%; Magnetite and others--1%.
Non-calcareous. Several grains are oxidized. Light gray.

Sedimentary Structures:

The structures observed in this pit consist of dark, coarse-grained sand laminae and beds interstratified with light, massive fine-grained sand. The coarse-grained strata range between 0.5 to 5.0 cm thick. The lower most strata are the thickest and steepest dipping. Attitudes of the coarse-grained beds and laminae are as follows:

Depth of Strata	Strike	Dip	Thickness
29 cm	N44W	4N	1 cm
32 cm	N55W	6NE	1 cm
36 cm	N80W	18N	4 cm
45 cm	N82W	28N	5 cm

Interpretation:

The strata in this pit record the recent transport , deposition, and stabilization of eolian (dune) sands. The majority of the sand in this profile reflects periods of relatively slow aggradation in the form of subcritically climbing translatent strata. The lack of soil properties, including no carbonate accumulation indicates that the strata in this pit are quite recent and are younger than 1000 years old since carbonate will accumulate on the order of 100's of years in stable sediments in an arid environment.

Figure 21c.

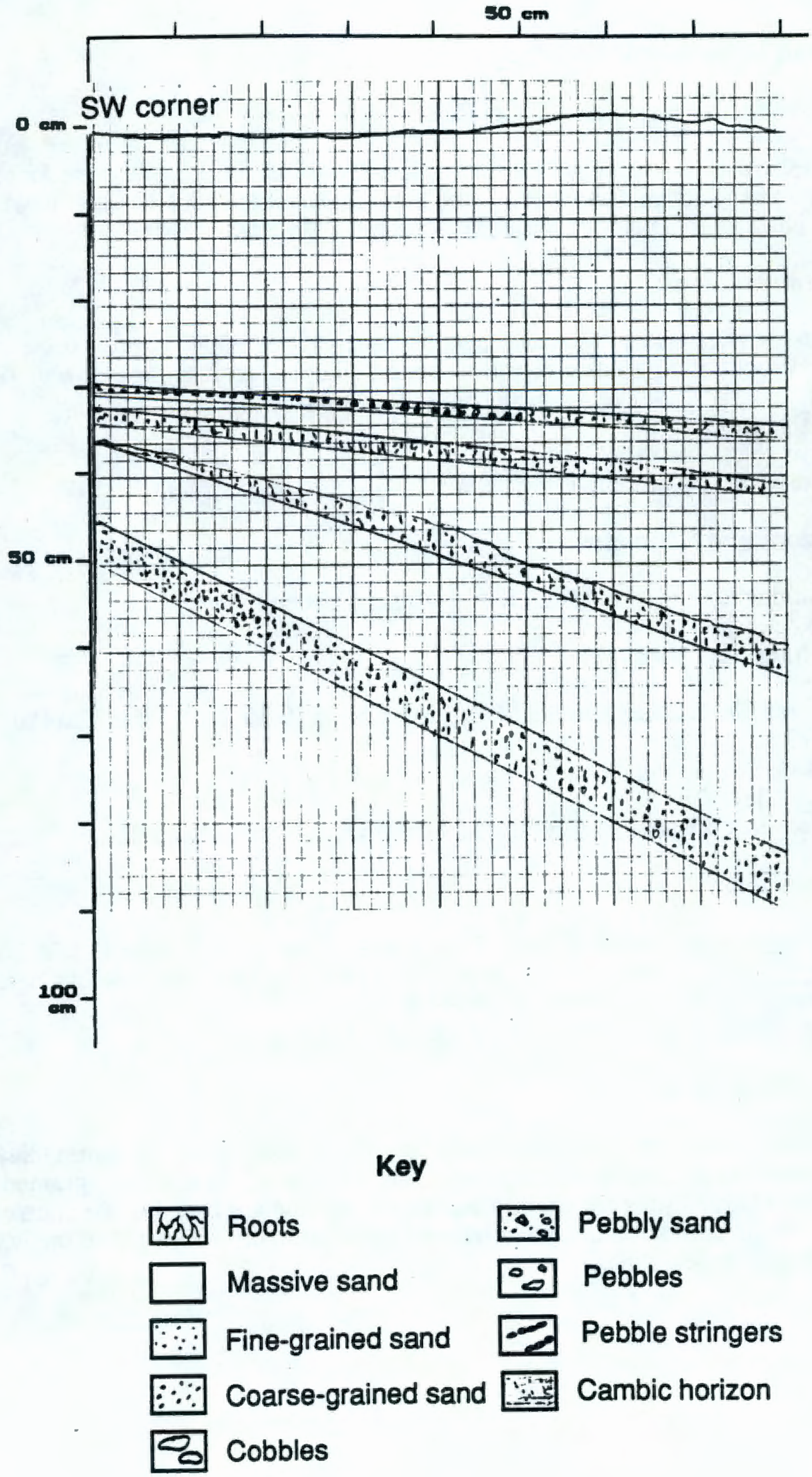
50 cm
SW corner
0 cm
50 cm
100 cm
Key
Roots
Massive sand
Fine-grained sand
Coarse-grained sand
Cobbles
Pebbly sand
Pebbles
Pebble stringers
Cambic horizon

Figure 21d.

Pit Stratigraphy

Location and Morphologic Setting:

HA-90-6 SE1/4SE1/4 Sec 8 T12N R28E

Sample from southern trailing arm of large, stabilized parabolic dune located on northern periphery of active dune area. Dune trend is 90°, it is about 30 to 40 m wide, 4 to 5 m high, and has a well developed deflation surface on the upwind side.

% of Vegetative Cover:

Sparsely vegetated by grasses, sage, and rare cactus. ~30% cover. Roots are dense to 25 cm. Woody roots from sage follow coarse-grained laminae for entire pit depth.

Pedogenic Development:

There is no soil present at the pit site.

Pit Dimensions and Geometry:

1 m along a trend of N75E; 1.8 m N150E; 1 m deep

Textural Characteristics:

Average Grain Size: Bimodal--Coarse: 1.5 Phi (0.35 mm); Fine: 2.5 Phi (0.177 mm).
Sorting: Moderate, clean
Silt & Clay: Tr
Roundness: Coarse--subangular to subrounded; Fine--subangular.

Sand Composition:

Coarse Fraction: (65% of total) Basalt--65%; Quartz--30%; Chert--3%; Lithics--2%
Fine Fraction: (35% of total) Quartz--75%; Basalt--15%; Mica--4%; Chert--3%; Magnetite--2%; Lithics and Oxides--1%.
Minor oxide stain on quartz. Well Packed. Light tan.

Sedimentary Structures:

Stratification in the pit is composed primarily of alternating 3 to 5 mm thick, light, fine-grained sand laminae and 3 to 5 mm thick, dark, basalt rich, coarse-grained sand laminae. Thickest laminations are slightly less than 1 cm and are found in the coarse-grained sand laminae. Stratification is near horizontal (maximum dip about 13° to the northeast) and is uniform in appearance.

Interpretation:

The strata exposed in this pit were deposited by eolian processes. The low-angle, fine-grained sand laminae are interpreted as subcritically climbing translatent cross-strata. Subcritically climbing translatent cross-strata result from the translation and accumulation of eolian ripples. Coarse-grained sand laminae which make up the remaining stratification in the pit are also interpreted as subcritically climbing translatent cross-strata formed as a result of translation and accumulation of coarse grain sized sand during high wind events.

Eolian sedimentation at the pit site appears to have been continuous with no significant erosional or pedogenic breaks. The dominance of low-angle stratification suggests that accumulation of sediment was slow during its history. The Mazama ash, although present regionally, was not encountered in this pit. The absence of this distinctive marker horizon along with the lack of any well-developed soil suggests that the deposit is quite young, and likely younger than the 6700 yr B.P. date assigned to the Mazama volcanic event.

Figure 21d.

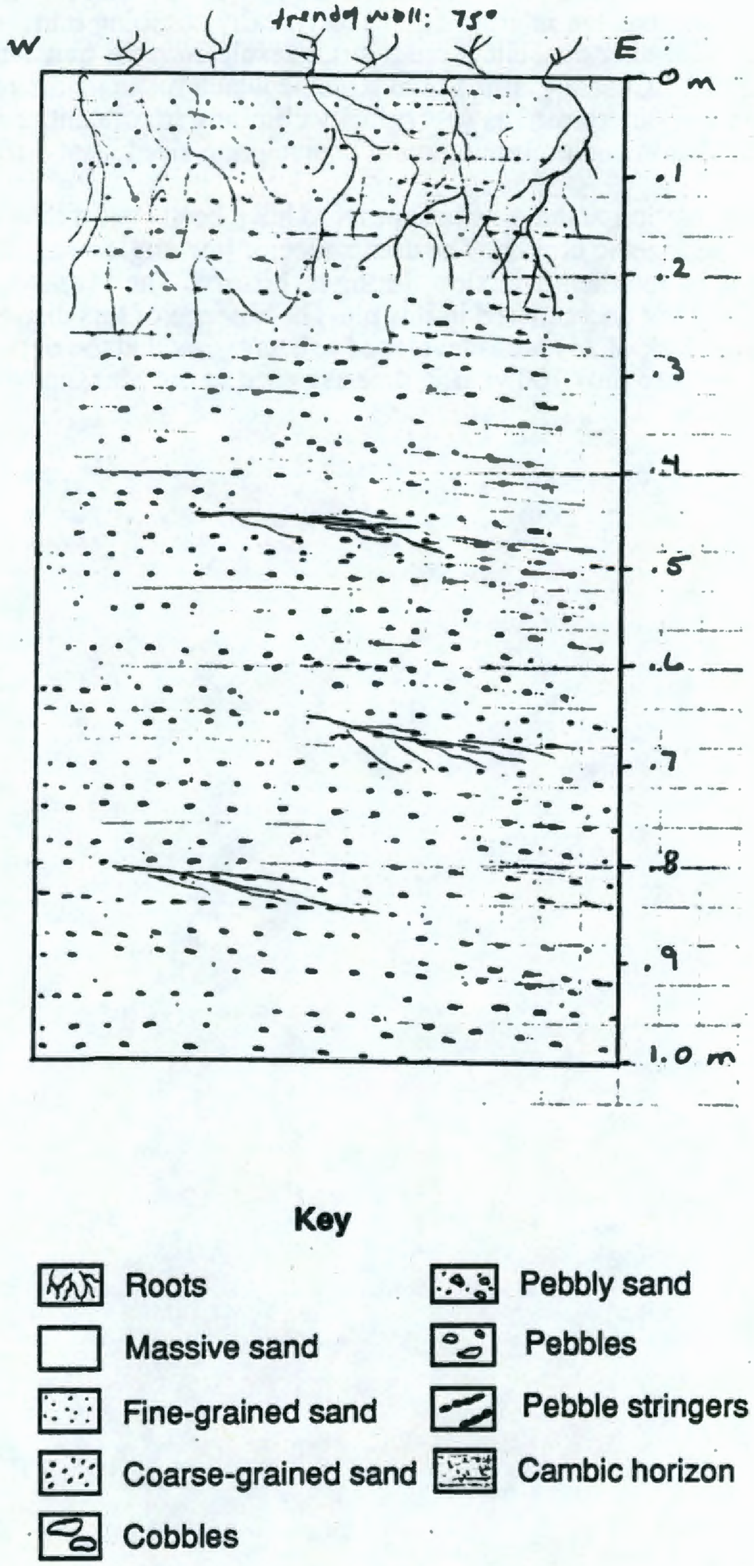
trend of wall: 75°
W
E
0 m
.1
.2
.3
.4
.5
.6
.7
.8
.9
1.0 m
Key
Roots
Massive sand
Fine-grained sand
Coarse-grained sand
Cobbles
Pebbly sand
Pebbles
Pebble stringers
Cambic horizon

Figure 21e.

Pit Stratigraphy

Location and Morphologic Setting:

HA-90-8 SW1/4SW1/4 Sec14 T12N R28E

Pit located 2 m upwind of the crest line on a transverse dune 100 m long, 8 m high, 20 m wide, possessing a well developed slipface inclined at 33°. This transverse dune is located 200 m west of the Columbia River in the east-central active dune field and forms the second major dune ridge west of the Columbia River. This transverse dune is not the same dune form as describes in sample HA-90-9. Trend of the transverse dune is N160E which is nearly parallel to the river.

% of Vegetative Cover:

There is no vegetation on this dune ridge. However, deflation surfaces upwind and downwind of the dune are heavily vegetated.

Pedogenic Development:

No soil development was observed in this pit.

Pit Dimensions and Geometry:

1 m along a trend of N65E; 1.6 m along a trend of N160E; 1.1 m deep

Textural Characteristics:

Average Grain Size: 1.5 to 2.0 Phi (0.35 to 0.25 mm)
Sorting: Moderate
Silt & Clay: <2%
Roundness: Subangular to rounded; finest grains are round.

Sand Composition:

Quartz--60%; Basalt--30%; Feldspar--5-8%; Chert--2%; Magnetite--<1%. Slightly calcareous. Light tan.

Sedimentary Structures:

The sedimentary structures observed in this pit are primarily composed of alternating low-angle, light and dark, one to two grain thick, fine-grained sand laminae and are interbedded with distinct, inversely graded, dark, 1 to 5 cm thick, coarse-grained sand beds. Contacts between fine- and coarse-grained laminae and beds are sharp and are inclined at about 10 to 12° to the east. The coarse-grained sand beds are located at depths of 40, 50, 70, 80, and 88 cm below the surface. Strata above 40 cm was obscured due to dry sand which did not allow a pit wall to be maintained.

Interpretation:

The strata exposed in this pit were deposited by eolian processes. Low-angle, one to two grain thick sand laminae are interpreted as subcritically climbing translatent cross-strata. Subcritically climbing translatent cross-strata are formed by the transportation and accumulation of eolian ripples. Inversely graded, coarse-grained sand beds comprise the thickest strata in this pit and are interpreted as subcritically climbing translatent cross-strata formed as a result of transportation and accumulation of surface granule ripples. Erosion of the surface producing a lag concentrate of coarse grains that are too large to be transported by the wind results in the formation of granule ripples. Surface creep through saltation is the primary mechanism responsible for the formation and growth of granule ripples.

Eolian sedimentation at the pit site appears to have been relatively continuous with no pedogenic break. The dominance of low-angle single to multiple grain thick sand laminae suggests that sedimentation was slow during its depositional history. Excessive erosion of the surface is marked by the presence of granule ripples. Granule ripples are ubiquitous in the active dune area on sparsely to non-vegetated dunes, especially in or near wind-induced scour-channels formed on the surface of the dune. The Mazama ash, though present regionally, was not encountered in this pit. The absence of this distinctive marker unit and the lack of any well-developed soil suggests that the deposit is quite young, and likely younger than the 6700 yr B.P. date assigned to the Mazama volcanic event.

Figure 21e.

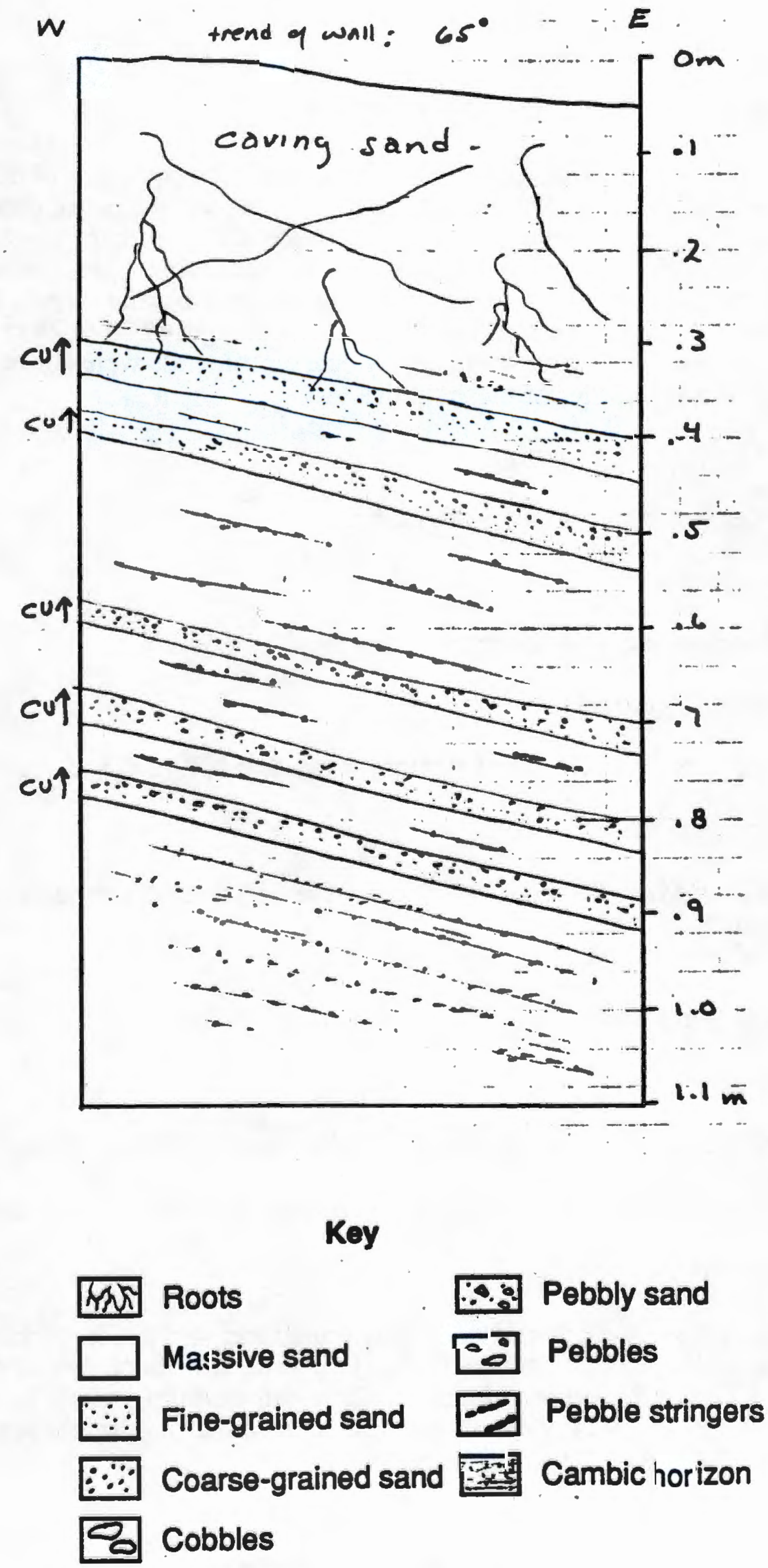
W
trend of wall: 65°
E
0m
.1
.2
.3
.4
.5
.6
.7
.8
.9
1.0
1.1 m
caving sand
CU↑
CU↑
CU↑
CU↑
CU↑
Key
Roots
Massive sand
Fine-grained sand
Coarse-grained sand
Cobbles
Pebbly sand
Pebbles
Pebble stringers
Cambic horizon

Figure 21f.

Pit Stratigraphy

Location and Morphologic Setting:

HA-90-9 SW1/4SW1/4 Sec 23 T12N R28E

This sample is along a transverse ridge formed by the coalescing of the leading edges of several parabolic dunes. This transverse dune is the second major dune form west of the Columbia River. It is not the same ridge as described in sample HA-90-8. The ridge has a strike of N160E. Sinuous, bifurcating, asymmetric wind-ripples were observed to be active on the dune surface during the passage of a storm front (winds approximately 40 mph). These ripples had a strike of N5W, a wavelength of 25 to 28 cm, and an amplitude of 1.5 to 2.0 cm. The darker and slightly coarser minerals were concentrated in small troughs on the stoss sides of these ripples.

% of Vegetative Cover:

Sparsely vegetated by grasses. ~5% cover.

Pedogenic Development:

No soil development was observed in this pit.

Pit Dimensions and Geometry:

1.4 m along a trend of N170E; 1 m along a trend of N80E; 1.1 m deep

Textural Characteristics:

Average Grain Size: Bimodal at 1.0 to 1.5 Phi (0.5 to 0.35 mm) and 2.5 to 3.0 Phi (0.177 to 0.125 mm).
Sorting: Moderately sorted
Silt & Clay: <2%
Roundness: Subrounded

Sand Composition:

Quartz--60%; Basalt--30%; Feldspar--5%; Micas--2%; Chert--1%; Magnetite--1%; Others--1%.
Slightly calcareous. Minor oxide stain on quartz. Few quartz are included. Light-gray.

Sedimentary Structures:

This pit consists of subcritically climbing translatent strata. The strata are composed of alternating light, medium-grained (0.5 to 0.35 mm) sand laminae and dark, coarse-grained (0.71 to 0.5 mm) sand laminae. The light, medium-grained sand laminae are quartz-rich and are much more abundant than the dark, basalt rich, coarse-grained sand laminae. Attitudes of the strata are as follows:

Depth	Strike	Dip	Thickness
21 cm	N52W	3NE	1 cm
24 cm	N52W	3NE	1 cm
41 cm	N32W	11NE	4 cm
50 cm	N32W	11NE	1 cm
55 cm	N41W	12NE	1 cm
65 cm	N30W	8NE	1 cm

Interpretation:

The strata in this pit record the transport and deposition of eolian (dune) sands. The presence of wavy, low-angle, subcritically climbing translatent strata suggests that vegetation played an important role in the final deposition of this sand. The presence of a carbonate coating on few sand grains suggests that these eolian sediments resided in a buried and inactive state for an undetermined, though relatively lengthy period of time. While this area is presently sparsely vegetated, it appears that a period of stability and possible plant growth existed in the recent past at this particular locale. The lack of a well developed soil profile suggests that the strata in the pit are quite recent and probably younger than the Mazama ash (ca. 6700 to 6800 yr B.P.).

Figure 21f.

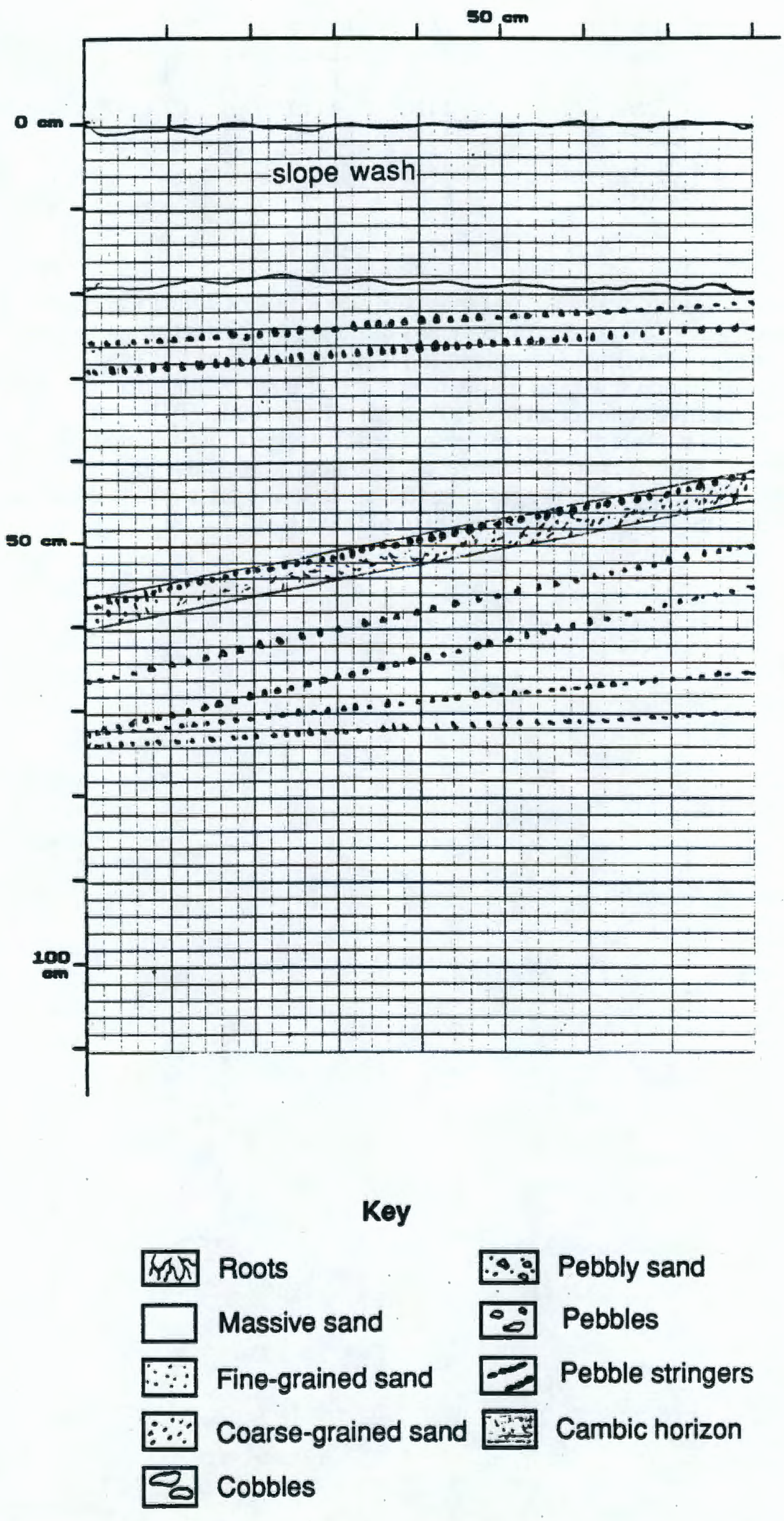
50 cm
0 cm
slope wash
50 cm
100 cm
Key
Roots
Massive sand
Fine-grained sand
Coarse-grained sand
Cobbles
Pebbly sand
Pebbles
Pebble stringers
Cambic horizon

Figure 21g.

Pit Stratigraphy

Location and Morphologic Setting:

HA-90-10 SW1/4SW1/4 Sec 22 T12N R28E

This sample is on the crest of a large transverse dune trending N160E. The transverse dune is formed from a coalescence of several parabolic dunes. The slipface of the dune is 33° to the horizontal and overrides the stoss side of downwind dune forms. No interdunal areas are present here. Small asymmetric, sinuous-crested wind-ripples cover the surface of the dune striking at 180° having an amplitude of 4 to 6 mm, and a wavelength of 8 to 10 cm.

% of Vegetative Cover:

Sparsely vegetated by small, green plants. ~5% cover.
No soil present.

Pedogenic Development:

No soil is developed at the pit site.

Pit Dimensions and Geometry:

1.9 m along a trend of N170E; 1.2 m along a trend of N80E; 1 m deep

Textural Characteristics:

Average Grain Size: Bimodal at 1.0 to 1.5 Phi (0.5 to 0.35 mm) and 2.5 to 3.0 Phi (0.177 to 0.125 mm)
Sorting: Moderate
Silt & Clay: <2%
Roundness: Subangular to subrounded in fine-grained sand.

Sand Composition:

Quartz--60%; Basalt--25%; Feldspar--10%; Micas--3%; Magnetite--1%; Others--1%. Slightly calcareous. Few quartz grains are included. Oxide coatings common on quartz grains. Light pinkish-gray.

Sedimentary Structures:

This pit consists of subcritically climbing translatent strata. The strata are composed of alternating light, fine-grained sand laminae interbedded with dark, coarse-grained sand laminae and beds. Strata are mainly few millimeters thick in both the fine- and coarse-grained sand up to a maximum of 2 cm in the coarse-grained sand. Light, fine-grained sand laminae are quartz-rich, and are much more abundant than the dark, coarse-grained sand laminae and beds. Attitudes of the strata are as follows:

Depth	Strike	Dip	Thickness
12 cm	N5W	4E	1 cm
45 cm	N22E	9E	1 cm
47 cm	N20E	8E	1 cm
50 cm	N10W	7E	1 cm
65 cm	N10W	7E	1 cm
70 cm	N22W	4E	1 cm
81 cm	N31W	21NE	1 cm
87 cm	N38W	11NE	1 cm
92 cm	N38W	11NE	1 cm

Interpretation:

The strata exposed in this pit were deposited predominantly by eolian processes. Inversely graded sand laminae comprise nearly 50% of the low-angle cross-strata observed and are interpreted as subcritically climbing translatent cross-strata. Subcritically climbing translatent cross-strata result from translation and accumulation of eolian ripples. Normally graded low-angle cross-laminae make up the bulk of the remaining low-angle cross-strata and are interpreted as vegetatively induced stratification; as envisioned here, vegetation at the surface acted as a baffle to sediment transport, thus encouraging deposition. The tangential foresets exposed at the 70 cm level record rapid fallout of suspended silt and very fine sand detritus during the migration and preservation of an eolian bedform. Accumulations of massive sand in the pit are associated with rapid deposition of suspended eolian sediment.

Eolian sedimentation at the pit site appears to have been relatively continuous with no significant erosional or pedogenic breaks. the dominance of low-angle stratification suggests that accumulation of sediment was slow and likely influenced by vegetation during much of its history. The Mazama ash, though present regionally, was not encountered in this pit. The absence of this distinctive marker unit and the lack of any well-developed soil suggests that the deposits are quite young, and likely younger than the 6700 yr B.P. date assigned to the Mazama volcanic event.

Figure 21g.

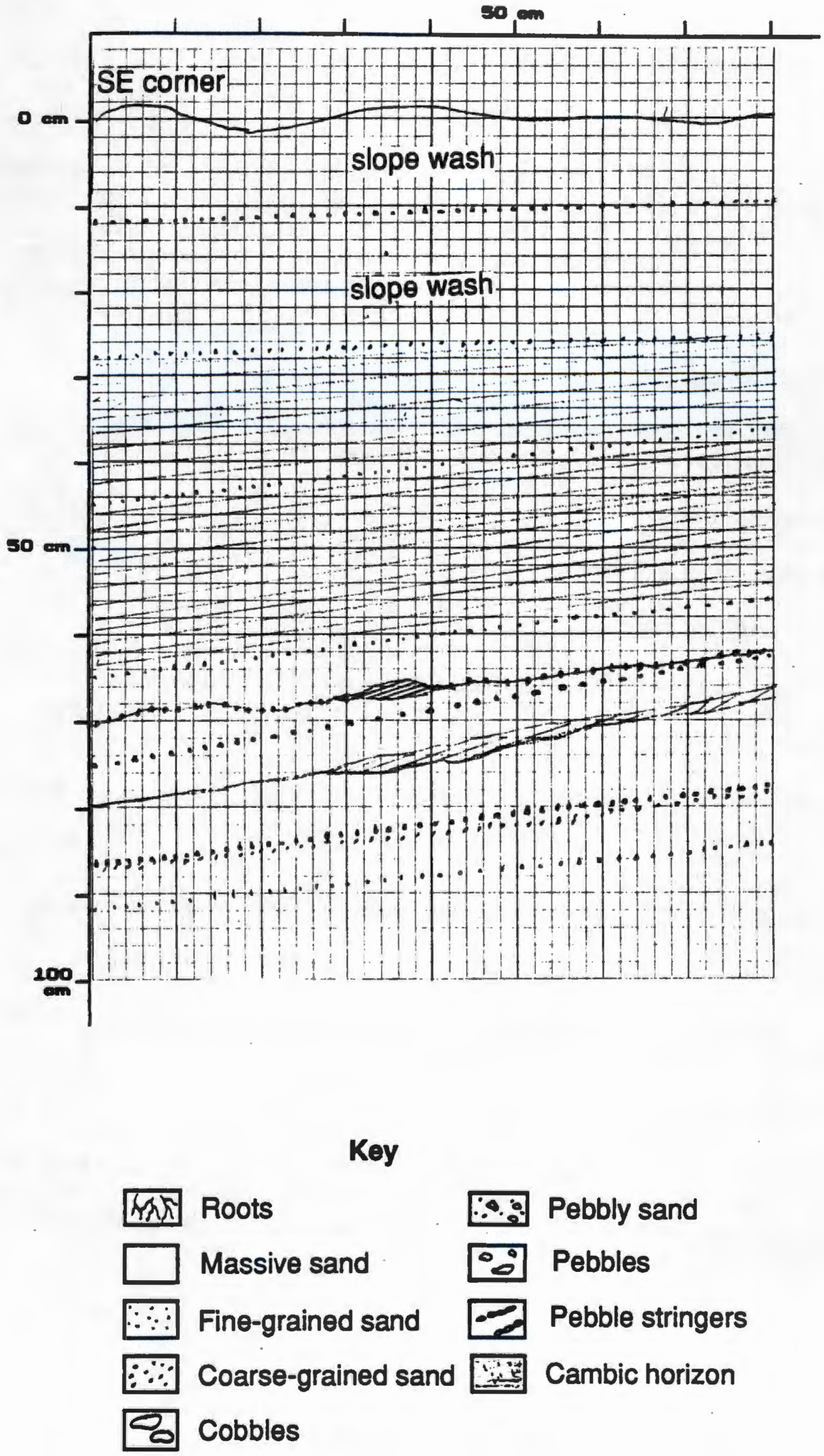
50 cm
SE corner
0 cm
slope wash
slope wash
50 cm
100 cm
Key
Roots
Massive sand
Fine-grained sand
Coarse-grained sand
Cobbles
Pebbly sand
Pebbles
Pebble stringers
Cambic horizon

Figure 21h.

Pit Stratigraphy

Location and Morphologic Setting:

HA-90-12 SW1/4SW1/4 Sec 21 T12N R28E

This sample is from the stabilized, southern trailing arm of a partially stabilized parabolic dune about 100 m upwind of the brink point. The slipface of the dune combines with other parabolic dunes to form a transverse dune ridge trending N180E. A large (100 m wide by 150 m long) deflation bowl exists immediately to the north of the sample area. About 25 m west of the pit location, the trailing arm is being overridden by a smaller parabolic dune.

% of Vegetative Cover:

Vegetation consists of grass, green plants, and some sage. ~30% cover. Upper 40 cm of pit was dry and was held in place by a dense root mass.

Pedogenic Development:

There is no soil at this pit site.

Pit Dimensions and Geometry:

1 m along a trend of N10E; 1 m along a trend of N100E; 1.3 m deep

Textural Characteristics:

Average Grain Size: Bimodal at 1.0 to 1.5 Phi (0.5 to 0.35 mm) and 2.5 to 3.0 Phi (0.177 to 0.125 mm)
Sorting: Moderate
Silt & Clay: <2%
Roundness: Largest grains--subangular, medium to fine grains--sub-rounded.

Sand Composition:

Quartz--65%; Basalt--20%; Feldspar--10%; Mica--4%; Magnetite and others--1%. Slightly carbonaceous. Light pinkish-gray.

Sedimentary Structures:

This pit consists of subcritically climbing translatent strata. The strata are composed of light, fine-grained sand laminae and beds interbedded with dark, coarse-grained sand laminae. Strata below about 60 cm dip between 10 to 15°. Strata above 60 cm dip 21°. Attitudes of the strata are as follows:

Depth	Strike	Dip	Thickness
49 cm	N5W	21E	1 cm
64 cm	N5W	21E	1 cm
69 cm	N14W	10E	1 cm
70 cm	N14W	12E	1 cm
76 cm	N10W	13E	1 cm
82 cm	N10W	13E	1 cm
93 cm	N6W	14E	1 cm
120 cm	N6W	14E	1 cm

Interpretation:

The strata exposed in this pit were deposited predominantly by eolian processes. Inversely graded sand laminae comprise nearly 50% of the low-angle cross-strata observed and are interpreted as subcritically climbing translatent cross-strata. Subcritically climbing translatent cross-strata result from translation and accumulation of eolian ripples. Normally graded low-angle cross-laminae make up the bulk of the remaining low-angle cross-strata and are interpreted as vegetatively induced stratification; as envisioned here, vegetation at the surface acted as a baffle to sediment transport, thus encouraging deposition

Eolian sedimentation at the pit site appears to have been relatively continuous with no significant erosional or pedogenic breaks. The dominance of low-angle stratification suggests that accumulation of sediment was slow and likely influenced by vegetation during much of its history. The Mazama ash, though present regionally, was not encountered in this pit. The absence of this distinctive marker unit and the lack of any well-developed soil suggests that the deposits are quite young, and likely younger than the 6700 yr B.P. date assigned to the Mazama volcanic event.

Figure 21h.

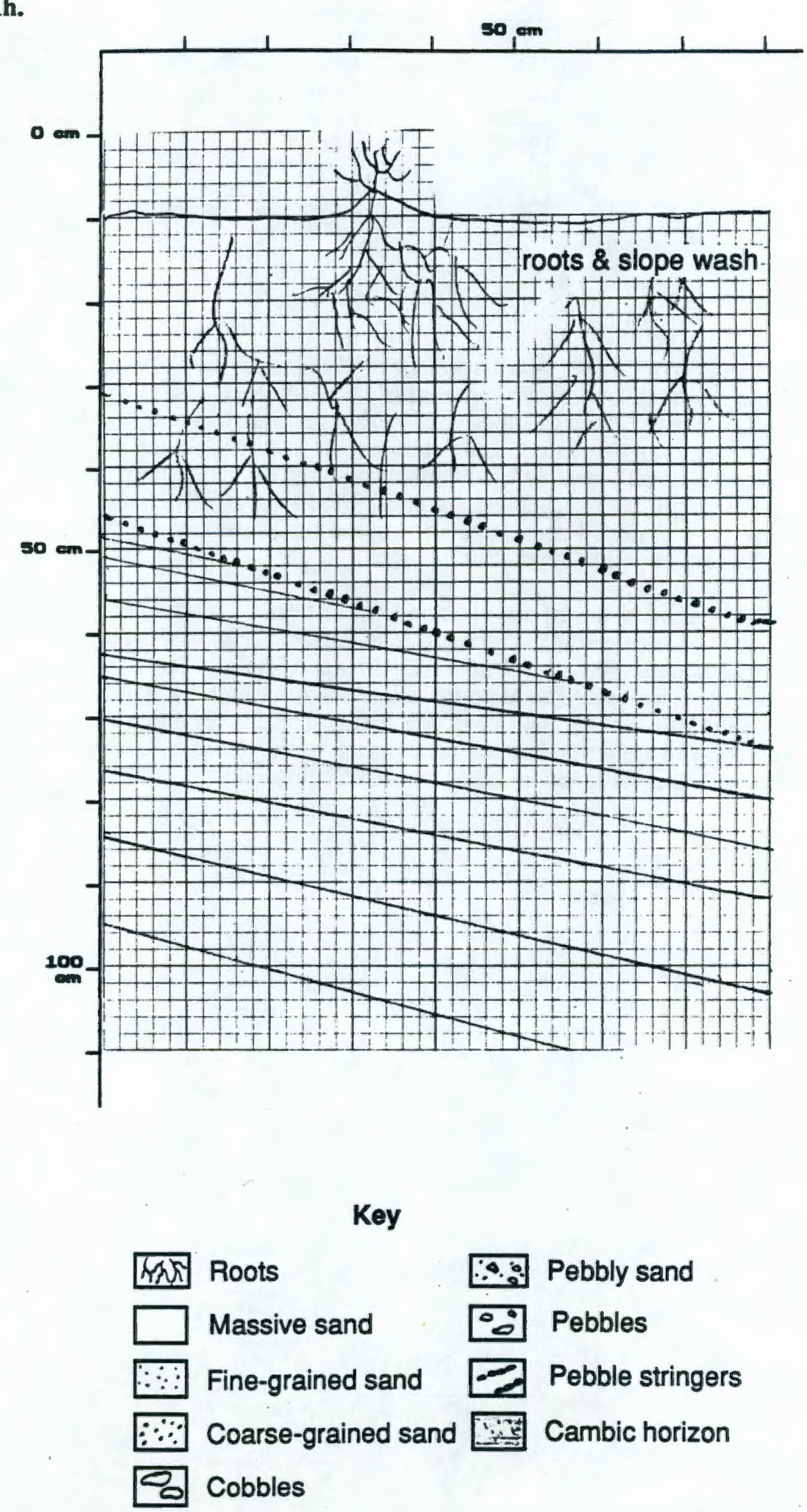
50 cm
0 cm
50 cm
100 cm
roots & slope wash
Key
Roots
Massive sand
Fine-grained sand
Coarse-grained sand
Cobbles
Pebbly sand
Pebbles
Pebble stringers
Cambic horizon

Figure 21i.

Pit Stratigraphy

Location and Morphologic Setting:

HA-90-13 SE1/4SE1/4 Sec 16 T12N R28E

This sample is on the crest of a parabolic dune (10 to 15 m high) which coalesces with other dunes in the area to form a transverse ridgeline which strikes at N10W.

% of Vegetative Cover:

There is no vegetation on the crest of the dune.

Pedogenic Development:

There is no soil at this pit site.

Pit Dimensions and Geometry:

2 m along a trend of N0E; 2 m along a trend of N80E; 1.3 m deep

Textural Characteristics:

Average Grain Size: Bimodal at 1.0 to 1.5 Phi (0.5 to 0.35 mm) and 2.5 to 3.0 Phi (0.177 to 0.125 mm).
Sorting: Lower moderate
Silt & Clay: 2%
Roundness: Medium-grained--subangular to subrounded; Fine-grained--subrounded.

Sand Composition:

Quartz--58%; Basalt--30%; Feldspar--2-3%, Mica--2-3%; Magnetite and chert--1-2%; Lithics--1-2%.
Slight carbonate reaction. Light pinkish-gray.

Sedimentary Structures:

Two distinct periods of deposition are recorded in this pit. The lower 60 cm of the pit consists of strata dipping at approximately 21 to 27°. It consists of light, dense packed, medium-grained sand laminae and beds interbedded with dark, loose packed, coarse-grained sand laminae and beds. Strata between few mm to 2 cm thick. Strata between 40 and 60 cm are at the angle-of-repose (~32°). The upper 40 cm of the pit consists of subcritically climbing translatent strata. It consists of light, dense packed, medium-grained sand laminae and beds interbedded with dark, loose packed, coarse-grained sand laminae and beds. Attitudes of the strata are as follows:

Depth	Strike	Dip	Thickness
40 cm	N15W	13E	1 cm
50 cm	N8W	28E	2 cm
65 cm	N6W	27E	1 cm
70 cm	N11W	21E	1 cm
75 cm	N10W	27E	1 cm
87 cm	N10W	22E	2 cm

Interpretation:

The strata exposed in this pit were deposited predominantly by eolian processes. Strata below 40 cm are interpreted as grainflow deposits interbedded with grainfall deposits. The high angle of dip and dip direction help identify the grainflow deposits. These processes occurred along the active face of an advancing dune. These dune face deposits are probably not very old in lieu of the fact that the modern dune avalanche face is only 3 m from the pit. Angle-of-repose strata between 40 and 60 cm probably represent avalanche-flow processes as they are inversely graded and thin downdip. In the upper 40 cm of the pit, inversely graded sand laminae comprise nearly all of the low-angle cross-strata observed and are interpreted as subcritically climbing translatent cross-strata. Subcritically climbing translatent cross-strata result from translation and accumulation of eolian ripples. An erosional truncation surface exists at 40 cm separating the steep dipping strata below from the low-angle strata above.

Eolian sedimentation at the pit site appears to have been interrupted by at least one major erosional period. There are no pedogenic breaks. The dominance of high-angle stratification suggests that accumulation occurred by sediment fallout and avalanche processes during much of its history. The Mazama ash, though present regionally, was not encountered in this pit. The absence of this distinctive marker unit and the lack of any well-developed soil suggests that the deposits are quite young, and likely younger than the 6700 yr B.P. date assigned to the Mazama volcanic event.

Figure 21i.

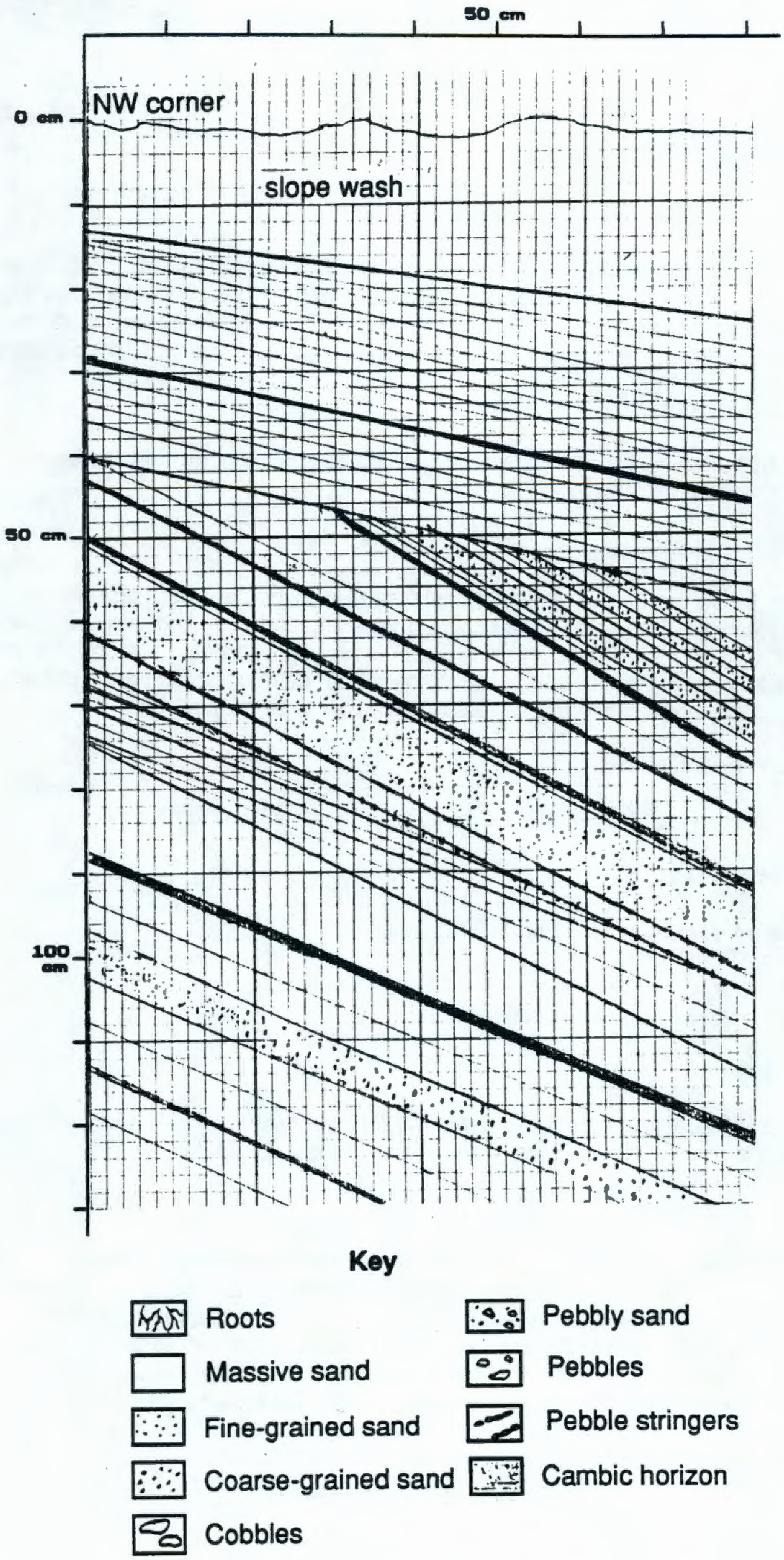
50 cm
0 cm
NW corner
slope wash
50 cm
100 cm
Key
Roots
Massive sand
Fine-grained sand
Coarse-grained sand
Cobbles
Pebbly sand
Pebbles
Pebble stringers
Cambic horizon

Figure 21j.

Pit Stratigraphy

Location and Morphologic Setting:

HA-90-17 SE1/4SE1/4 Sec 9 T12N R28E

Pit is located on top of a small sand ridge which is part of a partially stabilized compound parabolic dune. The surface is composed of small, 1 m high sand swells/ridges about 3 m above the deflation surface. Dune is located near the northeast corner of the active dune field about 200 m west of the Columbia River. Trend of the sand swell/ridges are N75E.

% of Vegetative Cover:

Dune surface is moderately vegetated by grass, green plants, and rare sage. Surface coverage is about 60%.

Pedogenic Development:

The upper 30 cm of this pit may be undergoing early stages of pedogenesis. This horizon is well-packed, darker than the underlying strata, and devoid of stratification due to re-working by root action. A thin (2 cm) layer of bioturbated silty sand is present at about 45 cm and probably is a thin soil horizon which developed beneath a stable surface represented by an overlying pebble rich, coarse-grained sand bed.

Pit Dimensions and Geometry:

1.4 m along a trend of N65E; 1.2 m along a trend of N165E; 1.2 m deep

Textural Characteristics:

Average Grain Size: 1.0 Phi (0.5 mm)
Sorting: Poor
Silt & Clay: 5 to 8%
Roundness: Subangular to subrounded.

Sand Composition:

Quartz--65%; Basalt--30%; Feldspar--2-3%; Mica--3%. Few quartz grains are oxidized, many are coated with caliche. Sand is calcareous. Light tan.

Sedimentary Structures:

Strata below 75 cm are alternations of one to two grain thick, well-packed, light and dark, fine-grained sand laminae interbedded with normally-graded, 1 to 2 cm thick, loosely packed, dark, coarse-grained sand beds. Contacts between the fine- and coarse-grained laminae and beds are sharp and are inclined about 15 to 18° to the northeast. Between 75 and 95 cm are two pebble rich (3 to 5 mm), coarse-grained sand beds, the lowermost of which is inclined about 15° to the northeast and the upper dipping about 8 to 10° to the southeast. Both of these pebble rich, coarse-grained sand beds have undulating surfaces. Between these beds are light, grain thick, fine-grained, undulating sand laminae. Strata between 45 to 75 cm are alternating one-to-two- grain-thick, fine-grained sand laminae interbedded with 0.5 to 2.0 cm thick, coarse-grained sand laminae and beds. Contacts are sharp and inclined 8 to 10° to the southeast. A 2 cm thick, pebble rich (3 to 5 mm diameters), coarse-grained sand bed occurs at a depth of 0.4 m. Both upper and lower contacts are sharp and undulating and are inclined about 3° to the southeast. Immediately below this pebble rich, coarse-grained sand bed is a 1 to 2 cm thick, silty, fine-grained sand bed that is bioturbated. Strata from 30 to 40 cm are 1 to 2 cm thick, normally graded, coarse- and fine-grained sand beds. Contacts are sharp and are inclined about 3 to 5° to the southeast. The uppermost 30 cm of the pit are rooted and bedding has been completely disrupted.

Interpretation:

The strata in this pit were deposited primarily by eolian processes. Alternating light and dark, one-to-two-grain-thick, fine-grained sand laminae dominate the low-angle stratification that are interpreted as subcritically climbing translatent eolian cross-strata. Normally-graded, low-angle cross-laminae are interpreted as vegetatively induced strata; as envisioned here, vegetation at the surface acted as a baffle to sediment transport, thus encouraging deposition. The accumulations of pebbly, coarse-grained sand beds probably record fluvial reworking of the surface during brief meltwater and/or storm events. Concentration of such coarse-grained detritus into discrete beds by wind action alone seems unlikely in lieu of the extreme strengths of sustained winds (43.0 to 52.5 mph calculated for 3 to 5 mm diameter sand) needed to initiate and maintain transport.

Eolian sedimentation at this pit site appears to have been somewhat sporadic with three erosional breaks, the uppermost of which contains a thin soil horizon. The dominance of low-angle stratification suggests that accumulation of sediment was slow and likely influenced by vegetation during parts of its history. The Mazama ash, though present regionally, was not encountered in this pit. The absence of this distinctive marker unit and the lack of any well-developed soil suggests that the deposit is quite young, and likely younger than the 6700 yr B.P. date assigned to the Mazama volcanic event.

Figure 21j.

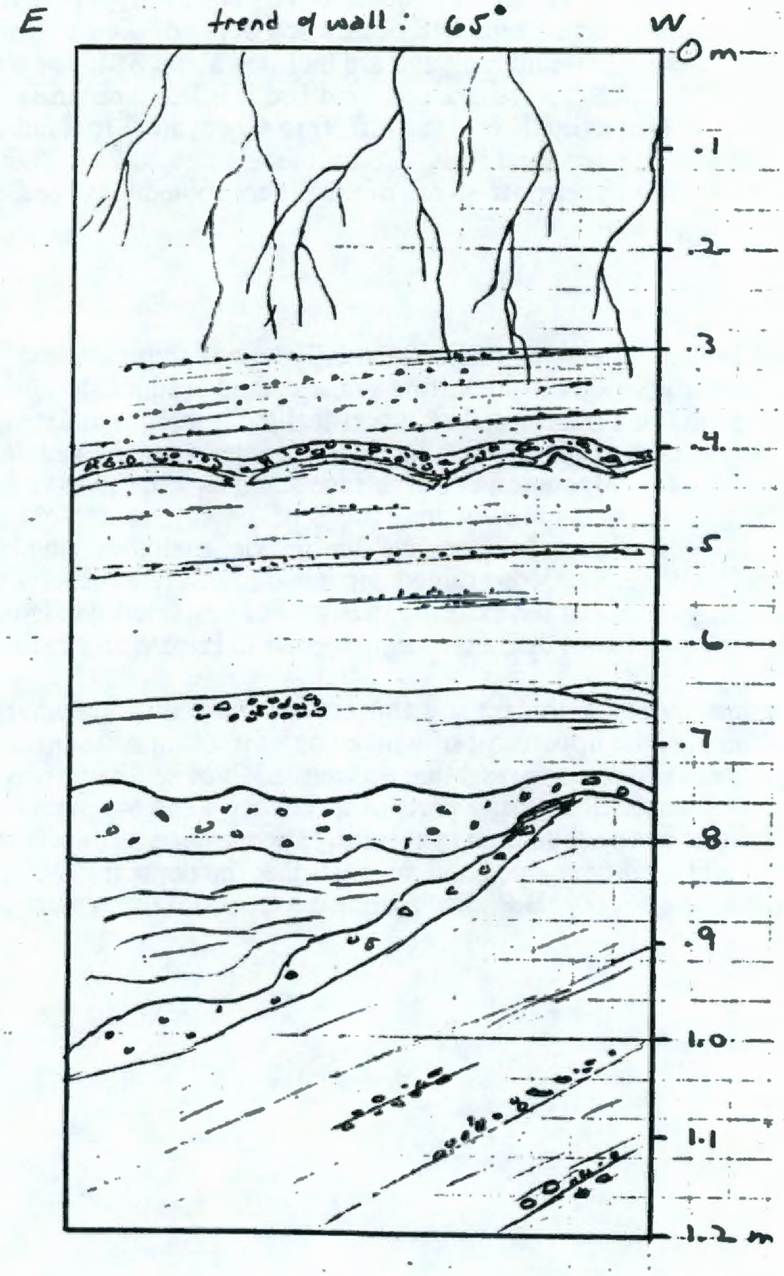

Key

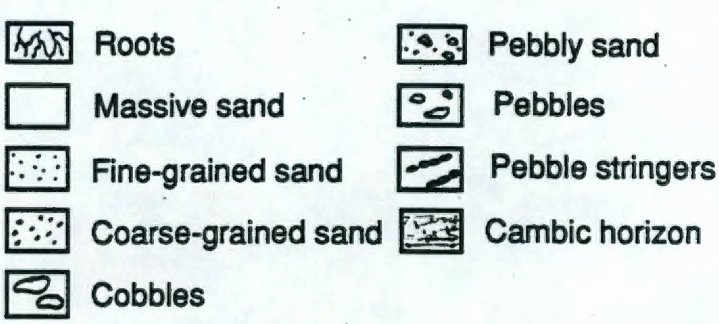

Figure 21k.

Pit Stratigraphy

Location and Morphologic Setting:

HA-90-18 NW1/4SW1/4 Sec27 T12N R28E

Pit located on a sparsely vegetated trailing arm of a parabolic dune which is 1 to 2 m high. Site is about 100 m south of the first active dunes at the southern edge of the active dune field.

% of Vegetative Cover:

Vegetation is spare, comprised mainly of grasses and green plants. About 30 to 40% of the surface is vegetated. A weak concentration of roots extend to about 30 cm.

Pedogenic Development:

No soil is present in this pit.

Pit Dimensions and Geometry:

1.2 m along a trend of N60E; 1.8 m along a trend of N150E; 1.2 m deep

Textural Characteristics:

Average Grain Size: 2.0 Phi (0.25 mm)
Sorting: Moderate to good.
Silt & Clay: 2%
Roundness: Subangular to rounded. Few have sharp fractured edges.

Sand Composition:

Quartz--65%; Basalt--28 to 30%; Feldspar--2 to 3%; Mica--2 to 3%; Chert--1%

Sedimentary Structures:

Strata in this pit consists predominantly of light, one grain to 2 mm thick, well packed fine-grained sand laminae interbedded with dark, 0.5 to 2 cm thick, normally-graded coarse-grained sand laminae and beds. Bedding is uniformly inclined 15° to the northeast. Dry sand leading to a caving slope within the upper 30 cm of the pit obscured any stratification that might exist there. Contacts between the coarse- and fine-grained sand laminae and beds are sharp.

Interpretation:

The strata exposed in this pit were deposited by eolian processes. Low-angle, grain thick to mm thick fine-grained sand laminae are interpreted as subcritically climbing translatent cross-strata that formed during translation and accumulation of eolian ripples. Normally-graded, low-angle, coarse-grained sand laminae and beds make up the remainder of stratification in this pit and are interpreted as vegetatively induced stratification. As envisioned here, vegetation at the surface acted as a baffle to sediment transport thus encouraging deposition.

Eolian sedimentation at the pit site appears to have been continuous with no erosional or pedogenic breaks. The dominance of low-angle stratification suggests that accumulation of sediment was slow and likely influenced by vegetation throughout parts of its history. The Mazama ash, though present regionally, was not encountered in this pit. The absence of this distinctive marker unit and the lack of any well-developed soil suggests that the deposit is quite young, and likely younger than the 6700 yr B.P. date assigned to the Mazama volcanic event.

Figure 21k.

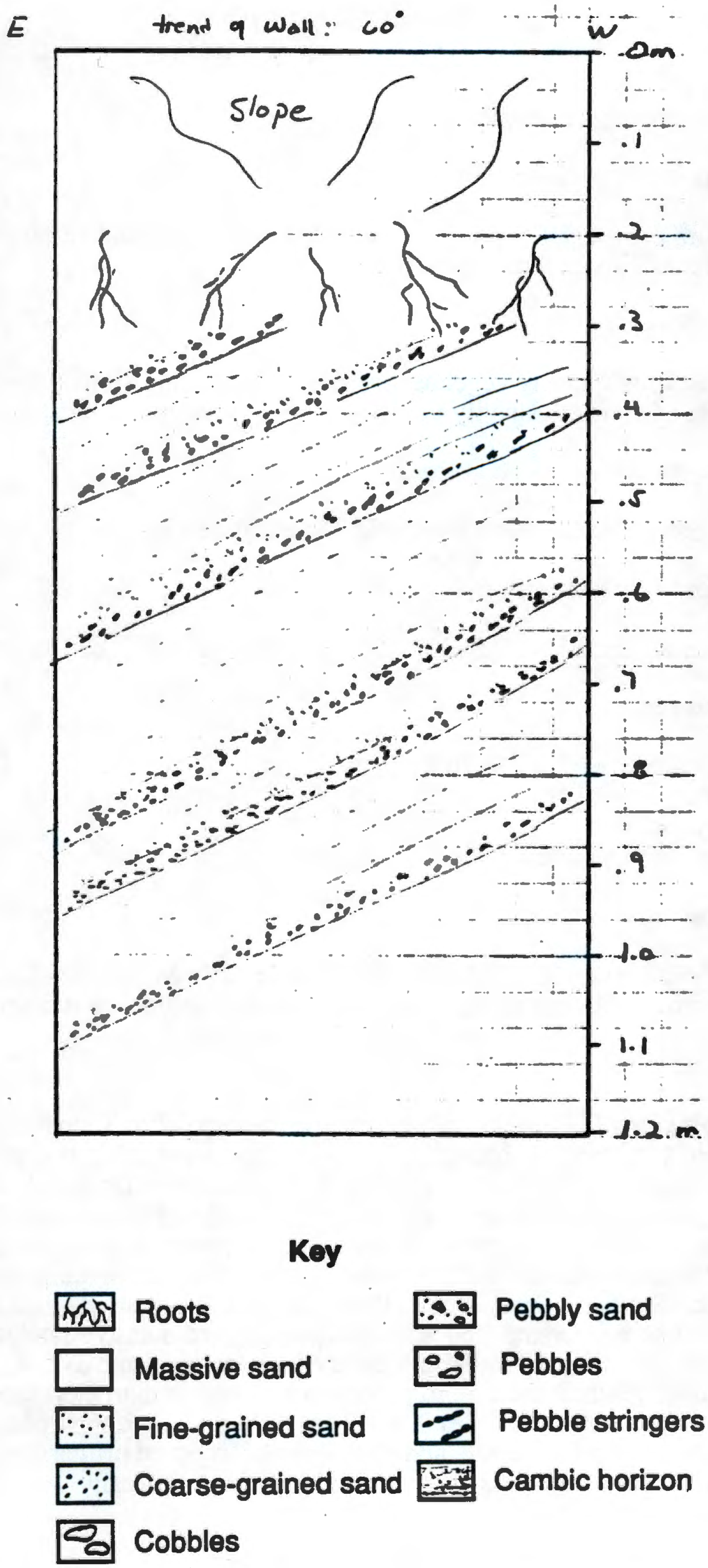
E
trend of Wall: 60°
W
Slope
0m
.1
.2
.3
.4
.5
.6
.7
.8
.9
1.0
1.1
1.2 m
Key
Roots
Massive sand
Fine-grained sand
Coarse-grained sand
Cobbles
Pebbly sand
Pebbles
Pebble stringers
Cambic horizon

Figure 21l.

Pit Stratigraphy

Location and Morphologic Setting:

HB-90-3 SE1/4 NE1/4 Sec 34 T12N R26E

Sample from central deflation bowl on lee side of a stabilized parabolic dune which trends N70°E. Dune is about 2 m high and 20 m wide.

% of Vegetative Cover:

Deflation bowl is sparsely vegetated by grasses providing 10 to 15% cover. Trailing arms and lee side of dune are heavily vegetated (~80%) and are stable.

Pedogenic Development:

No soil is present in deflation bowl or in the excavated pit.

Pit Dimensions and Geometry:

80 cm along a trend of N55°E; 1.2 m along a trend of N160°E; 1 m deep

Textural Characteristics:

Average Grain Size: 2.0 PHI (0.25 mm)
Sorting: Poor
Silt & Clay: <2%
Roundness: Sub-angular to slightly rounded.

Sand Composition:

Quartz--75%; Basalt--20%; Mica--2%; Feldspar--2%; Magnetite--1%; Chert--<1%. Non-calcareous. Several quartz grains are included and/or are oxidized. Light brown.

Sedimentary Structures:

Lower most strata (50 to 100 cm) consists primarily of 2 to 3 mm thick, normally graded, fine-grained sand laminae interstratified with dark, 1 cm thick, coarse-grained sand beds. Fine-grained sand cross-laminae at a depth of 60 cm form tangential foresets with the underlying coarse-grained sand bed and are inclined at 31° to the northeast. All other bedding contacts between fine- and coarse-grained strata are sharp and slightly inclined at 12° to 15° to the northeast. Sand between 35 and 50 cm is medium-grained, massive, and unstratified. Strata between 12 and 35 cm are dark, 1 cm thick, normally-graded, coarse-grained sand beds interstratified with medium-grained massive sand. Sand bed contacts are sharp but pinch out laterally into the medium-grained massive sand. Three normally graded, coarse-grained, granule to pebbly (3 to 5 mm in diameter) sand lenses are located in the upper 12 cm ranging from 0.5 to 2 cm thick and are interstratified with medium-grained massive sand. Granule and pebbles are composed primarily of basalt, quartz, feldspar, and chert. Contacts are sharp and interfinger laterally with medium-grained massive sand.

Interpretation:

The strata exposed in this pit were deposited predominatly by eolian processes. Normally graded low-angle laminae make up the bulk of observed structures and are interpreted as vegetatively-induced stratification; as envisioned here, vegetation at the surface acted as a baffle to sediment transport thus encouraging deposition. The tangential foresets at the 60 cm level record rapid fallout of suspended silt and very fine sand detritus during the migration and preservation of an eolian bedform. The accumulations of massive (structureless) sand identified in the pit are also associated with rapid deposition of suspended eolian sediment. Coarse-grained granule and pebble sand lenses within the upper 12 cm of the pit probably record fluvial reworking during brief meltwater and/or storm events. Concentrations of such coarse-grained detritus into discrete strata by the wind alone seems unlikely in lieu of the extreme strengths of sustained winds (43.0 to 52.5 mph calculated for 3 to 5 mm diameter sand) needed to initiate and maintain transport.

Eolian sedimentation at the pit site appears to have been relatively continuous with no significant erosional or pedogenic breaks. The dominance of low-angle stratification suggests that accumulation of sediment was slow and likely influenced by vegetation during much of its history. The Mazama ash, though present regionally, was not encountered in this pit. The absence of this distinctive marker unit and the lack of any well-developed soil suggests that the deposits are quite young, and likely younger than the 6700 yr B.P. date assigned to the Mazama volcanic event.

Figure 21l.

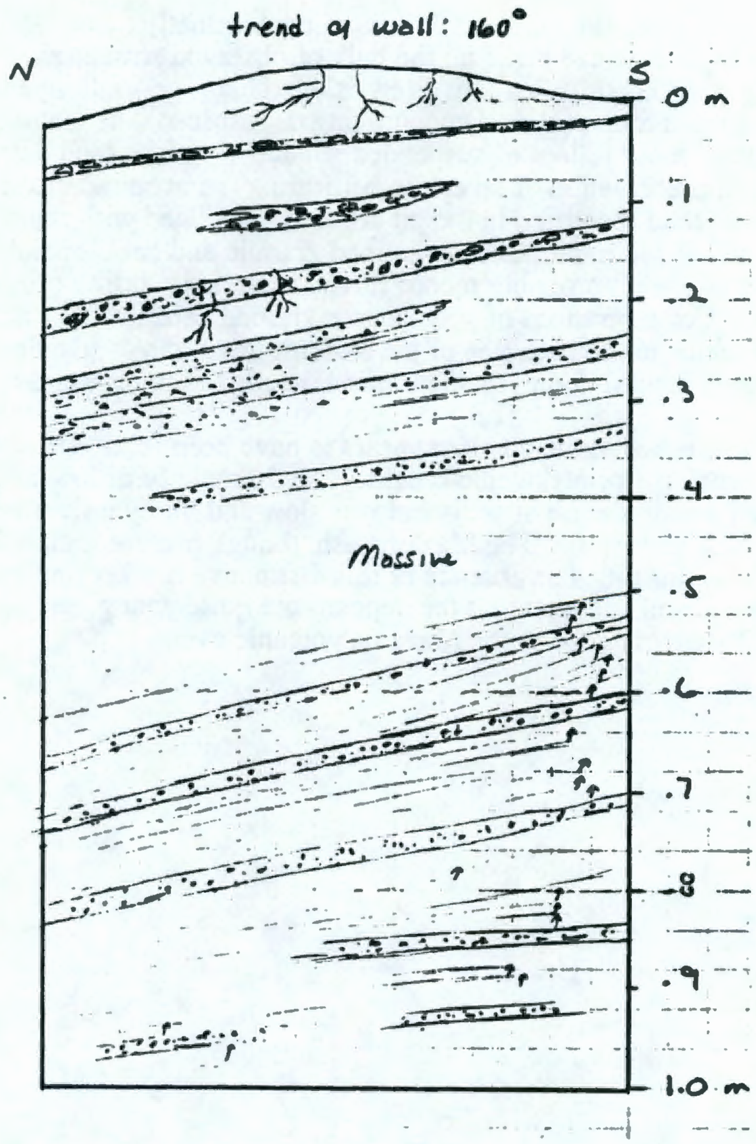

Key

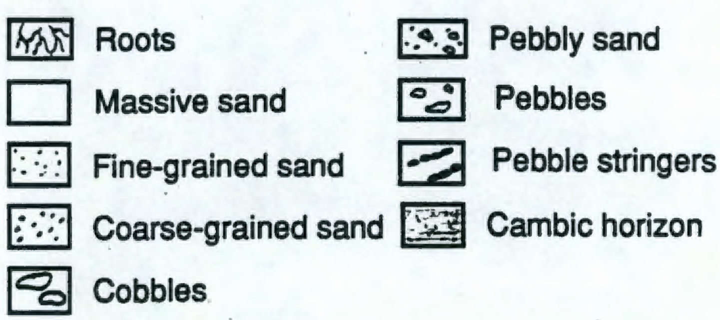

Figure 21m.

Pit Stratigraphy

Location and Morphologic Setting:

HB-90-4 NE1/4SE1/4 Sec 29 T12N R26E

Sample from center of small deflation surface on the stoss side of a partially stabilized trailing arm of a stabilized parabolic dune trending N55E and which builds in height downwind. Maximum relief about 2 m. Dune front is not present.

% of Vegetative Cover:

Sparsely vegetated by grasses, sage rare. ~30% cover. Root mass dense to 30 cm.

Pedogenic Development:

No soil development is present in this pit. Cobbles present at the 20 cm level are coated by caliche on the undersides and possibly represent the early development of a soil horizon.

Pit Dimensions and Geometry:

70 cm along a trend of N55E; 1 m along a trend of N145E; 1 m deep.

Textural Characteristics:

Average Grain Size: 2.5 to 3.0 Phi (0.177 to 0.125 mm)
Sorting: Moderate
Silt & Clay: <2%
Roundness: coarse grains-subangular, medium grains-subangular to rounded.

Sand Composition:

Coarse Fraction: (10% of total) Basalt--70%; Quartz--30%
Medium-Fine Fraction: (90% of total) Quartz--80%; Basalt--15%; Mica and Feldspar--3%; Magnetite--2% Calcareous. Minor oxide stain on quartz. Light brown.

Sedimentary Structures:

The lower 60 cm is composed of medium- to fine-grained, pebble rich (3 to 5 mm diameters), well packed massive sand. The densest concentration of pebbles are located at 40 cm but do not continue across the entire width of the pit wall. Overlying the medium- to fine-grained massive sand are medium- to fine-grained, well packed, one-grain-thick sand laminae which contains few pebbles, extends between 25 and 40 cm, and dip 7° northeast. Alternations between laminae are distinguished by color and grain size variations. The upper 25 cm are medium- to fine-grained, pebble rich, well packed massive sand. Several cobbles (up to 5 cm across) with undersides coated by caliche are located at 20 cm.

Interpretation:

Sedimentary features exhibited in the lower and upper most medium- to fine-grained, pebble rich massive sand suggest lower flow regime deposition. Close proximity to Cold Creek Valley and the presence of nearby fluvial deposits consisting of cobble and boulder lag support this interpretation. Deposition appears to have been largely en-masse. Brief sheet flow processes from meltwater and/or storm events concentrated a pebble lag at 40 cm that delineates a semi-stable surface across which a sand dune migrated. Low-angle, eolian strata between 25 to 40 cm are interpreted as subcritically climbing translatent cross-strata. Sub-critically climbing translatent cross-strata result from translation and accumulation of eolian ripples. Deposition of cobbles at the 20 cm level suggests a brief high velocity fluvial event sufficiently competent to transport cobble sized detritus to this location from the nearby cobble and boulder lag deposits.

The overall fluvial character of the cross-strata and lack of significant eolian breaks suggests a rapid depositional history in a fluvial setting for much this location. Eolian sedimentation capping the fluvial sequence appears to be continuous with no erosional or pedogenic breaks. The Mazama ash, though present regionally, was not encountered in this pit. The absence of this distinctive marker unit and the lack of any well-developed soil suggests that the deposit is quite young, and likely younger than the 6700 yr B.P. date assigned to the Mazama volcanic event.

Figure 21m.

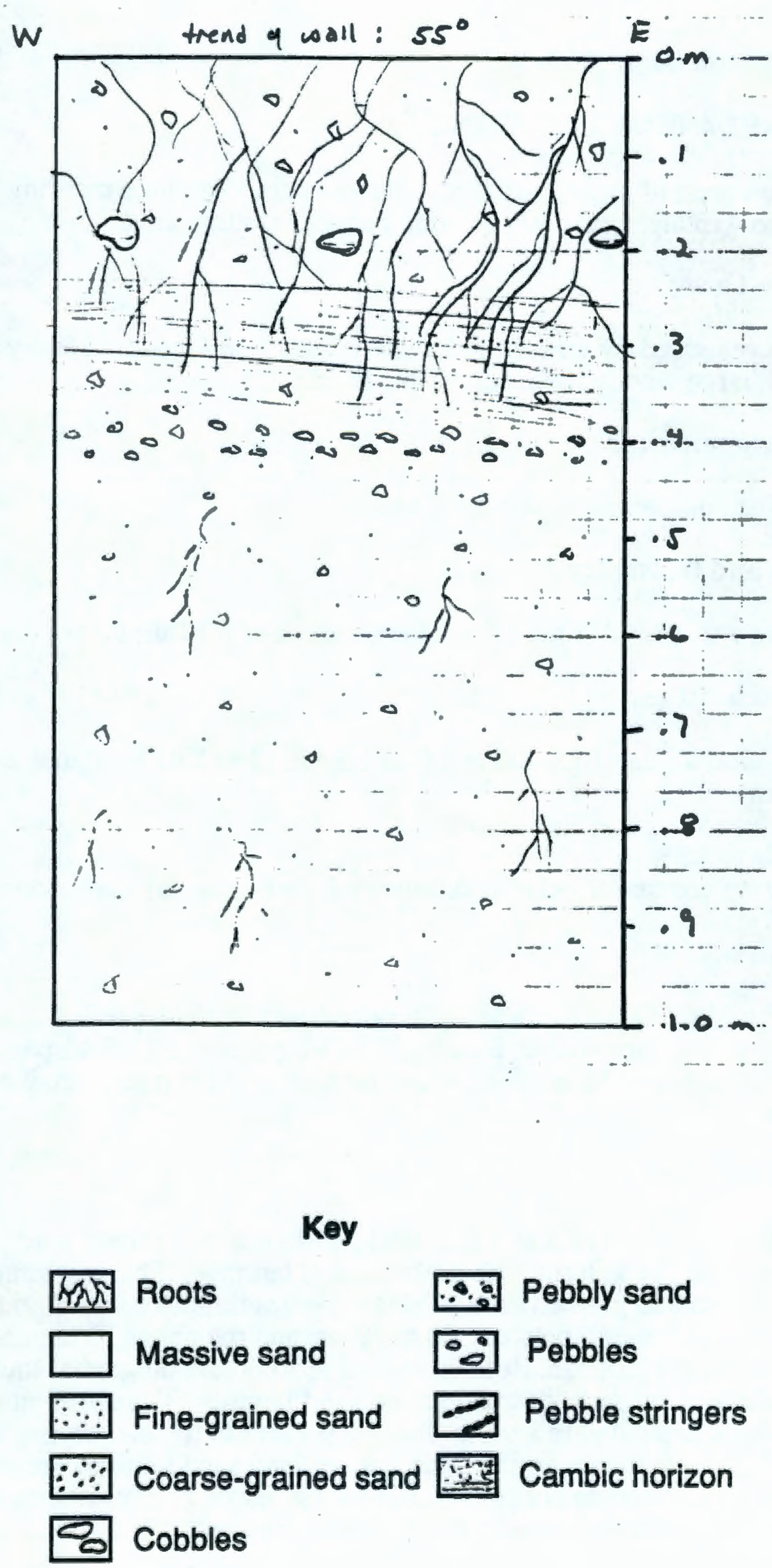
W
trend of wall : 55°
E
0 m
.1
.2
.3
.4
.5
.6
.7
.8
.9
1.0 m
Key
Roots
Massive sand
Fine-grained sand
Coarse-grained sand
Cobbles
Pebbly sand
Pebbles
Pebble stringers
Cambic horizon

Figure 21n.

Pit Stratigraphy

Location and Morphologic Setting:

HB-90-5 NE1/4NE1/4 Sec20 T12N R27E

Sample on crest of large, partially stabilized parabolic dune trending N70E. Dune crest is about 3 to 4 m high and 100's m wide between trailing arms.

% of Vegetative Cover:

Sparsely vegetated by grasses and small plants. ~30% cover. Heavy root mass to 50 cm with few, large woody roots below this level.

Pedogenic Development:

There is no soil present at this location.

Pit Dimensions and Geometry:

1 m along a trend of N50E; 1.5 m along a trend of N140E; 90 cm deep

Textural Characteristics:

Average Grain Size: Bimodal at 1.0 to 1.5 Phi (2 to 1.41 mm) and 2 to 3 Phi (0.25 to 0.125 mm).
Sorting: coarse--poor; fine--moderate
Silt & Clay: <2%
Roundness: coarse--angular to subrounded; fine--angular to rounded.

Sand Composition:

<u>Coarse Fraction:</u> Quartz--50-55%; Basalt--40-45%; Feldspar & Mica--<5%
<u>Fine Fraction:</u> Quartz--70%; Basalt--20%; Magnetite--5%; Feldspar & Mica--5%
Slightly calcareous. Minor oxide stain on quartz. Few quartz are included.
Light tan.

Sedimentary Structures:

Stratification consists of 2 to 3 mm thick, dark, coarse-grained sand laminae interbedded with 2 to 3 mm thick, light, fine-grained sand laminae. Thickest strata are 0.5 cm and occur in the coarse-grained sand laminae. No grading is observed in this pit. Cross-stratification is present between 60 to 70 cm and the upper 10 cm and are composed of fine-grained sand laminae. Both cross-bed sets contain tangential lower contacts and are truncated above by dark, coarse-grained sand laminae. The upper-most cross-laminae appears to be deposited in a scour channel present in the underlying sand. All other contacts between coarse-grained and fine-grained sand laminae are sharp. The apparent dip direction of laminae changes from 4° west below to 3° east above at approximately the 40 cm level. However, true dip for the strata are about 12° northeast.

Interpretation:

The strata exposed in this pit were deposited by eolian processes. Low-angle laminations are interpreted as subcritically climbing translatent cross-strata resulting from translation and accumulation of eolian ripples. The tangential foresets exposed between 60 to 70 cm and again at 10 cm record rapid fallout of suspended silt and very fine sand detritus during the migration and preservation of an eolian bedform. A wind-scour channel was formed into the surface of the sand dune prior to the deposition of the upper set cross-laminae. Wind-induced scour-channels, such as described here, are ubiquitous within and around the active dune field, primarily on partially and sparsely vegetated dunes.

Eolian sedimentation at the pit site appears to have been relatively continuous with no significant erosional or pedogenic breaks. The dominance of low-angle stratification suggests that accumulation of sediment was slow during much of its history. Wind-induced scour-channels are features present within the upper few cm of stratification within a pit or more commonly, on an active dune surface between patches of vegetation, suggesting their formation is probably controlled by recent vegetation deflecting the wind locally into high velocity zones. The Mazama ash, though present regionally, was not encountered in this pit. The absence of this distinctive marker unit and the lack of any well-developed soil suggests that the deposit is quite young, and likely younger than the 6700 yr B.P. date assigned to the Mazama volcanic event.

Figure 21n.

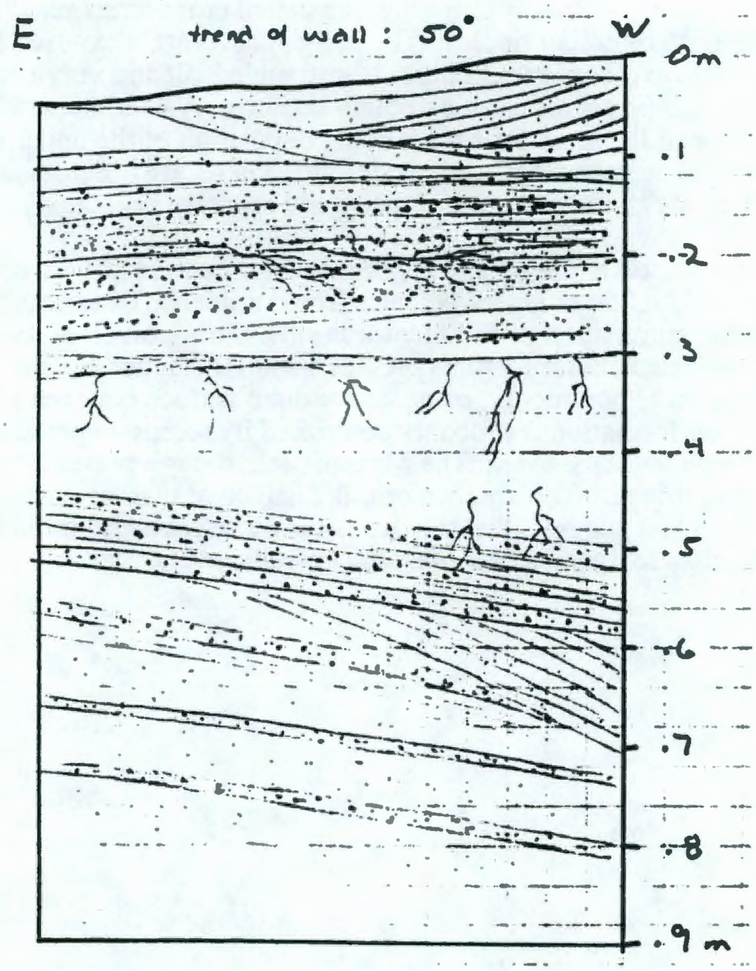

Key

- Roots
- Massive sand
- Fine-grained sand
- Coarse-grained sand
- Cobbles
- Pebbly sand
- Pebbles
- Pebble stringers
- Cambic horizon

Figure 21o.

Pit Stratigraphy

Location and Morphologic Setting:

HB-90-6 SE1/4 NW1/4 Sec 28 T12N R27E

This sample is on the north limb of a stabilized parabolic dune. The strike of the crest on the north limb of the dune is N85E. The center of the parabolic dune has been truncated by a blowout.

% of Vegetative Cover:

lightly vegetated with grass and brush
15% cover.

Pedogenic Development:

There is no soil present at this pit site..

Pit Dimensions and Geometry:

1.4 m along a trend of N10W; 1.2 m along a trend of N80E; 1 m deep

Textural Characteristics:

Average Grain Size: Bimodal at 1.0 to 1.5 Phi (0.5 to 0.35 mm) and 2.5 to 3.0 Phi (0.177 to 0.125 mm)
Sorting: Poor
Silt & Clay: <2%
Roundness: Angular to subrounded.

Sand Composition:

Medium Fraction: Quartz--58%; Basalt--58%; Chert--2%; Spar--2%
Fine Fraction: Quartz--60%; Basalt--30%; Feldspar--3%; Chert--2%; Muscovite--2%; Magnetite--1%; Mica--2%
Slight carbonate reaction. Light grayish-orange.

Sedimentary Structures:

This pit consists of subcritically climbing translatent strata interbedded with grainfall deposits. The subcritically climbing translatent strata occur as approximately 3 mm thick fining upward couplets located below 80 cm and above 30 cm. The strata are composed of alternating light, medium-grained sand laminae interbedded with dark, coarse-grained sand laminae. Between 30 and 80 cm is a massive, medium-grained sand. Four dark, coarse-grained thin sand beds (1 cm thick) are located within the massive sand; these are at 80, 70, 62, and 30 cm deep. Attitudes of the strata are as follows:

Depth	Strike	Dip	Thickness
2 cm	N10W	2E	1 cm
32 cm	N10W	2E	1 cm
62 cm	N10W	5E	1 cm
100 cm	N10W	3E	1 cm

Interpretation:

The strata exposed in this pit were deposited predominantly by eolian processes. Normally-graded sand laminae comprise nearly all of the low-angle cross-strata observed and are interpreted as low-angle cross-laminae and grainfall deposits. Normally-graded low-angle cross-laminae are interpreted as vegetatively induced stratification; as envisioned here, vegetation at the surface acted as a baffle to sediment transport, thus encouraging deposition.

Eolian sedimentation at the pit site appears to have been relatively continuous with no significant erosional or pedogenic breaks. The dominance of low-angle stratification suggests that accumulation of sediment was slow and likely influenced by vegetation during much of its history. The Mazama ash, though present regionally, was not encountered in this pit. The absence of this distinctive marker unit and the lack of any well-developed soil suggests that the deposits are quite young, and likely younger than the 6700 yr B.P. date assigned to the Mazama volcanic event.

Figure 21o.

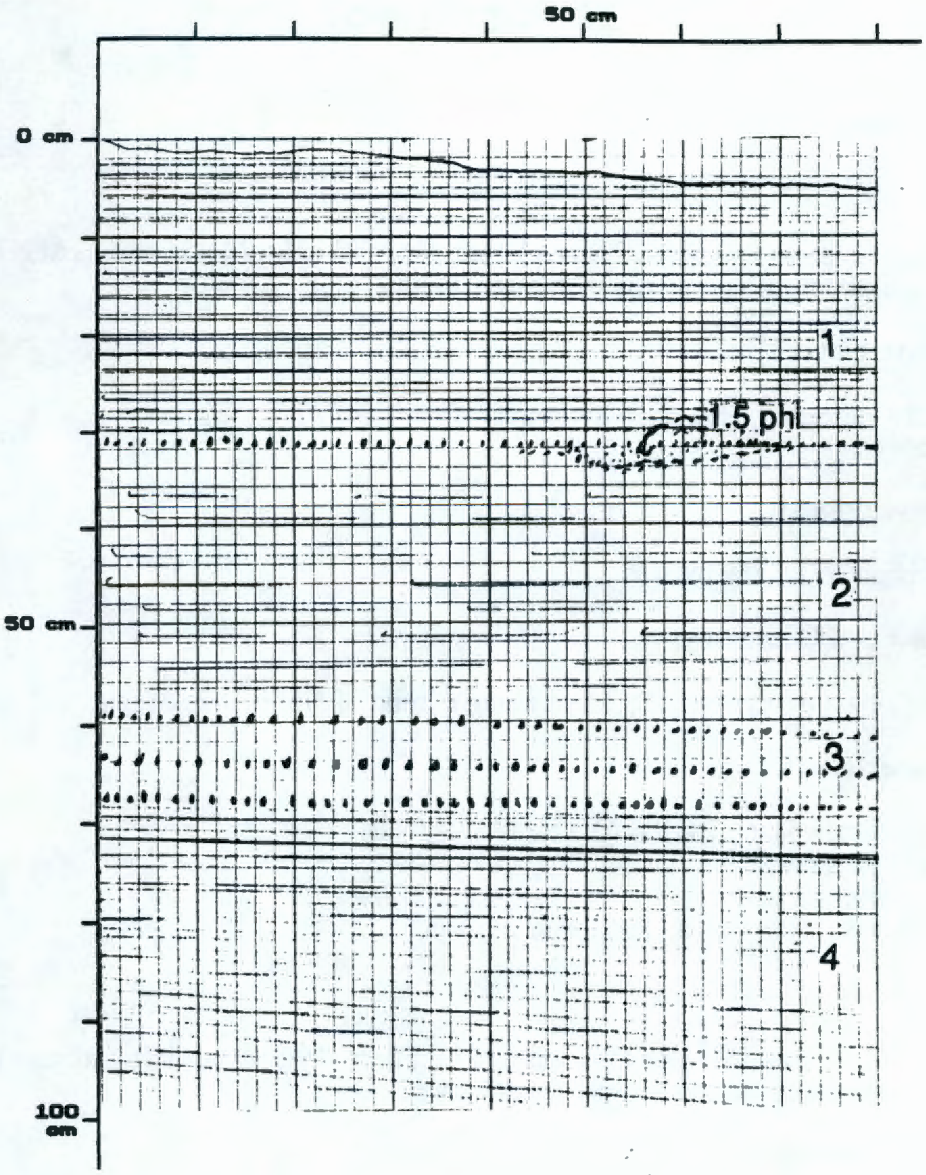
50 cm
0 cm
50 cm
100 cm
1
1.5 phi
2
3
4

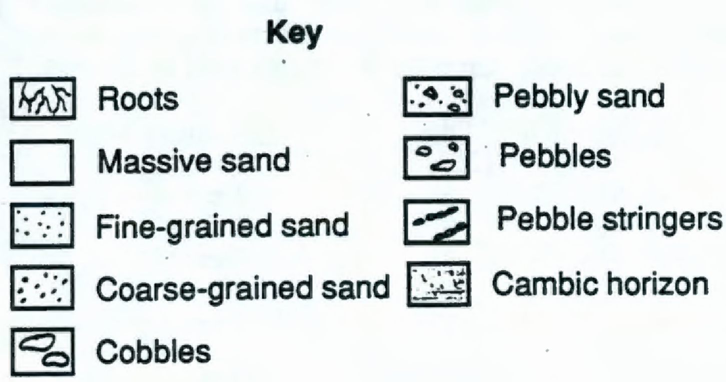
Key
Roots
Massive sand
Fine-grained sand
Coarse-grained sand
Cobbles
Pebbly sand
Pebbles
Pebble stringers
Cambic horizon

Figure 21p.

Pit Stratigraphy

Location and Morphologic Setting:

HB-90-8 SW1/4SW1/4 Sec 14 T12N R27E

This sample is on top of a stabilized linear dune (10 m high) that strikes at N75E. The surface of the dune is covered with a coarse basalt lag.

% of Vegetative Cover:

Sparsely vegetated with grass and brush
15% cover.

Pedogenic Development:

There is no soil at the pit site.

Pit Dimensions and Geometry:

1.6 m along a trend of S35E; 1.1 m along a trend of N55E; 1 m deep

Textural Characteristics:

Average Grain Size: 1.0 Phi (0.5 mm)
Sorting: Moderate
Silt & Clay: <2%
Roundness: Subrounded to rounded

Sand Composition:

Quartz--60%; Basalt--35%; Magnetite--2%; Chert--1%; Mica--1%; Lithics--1%
Slight carbonate reaction. Light tan to brown.

Sedimentary Structures:

This pit consists of subcritically climbing translatent strata. The strata are composed of alternating light, medium-grained sand laminae and beds interbedded with dark, coarse-grained sand laminae and beds. Below 60 cm, the dark, coarse-grained sand laminae and beds are regularly spaced about 5 cm apart. The interbedded fine-grained strata contain faint foreset laminations. Between 15 and 30 cm is a massive sand. The upper 15 cm of the pit is weakly stratified. Attitudes of the strata are as follows:

Depth	Strike	Dip	Thickness
15 cm	N27E	12SE	1 cm
32 cm	N15E	8E	1 cm
40 cm	N15E	8E	1 cm
45 cm	N0E	7E	1 cm
62 cm	N1W	6E	1 cm
75 cm	N5E	7E	1 cm

Interpretation:

The strata exposed in this pit were deposited predominantly by eolian processes. Inversely graded sand laminae comprise nearly 50% of the low-angle cross-strata observed and are interpreted as subcritically climbing translatent cross-strata. Subcritically climbing translatent cross-strata result from translation and accumulation of eolian ripples. Normally graded low-angle cross-laminae make up the bulk of the remaining low-angle cross-strata and are interpreted as vegetatively induced stratification; as envisioned here, vegetation at the surface acted as a baffle to sediment transport, thus encouraging deposition.

Eolian sedimentation at the pit site appears to have been relatively continuous with no significant erosional or pedogenic breaks. The dominance of low-angle stratification suggests that accumulation of sediment was slow and likely influenced by vegetation during much of its history. The Mazama ash, though present regionally, was not encountered in this pit. The absence of this distinctive marker unit and the lack of any well-developed soil suggests that the deposits are quite young, and likely younger than the 6700 yr B.P. date assigned to the Mazama volcanic event.

Figure 21p.

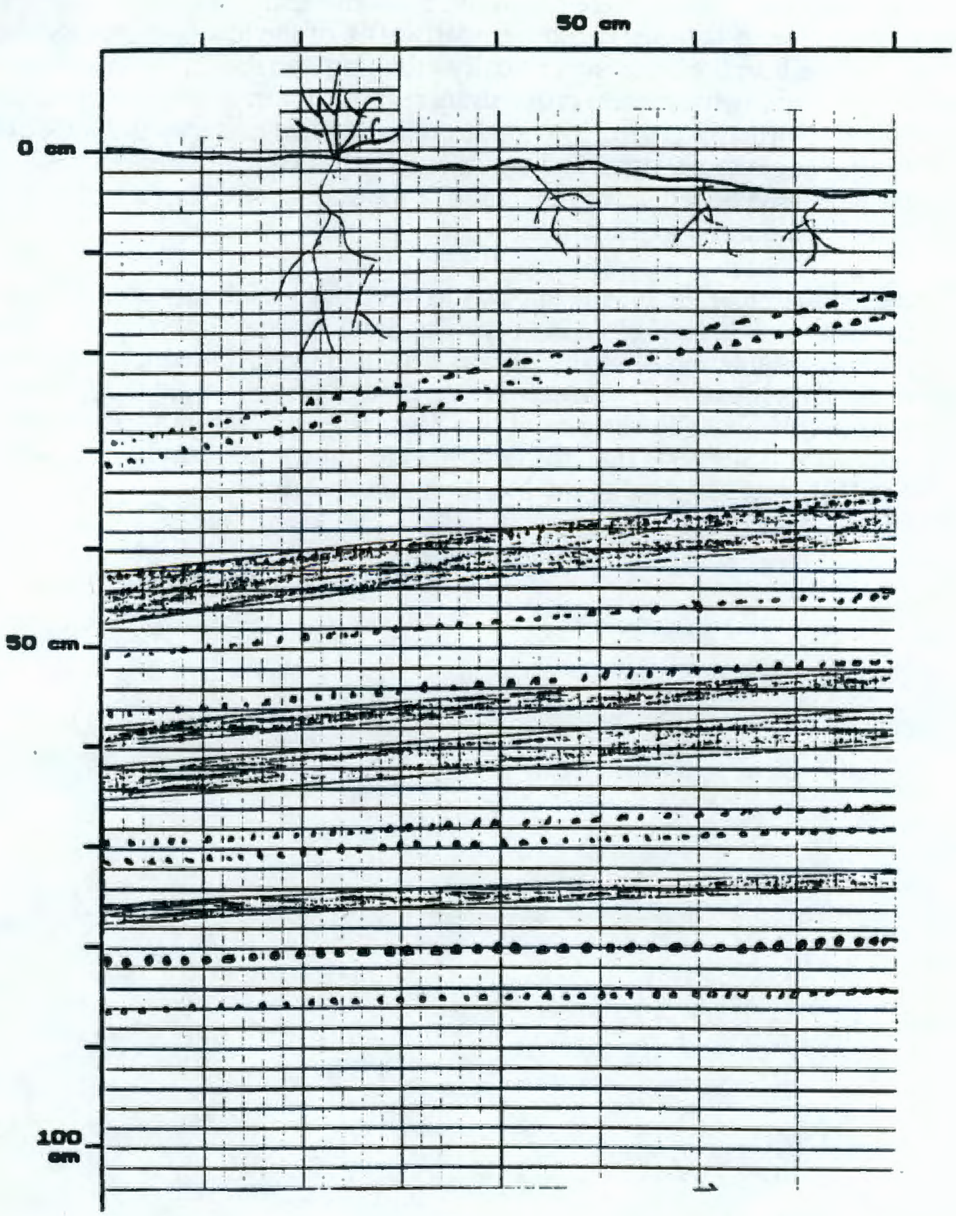

Key

- Roots
- Massive sand
- Fine-grained sand
- Coarse-grained sand
- Cobbles
- Pebbly sand
- Pebbles
- Pebble stringers
- Cambic horizon

Figure 21q.

Pit Stratigraphy

Location and Morphologic Setting:

HC-90-4 NE1/4NW1/4 Sec21 T11N R27E

Pit located at the intersection of a stabilized trailing arm of a stabilized parabolic dune and the downwind edge of a large deflation surface (800 m long by 200 m wide) about 2 km northeast of Cold Creek Valley.

% of Vegetative Cover:

This area is heavily vegetated by grasses, green plants, and rare sage covering up to 70% of the surface. Root mass is dense to 10 cm with woody roots extending the entire pit depth.

Pedogenic Development:

A dark, well packed, developing cambic horizon extends from the surface to a depth of 40 cm. It is composed of silty, medium- to fine-grained sands. Below 40 cm, color becomes lighter.

Pit Dimensions and Geometry:

80 cm along a trend of N70E; 1 m along a trend of N160E; 90 cm deep

Textural Characteristics:

Average Grain Size: 1.5 Phi (0.35 mm)
Sorting: Poor
Silt & Clay: 5 to 8%
Roundness: Majority of grains are subangular to subrounded. Many have sharp, fractured edges.

Sand Composition:

<u>Sand:</u> Basalt--50%; Quartz--45%; Feldspar--2-3%; Mica--2%
<u>Others:</u> Pebbles mainly quartz and basalt; Cobbles mainly granite, gneiss, quartzite.

Sedimentary Structures:

Sediment is a dark, poorly sorted, unstratified pebbly sand. Cobbles (up to 12 cm) are found below 45 cm and do not have a preferred orientation. Cobbles are encountered at 45, 60, 70, and 80 cm below the surface. One or more sides of the cobbles are coated with caliche. Above 45 cm, the sediment is unchanged except for the absence of cobbles. A cambic horizon appears to have developed between 0 and 40 cm.

Interpretation:

The strata in this pit were deposited by fluvial processes as indicated by the textural and depositional character of the pebbly sands. The presence of cobbles in a poorly sorted matrix, and lack of sedimentary structures suggests rapid deposition of a homogeneous mass. It is not probable that bedding was disrupted by bioturbation since no such activity was observed at any other sample sites. Several exposures of cobble and boulder lag deposits which were fluvially derived were clearly evident near the pit.

Fluvial sedimentation at the pit site appears to have been rapid. Pedogenic activity is evident within the upper 40 cm suggesting that this area has undergone little if any depositional or erosional modifications during the recent past. The presence of a heavy vegetative cover on the surface supports this interpretation. The Mazama ash, though present regionally, was not encountered in this pit. The absence of this distinctive marker unit and the lack of any well-developed soil suggests that the deposit is quite young, and likely younger than the 6700 yr B.P. date assigned to the Mazama volcanic event.

Figure 21q.

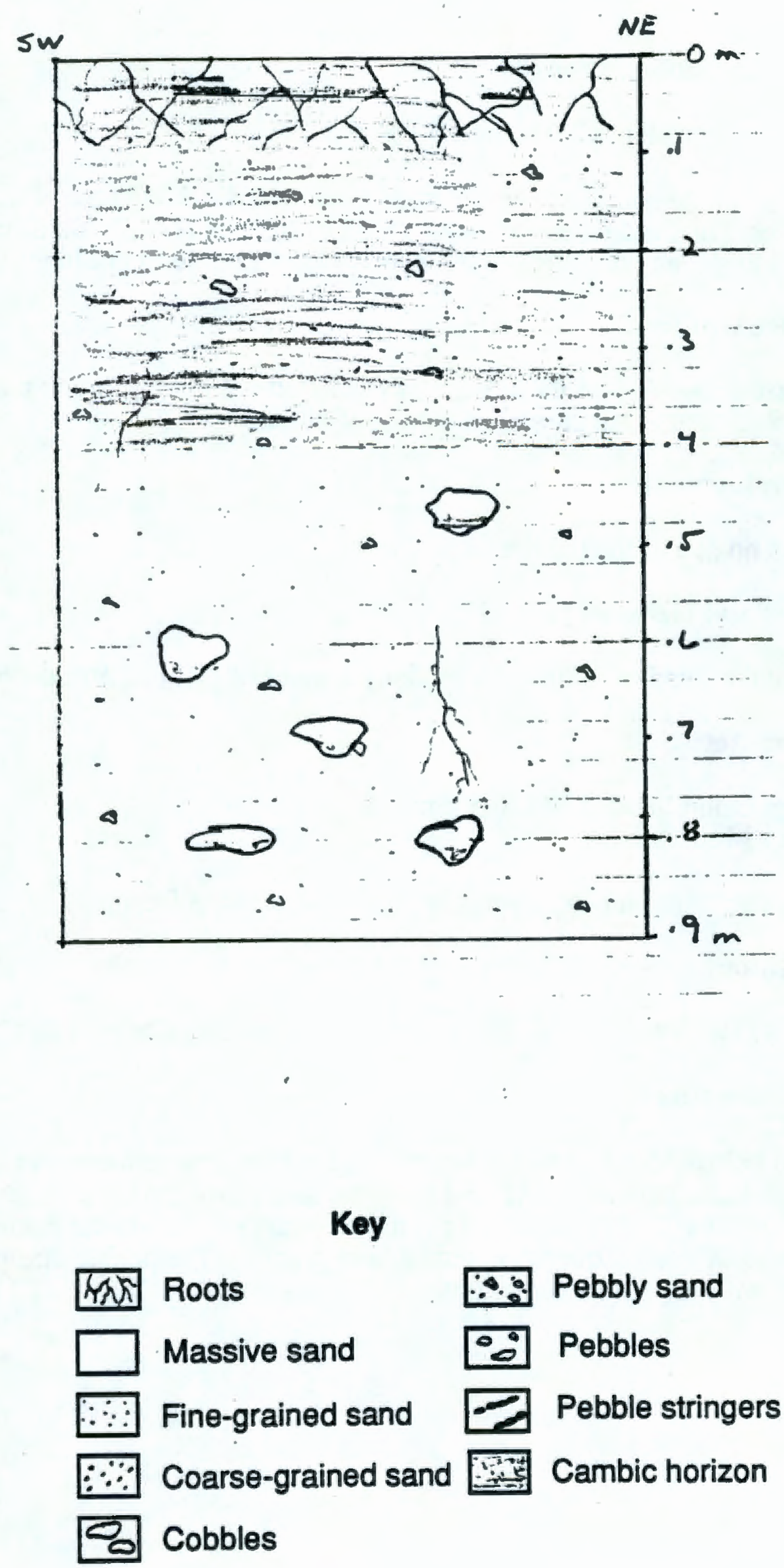
SW
NE
0 m
.1
.2
.3
.4
.5
.6
.7
.8
.9 m
Key
Roots
Massive sand
Fine-grained sand
Coarse-grained sand
Cobbles
Pebbly sand
Pebbles
Pebble stringers
Cambic horizon

Figure 21r.

Pit Stratigraphy

Location and Morphologic Setting:

HC-90-6 NE1/4SE1/4 Sec12 T11N R26E

Pit site is on the south side of a partially stabilized trailing arm of a parabolic dune located about 1/2 mi. east of Cold Creek Valley. Trend of dune is N70E. Maximum relief is about 1 to 2 m. Surrounding area contains several exposures of cobble to boulder lag deposits.

% of Vegetative Cover:

Approximately 60% of the surface is vegetated with grass, green plants, and sage. Root density in the pit is sparse but extend to depths of 80 cm.

Pedogenic Development:

There is no soil at the pit site.

Pit Dimensions and Geometry:

1 m along a trend of N70E; 1.2 m along a trend of N160E; 1 m deep

Textural Characteristics:

Average Grain Size: 1 Phi (0.5 mm)
Sorting: Moderate
Silt & Clay: <2%
Roundness: Angular to subangular, many with sharp fractured edges. Fine grains are rounded.

Sand Composition:

Quartz--75%; Basalt--20%, Mica--2%, Feldspar--2%, Chert--1%. Calcareous. Light gray.

Sedimentary Structures:

Deposit below 45 cm is a light coarse- to medium-grained massive sand. Overlying the massive sand is a light, pebble rich (3 to 8 cm) coarse-grained massive sand which extends from the surface to 45 cm. At 20 cm there is a well-rounded, matrix supported cobble lag. Cobbles are composed of quartz, quartzite, basalt, and granite. The pebble composition is the same as the cobbles with the addition of chert.

Interpretation:

Sedimentation at this pit site appear to be deposited primarily by fluvial processes. The lower 45 cm of massive sand is interpreted as being deposited rapidly by the waning stages of a flood event. Similarly, the overlying massive, pebbly sand is also interpreted as forming from rapid deposition by a flood event. The presence of sharp, fractured edges on the majority of the grains and the close proximity to Cold Creek Valley support this interpretation. Deposits of cobble and boulder lag are ubiquitous in this area and probably were the source of the cobbles which were transported to this location during a brief but intense meltwater and/or storm event. Erosion of the surface is currently removing the fine grain sand sized material and concentrating a pebble lag on the surface.

Fluvial sedimentation at the pit site appears to have been rapid and relatively continuous with no significant erosional breaks. The Mazama ash, although present regionally, was not encountered in this pit. The absence of this distinctive marker horizon and the lack of any well-developed soil suggests that the deposit is quite young, and likely younger than the 6700 yr B.P. date assigned to the Mazama event.

Figure 21r.

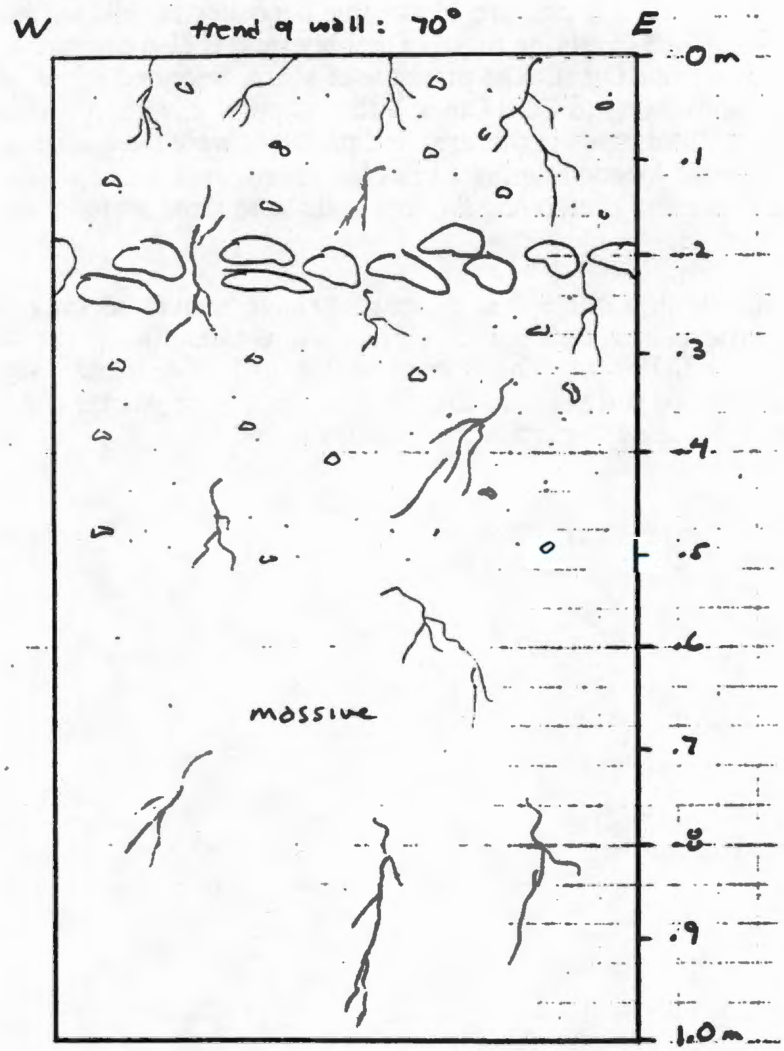
W
trend of wall: 70°
E
0 m
.1
.2
.3
.4
.5
.6
.7
.8
.9
1.0 m
massive

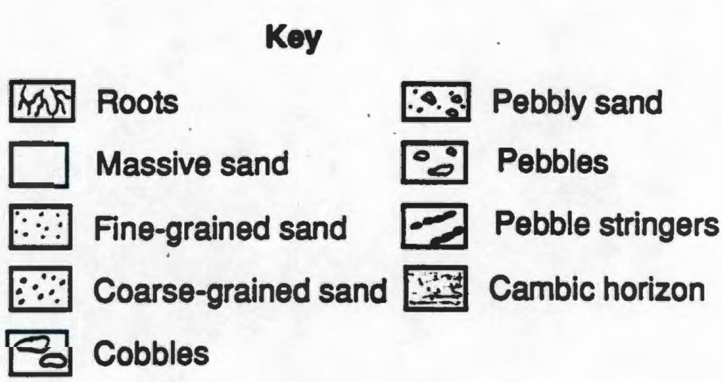
Key
Roots
Massive sand
Fine-grained sand
Coarse-grained sand
Cobbles
Pebbly sand
Pebbles
Pebble stringers
Cambic horizon

Figure 21s.

Pit Stratigraphy

Location and Morphologic Setting:

HD-90-2 SW1/4NE1/4 Sec 29 T10N R28E

This sample is in a slightly deflated area on top of a large (30 m) linear dune which strikes at N50E. This is the first major dune north of the flood plain of the Yakima River.

% of Vegetative Cover:

Sparsely vegetated with grass and brush. ~15% cover.

Pedogenic Development:

A weak cambic horizon is developing in the upper 20 cm of the pit. This is marked by a slightly brighter color than the lower sediments.

Pit Dimensions and Geometry:

0.80 m along a trend of S50E; 0.60 m along a trend of N50E; 0.77 m deep

Textural Characteristics:

Average Grain Size: 0.5 Phi (0.71 mm)
Sorting: Poor
Silt & Clay: Approximately 10% in upper 20 cm, <2% below 20 cm
Roundness: Angular to subangular

Sand Composition:

Quartz--60%; Basalt--25%; Feldspars--10%; Mica--4%; Chert--1%
No carbonate reaction. Light tan to yellow.

Sedimentary Structures:

This pit consists of subcritically climbing translatent strata. The strata are composed of light, medium-grained sand laminae interbedded with dark, coarse-grained sand laminae. Attitudes of the strata are as follows:

Depth	Strike	Dip	Thickness
30 cm	N35W	10NE	3 mm
54 cm	N35W	10NE	1 mm
64 cm	N35W	10NE	1 mm

Interpretation:

The strata in this pit were deposited predominantly by eolian processes. The low-angle cross-strata that are seen in this pit are interpreted as subcritically climbing translatent cross-strata. Normally-graded cross-laminae are interpreted as vegetatively induced stratification. The vegetation would have served as a baffle to sediment transport.

The presence of soil properties at the pit site indicates that this surface has been stable for some time. A cambic horizon is one of the first stages of Aridisol development. A cambic horizon, as seen in this pit, could have developed in approximately 100 years. The Mazama ash, though present regionally, was not encountered in this pit. The absence of this distinctive marker unit and the lack of any well-developed soil suggests that the deposits are quite young, and likely younger than the 6700 yr B.P. date assigned to the Mazama volcanic event.

Figure 21s.

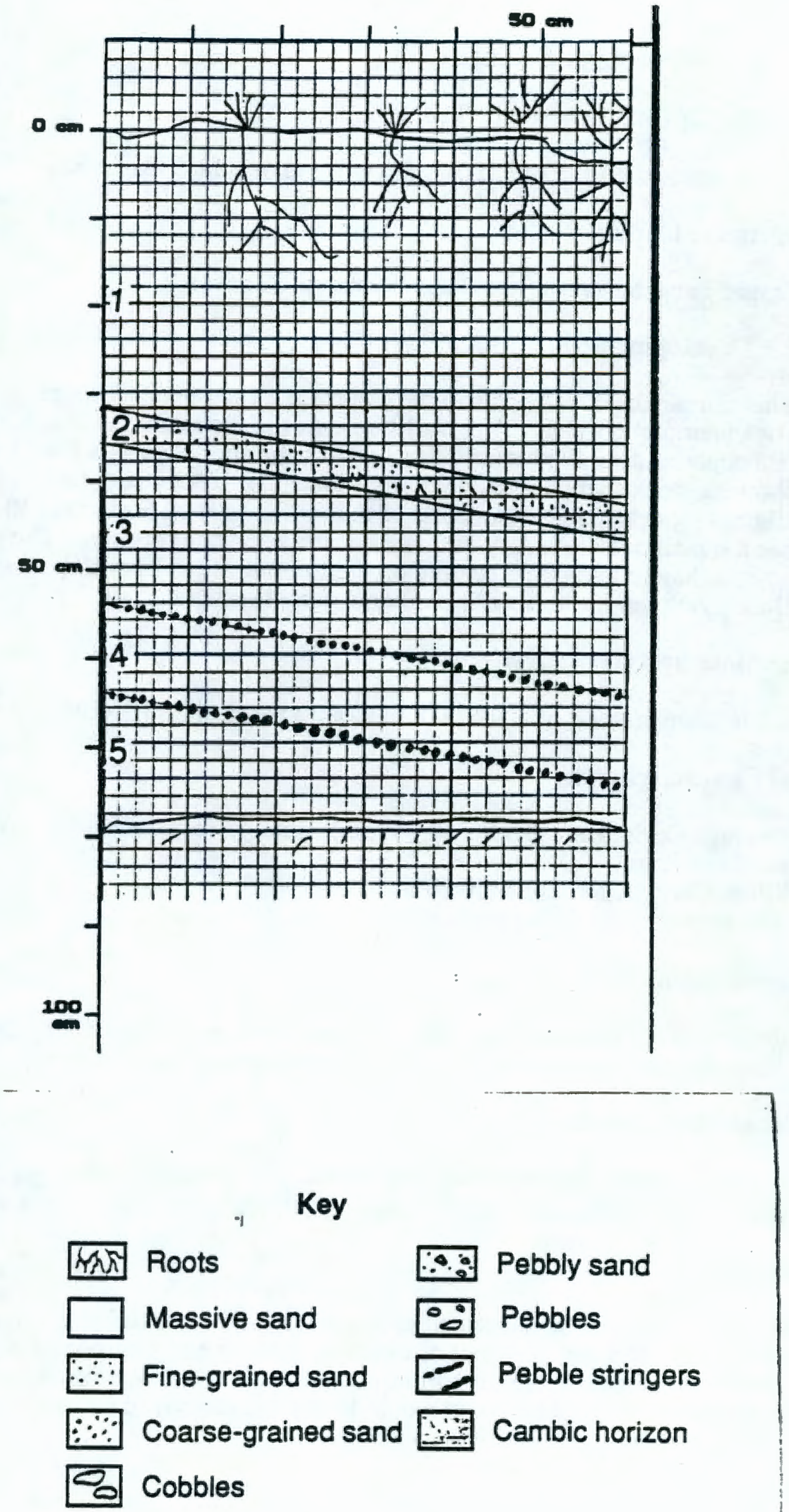
50 cm
0 cm
1
2
3
50 cm
4
5
100 cm
Key
Roots
Massive sand
Fine-grained sand
Coarse-grained sand
Cobbles
Pebbly sand
Pebbles
Pebble stringers
Cambic horizon

Figure 21t.

Pit Stratigraphy

Location and Morphologic Setting:

HD-90-4 SE 1/4NE1/4 Sec 13 T10N R27E

This sample is on top of a broad, flat ridge above the Yakima River flood plain.

% of Vegetative Cover:

Densely vegetated with grass and brush. ~50% cover.

Pedogenic Development:

This sample displays good soil development. The upper 15 cm of the soil forms a thin Bw1 (cambic) horizon. This Bw1 horizon is in the main root-mass. The Bw1 is loose and contains no soil structure. Below the main root-mass is a Bw2 (cambic) horizon showing weak to moderate, medium, subangular blocky structure. The Bw2 is just slightly more red than other parts of the soil. The Bw2 horizon is 40 cm thick. The Bw2 has a transitional boundary with a Bk (carbonate-rich) horizon. The pebbles in the Bk horizon have a carbonate coating on their bottomside. The Bk horizon is 20 cm thick. Underlying the Bk horizon is unaltered parent material.

Pit Dimensions and Geometry:

1.1 m along a trend of N50E; 0.8 m along a trend of S35E; 0.95 m deep

Textural Characteristics:

Average Grain Size: 0.5 Phi (0.71 mm); small (3 to 5 mm) pebbles throughout the pit
Sorting: Poor
Silt & Clay: Approximately 10%
Roundness: Angular to subangular

Sand Composition:

Quartz--60%; Basalt--30%; Feldspar--5-6%; Mica--2-3%; Others--2%
Minor iron oxide staining is present. Moderate carbonate reaction.

Sedimentary Structures:

No sedimentary structures were observed. The sand is medium-grained and massive. Small (3 to 5 mm) pebbles, primarily basalt, feldspar, and quartz occur throughout the pit.

Interpretation:

The extent of soil development at this pit site indicates that this soil has been stable for a long time. The development of a cambic horizon and a carbonate horizon suggests that this soil has been stable for a minimum of 1000 years. Any sedimentary structures that may have existed in this sand would have been destroyed by root activity over a 1000 year time period. This soil is an Aridisol.

Figure 21t.

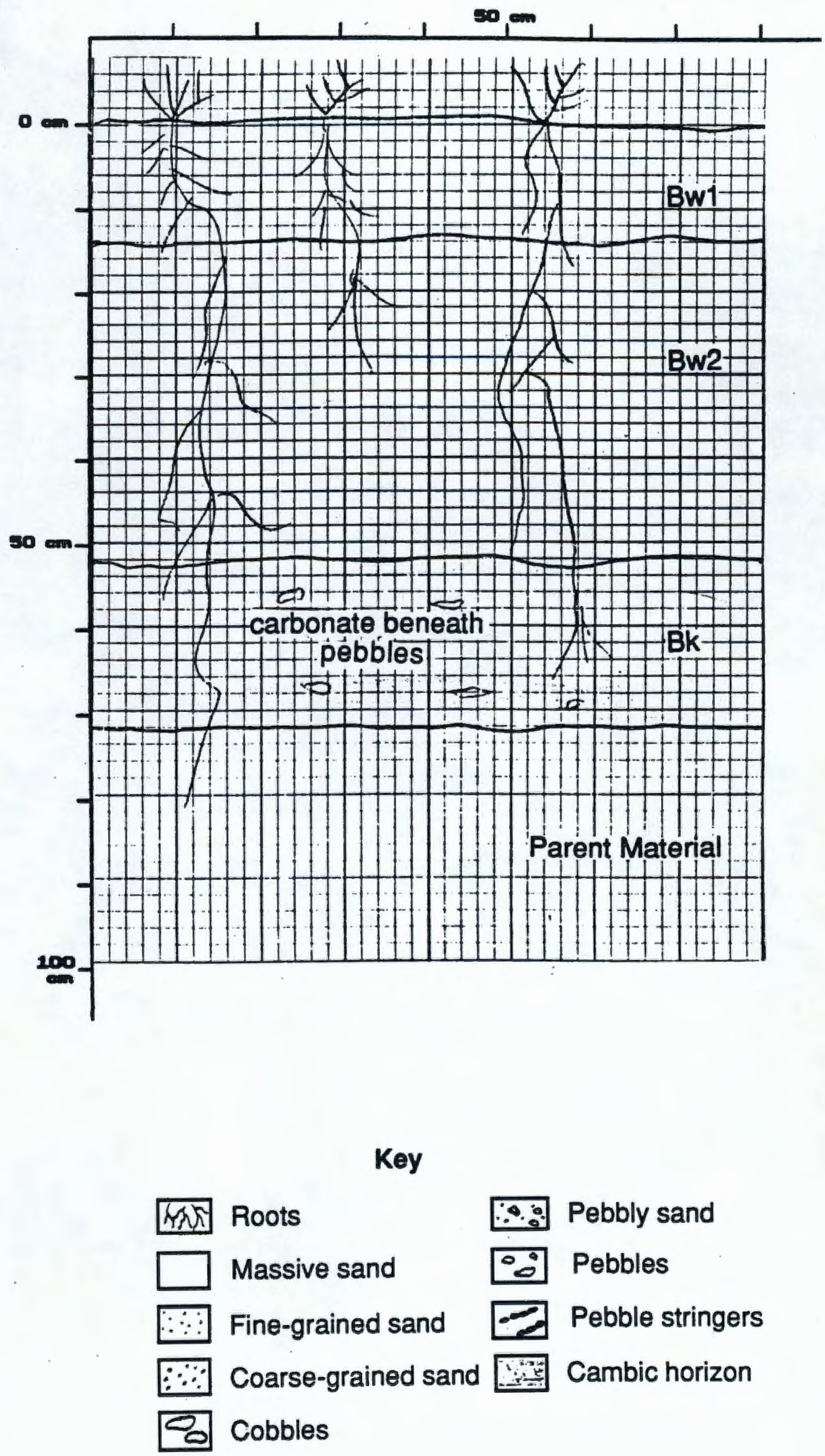
50 cm
0 cm
50 cm
100 cm
Bw1
Bw2
carbonate beneath pebbles
Bk
Parent Material
Key
Roots
Massive sand
Fine-grained sand
Coarse-grained sand
Cobbles
Pebbly sand
Pebbles
Pebble stringers
Cambic horizon

DISTRIBUTION

OFFSITE

12 DOE/Office of Scientific and Technical Information

C. S. Abrams
Argonne National Laboratory
P.O. Box 2528
Idaho Falls, ID 83401

3 Battelle Memorial Institute
Project Management Division
505 King Avenue
Columbus, OH 43201
ATTN: W. A. Carbeiner
W. S. Madia
Technical Library

C. Massimino
U.S. Environmental Protection Agency
1200 Sixth Avenue
Seattle, WA 98101

J. W. Nyhan
Los Alamos National Laboratory
P.O. Box 1663
Los Alamos, NM 87545

J. Rensel, M.S. PV-11
Washington State Department of Ecology
High-Level Waste Management
Olympia, WA 98504

2 Washington State Department of Ecology
7601 W. Clearwater, Suite 102
Kennewick, WA 99336
ATTN: D. Teal
N. Uziemblo

3 Washington State Department of Ecology
M.S. PV-11
Olympia, WA 98504-8711
ATTN: E. M. Carlin
C. Cline
R. B. Hibbard

11 Washington State University
Pullman, WA 99164
ATTN: D. Gaylord (10)
P. J. Mehringer

J. Waugh
Chem Nuclear Geotech
P.O. Box 14000
Grand Junction, CO 81502

ONSITE

11 DOE Richland Operations Office

G. J. Bracken	A4-02
J. J. Broderick	A7-27
R. D. Freeberg	A5-19
R. E. Gerton	A4-02
J. D. Goodenough	A5-19
A. C. Harris	A5-19
R. D. Izatt	A3-42
P. M. Pak	A5-19
R. K. Stewart	A5-19
D. E. Trader	A5-90
DOR-RL Reading Room 1	

2 US Army Corps of Engineers

W. L. Greenwald	A5-20
J. H. Jacobson	A3-61

US EPA/OGA

P. S. Innis	B5-01

Kaiser Engineers Hanford Company

D. L. Fort	E6-50

19 Westinghouse Hanford Company

M. R. Adams	H6-01
M. A. Buckmaster	H6-03
J. W. Cammann	H4-14
R. A. Carlson	H6-03
R. W. Hookfin	H6-28
D. R. Myers	S0-14
K. L. Petersen	H4-14
M. R. Sackschewsky	H4-14
W. A. Skelly	H6-03
J. C. Sonnichsen	H4-14
N. R. Wing	H4-14
D. D. (Don) Wodrich	B1-59
R. D. Wojtasek	H6-27
D. E. Wood	H0-32
Publishing Services (3)	
Environmental Data Management Center (2)	

20 Pacific Northwest Laboratory

L. L. Cadwell	P7-54
G. W. Gee (4)	K6-77
R. R. Kirkham	K6-77
G. V. Last	K6-84
M. W. Ligotke (2)	P7-54
S. O. Link	P7-54
R. A. Romine	P8-38
M. E. Thiede	K6-13
W. H. Walters	K6-06
Publishing Coordination	
Technical Report Files (5)	

Routing

R. M. Ecker	Sequim
M. J. Graham	K6-78
P. M. Irving	K6-98
C. S. Sloane	K6-04
P. C. Hays - Last	K6-86